DESSIN

DEMONSTRATE ECOSYSTEM SERVICES ENABLING INNOVATION IN THE WATER SECTOR

www.dessin-project.eu

D34.3 Evaluation of the results obtained in the demonstration and guidelines and recommendations for transfer to other Water Scarcity sites

NTUA, January 2018

The research leading to these results has received funding from the European Union Seventh Framework Programme (FP7/2007-2013) under grant agreement no. 619039

D34.3 Evaluation of the results obtained in the demonstration and guidelines and recommendations for transfer to other Water Scarcity sites

SUMMARY

Deliverable D34.3 is part of WP34 and it is closely related with T34.4. More specifically, D34.3 gives an overview of the results obtained by the Athens' sewer mining (SM) pilot and additionally provides guidelines and recommendations for transferring the solution (i.e., SM) to other sites. Furthermore, it includes the valuation of ESS that result from the utilization of the SM solution. The deliverable is organized in two main sections, 1) Evaluation of the results obtained in the demonstration and 2) Guidelines and recommendations for transfer to other water scarcity sites.

DELIVERABLE NUMBER	WORK PACKAGE
D34.3	WP34

LEAD BENEFICIARY	DELIVERABLE AUTHOR(S)
NTUA	Dr. Christos Makropoulos (Associate Professor, NTUA) Dr. Costas Noutsopoulos (Assistant Professor, NTUA) Dr. Daniel Mamais (Professor, NTUA) Dr. Andreas Andreadakis (Professor, NTUA) Dr. Efthymios Lytras (EYDAP) Dr. Evangelos Rozos (NTUA) c. PhD Ioannis Tsoukalas (NTUA) c. PhD Argyro Plevri (EYDAP) c. PhD Georgios Karakatsanis (NTUA) Msc Chem.Eng. Andriana Lazari (CHEMiTEC) Chem.Eng. Nikos Tazes (CHEMiTEC)

QUALITY ASSURANCE	
Christos Lioumis	CHEMiTEC
Konstantinos Papadopoulos	EYDAP

PLANNED DELIVERY DATE	ACTUAL DELIVERY DATE
31/12/2017	26/1/2018

DISSEMINATION LEVEL	
	☒ PU = Public ☐ PP = Restricted to other programme participants ☐ RE = Restricted to a group specified by the consortium. Please specify: _____ ☐ CO = Confidential, only for members of the consortium

The research leading to these results has received funding from the European Union Seventh Framework Programme (FP7/2007-2013) under grant agreement no. 619039
This publication reflects only the author's views and the European Union is not liable for any use that may be made of the information contained therein.

Table of contents

The research leading to these results has received funding from the European Union Seventh Framework Programme (FP7/2007-2013) under grant agreement no. 619039
This publication reflects only the author's views and the European Union is not liable for any use that may be made of the information contained therein.

List of Figures

The research leading to these results has received funding from the European Union Seventh Framework Programme (FP7/2007-2013) under grant agreement no. 619039
This publication reflects only the author's views and the European Union is not liable for any use that may be made of the information contained therein.

The research leading to these results has received funding from the European Union Seventh Framework Programme (FP7/2007-2013) under grant agreement no. 619039
This publication reflects only the author's views and the European Union is not liable for any use that may be made of the information contained therein.

The research leading to these results has received funding from the European Union Seventh Framework Programme (FP7/2007-2013) under grant agreement no. 619039
This publication reflects only the author's views and the European Union is not liable for any use that may be made of the information contained therein.

List of Tables

The research leading to these results has received funding from the European Union Seventh Framework Programme (FP7/2007-2013) under grant agreement no. 619039
This publication reflects only the author's views and the European Union is not liable for any use that may be made of the information contained therein.

List of Acronyms and Abbreviations

AMI: Advanced Monitoring Infrastructure
DALYs: Disability adjusted life years
DSS: Decision Support Systems
EDCs: Endocrine – disrupting compounds
EPS: extracellular polymeric substances
ESS: Ecosystem Services
IPTO: Independent Power Transmission Operator
JMD: Joint Ministerial Decree
MBR: Membrane Biological Reactor
MF: Microfiltration
NF: Nanofiltration
PhACs: Pharmaceutically active compounds
PLC: Programmable Logic Controller
PPP: Public-Private Partnership
QMRA: Quantitative microbial risk
RO: Reverse Osmosis
SM: Sewer Mining
TMP: Trans-membrane pressure
UF: Ultrafiltration
UHI: Urban Heat Island
US EPA: Environmental Protection Agency
UV: Ultraviolet radiation
WHO: World Health Organisation
WWTP: WasteWater Treatment Plant

The research leading to these results has received funding from the European Union Seventh Framework Programme (FP7/2007-2013) under grant agreement no. 619039
This publication reflects only the author's views and the European Union is not liable for any use that may be made of the information contained therein.

Executive summary

Deliverable D34.3 is part of WP34 and it is closely related with T34.4. More specifically, D34.3 gives an overview of the results obtained by the Athens' sewer mining (SM) pilot and additionally provides guidelines and recommendations for transferring the solution (i.e., SM) to other sites. Furthermore, it includes the valuation of ESS that result from the utilization of the SM solution. The deliverable is organized in two main sections, 1) Evaluation of the results obtained in the demonstration and 2) Guidelines and recommendations for transfer to other water scarcity sites. The results obtained from the demonstration are presented in section 1, which is subdivided in two main sections. Specifically, in section 1.1 that presents the results from the Athens' sewer mining pilot and assesses the performance of the MBR-RO pilot system aiming to explore the feasibility of reclamation and reuse of the treated effluent for urban use. Next. In section 1.2 we investigate the potential of the implemented solution to mitigate the heat-island effect. For this reason, we study the potential benefits of irrigating with treated water a green area in KEREFYT (where the pilot unit is located), the research centre of Athens Water Supply and Sewerage Company (EYDAP). Furthermore, section 2 provides guidelines and recommendations for transferring the solution to other water scarcity sites. Particularly, in section 2.1 we provide a discussion regarding the up-scaling of sewer mining at a city level as well as present a novel methodology for the optimal placement of sewer mining units. The latter is able to account for both the spatial properties and water demand characteristics of a given area while simultaneously accounts for the dynamics of sewer networks. Additionally, in section 2.2, we develop and apply a pricing system for the diffusion of the sewer-mining technology in a market environment as an economically viable investment. An indicative small-scale area with issues of water scarcity was selected for the simulation and valuation of ecosystem services. The main scenario was to use treated wastewater from the sewer-mining unit to water a local park. Hence, our analysis was based in three (3) main pillars: (1) the quantification of water scarcity mitigation, (2) the valuation of water-enhanced ecosystem services (the major service being microclimate regulation from the park's watering) and (3) a discussion on estimated derived economic activities as well as the business model for the sewer mining technology operation. Lastly, it is remarked, that in order to assist the reader and provide a straightforward narrative, each main subsection is structured in way that it has its own discussion and conclusions.

1 Evaluation of the results obtained in the demonstration

1.1 The Athens sewer mining pilot

1.1.1 Introduction

Global climate change and increasing growth of population enhance a worldwide effort to reduce water demand. Replacement of fresh water for non-potable uses with water from alternative sources such as rainwater or treated "blackwater" and "greywater" is being encouraged so as to decrease fresh water demand. Sewer mining (SM) is one of the latest wastewater recycling inventions and is gradually increasing in popularity due to its high treatment efficiency as well as the fact that smaller space is required to install the treatment unit. This practice belongs to the wider group of decentralized options for water recycle/reuse (Makropoulos & Butler, 2010). Sewer mining does not use traditional wastewater treatment schemes, but alternative ones that make the usage of a compact, portable and advanced treatment unit possible. Furthermore, direct sewer mining can reduce the need for additional infrastructure and ongoing energy consumption to transmit wastewater to a centralized treatment facility and then recycled water to the point of use (Marleni, et al., 1-6 December 2013)

In order to achieve goals of the project, an innovative small footprint SM packaged treatment unit for urban reuse, consisting of a membrane bioreactor (MBR) coupled with a reverse osmosis (RO) unit, has been installed in EYDAP's R&D department, in the Metamorphosis region (Athens, Greece). The concept of Athens demo site is to test the idea of sewer mining as an innovative tool for distributed reuse within the urban environment, exploiting state-of-the-art information and communication technology solutions for distributed monitoring and management. Reused water characteristics and their impacts on urban green are also being tested, via onsite irrigation. Conclusively, the demo site is examining a major component of ecosystem services (ESS) specifically relevant for arid regions: the mitigation of heat island effects due to irrigation of urban green. This is performed through sprinkling reclaimed water on a grass field, located near the unit.

The main advantages of the sewer mining unit installed in the Athens demo site are:

- the production of high quality recycled water due to the combination of membrane bioreactor with reverse osmosis, conforming to stringent performance requirements, including water and health quality standards
- the minimum landscape disruption due to the small size of the unit coupled with the lack of odors and noise pollution, making it suitable for installation in the urban environment. Adding to that, computational simulations can identify optimal installation spots, e.g. selection of placement areas for minimization of hydrogen sulphide build-up in sewer pipes (Tsoukalas, et al., 2016)
- the fully independent function of the system enabled by the installed automations, as well as the online monitoring system that guarantees a high quality of the treated water stream and
- the ability of mining sewage directly from the network, close to the point-of-use, with minimum infrastructure required and low transportation costs for the treated effluent.

In view of the above, the objectives of this study were to assess the performance of an MBR-RO pilot system and to explore the feasibility of reclamation and reuse of the treated effluent for urban use.

1.1.2 Description of the MBR-RO pilot system

1.1.2.1 General description of the decentralized wastewater treatment unit

The pilot unit for the treatment of wastewater, together with Advanced Monitoring Infrastructure (AMI) and Decision Support Systems (DSS) have been installed in the Research and Development center of EYDAP, in the Metamorphosi region, Athens. The goal of the unit is to highlight the use of versatile, mobile wastewater treatment units that pump untreated wastewater directly from the central network and treat it on site, close to the end-point of use. The installed pilot unit consists of: (1) a membrane bioreactor unit (MBR) and (2) a reverse osmosis unit (RO). Both of them have been constructed as individual modules that can be combined in one compact unit, offering ease of transportation. The daily treatment capacity is 12 m^3/day. The following Figure 1 presents the location of the unit as well as the nearby irrigation area.

Figure 1. Depiction of the DESSIN Athens pilot plant (left) and the area that is irrigated using retrieved water (right).

The treatment scheme is presented briefly in Figure 2. In the pilot system, feed wastewater is pumped from the local sewerage network to the satellite wastewater treatment plant (WWTP). The inlet pumping station is feeding the sewage to an equalization tank of a volume around 17 m^3 and from there, wastewater ends up to the MBR unit. The outlet stream of the MBR unit then enters the RO unit. As shown in Figure 3, the retrieved water is stored into tanks, from where it is pumped in order to irrigate, via a sprinkler irrigation system, a triangular green location of a total area of 50 m^2, which is located near the unit. The following paragraphs give a brief description of each treatment stage of this pilot unit.

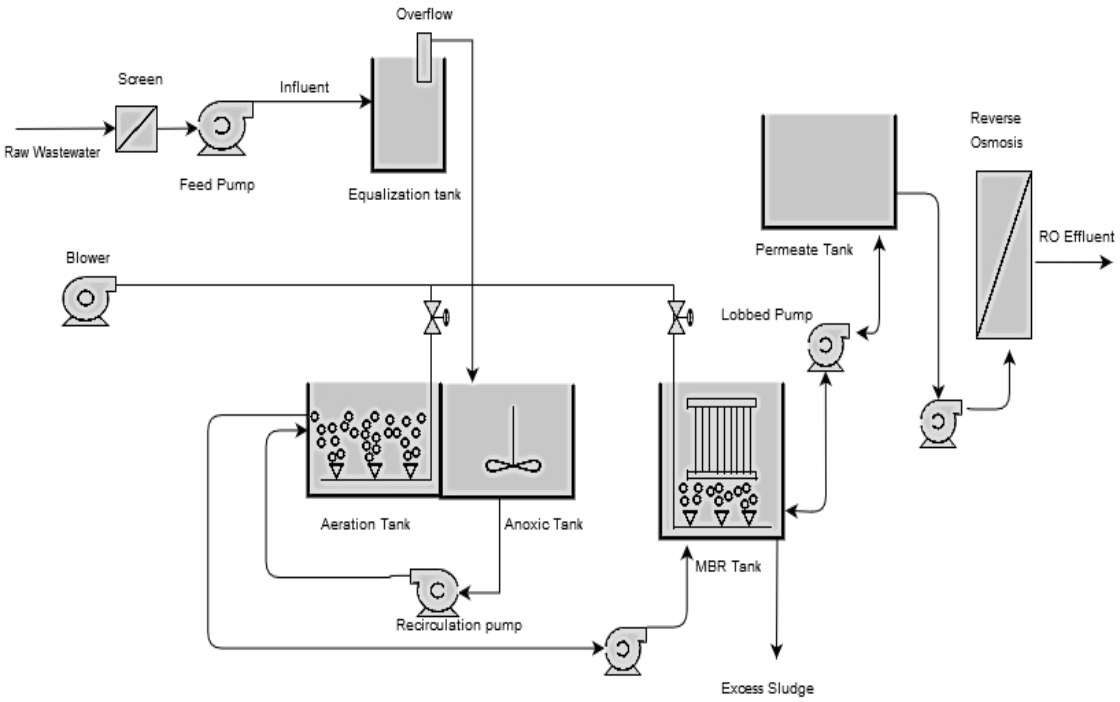

Figure 2. Flow chart of DESSIN Athens pilot plant.

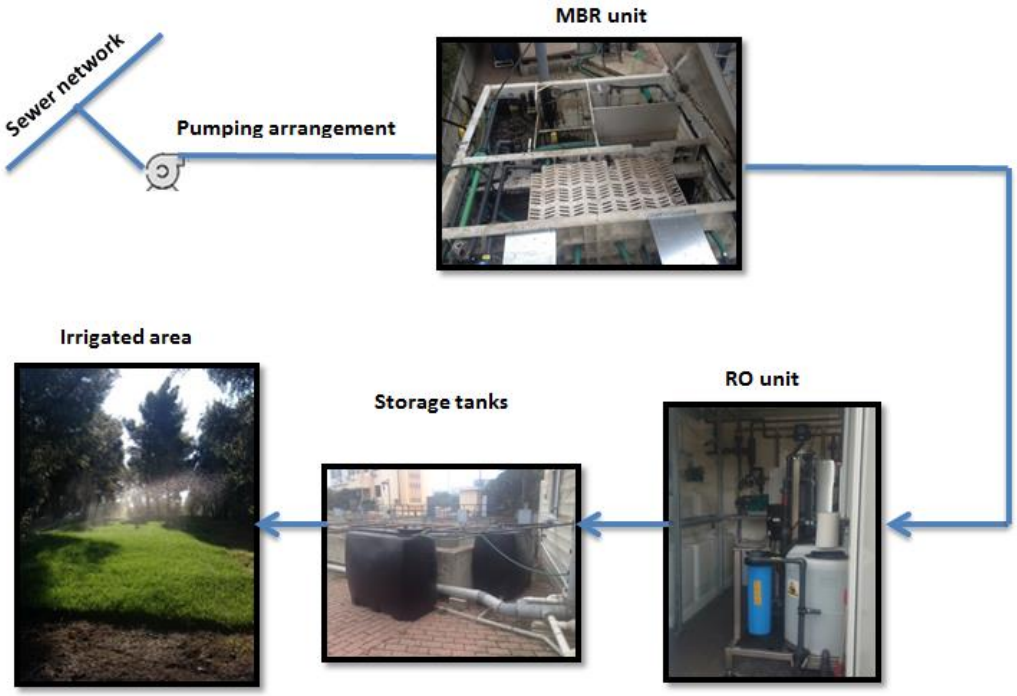

Figure 3. Schematic representation of the processing stages of the pilot plant, starting from the sewage pumping and ending in the sprinkling of the adjacent green space.

1.1.2.2 Preliminary treatment

The first pretreatment stage is realized inside the tank where the submerged feed pump of the unit is located (Figure 4). Wastewater passes through a coarse screen-grit system. The screens allow for the retention of solids, especially large and bulky material (e.g. paper, fabric and plastic materials etc.) and the grit-grease unit for the protection of the downstream equipment from sand particles, grease and oil. The second stage of the pretreatment process consists of a biotube filter (fine screen), placed in the equalization tank of the system. The biotube filter removes fine parts of the sand particles and suspended solids that are contained in wastewater streams.

Figure 4. Presentation of the coarse screen (≤5mm) -grit system (left) and the biotube filter fine screen (≤2mm) (right) which constitutes the pretreatment stage.

1.1.2.3 Biological treatment unit

The outlet flow from the pretreatment unit enters via overflowing-the main treatment units. The main treatment units consist of biological treatment with MBR. The MBR unit has been installed within a 2,16 m x 2,00 m x 2,87 m container, which is separated into 5 compartments, within which biological processes for the waste treatment take place (Figure 5). In Figure 6, the plan view of the biological unit is presented.

Figure 5. Presentation of the biological processing tank.

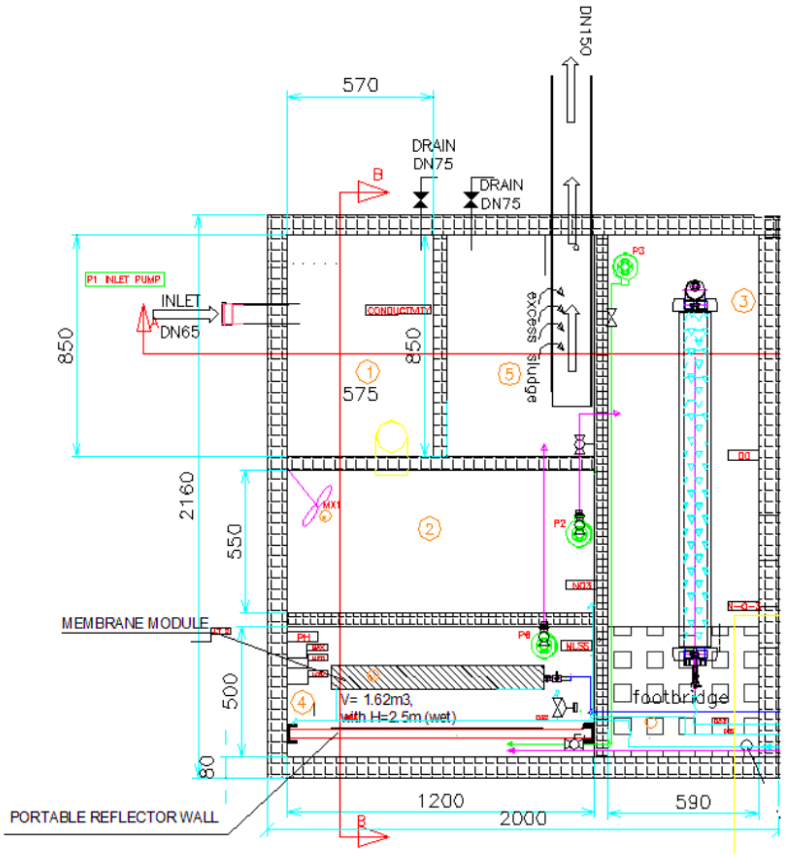

Figure 6. Plan view of DESSIN Athens pilot plant (dimensions in mm). The orange numbering presents discrete sub-tanks.

The first compartment is used as a pretreatment/equalization tank. Wastewater leaving this tank is fed through an overflow system that contains a filter to the denitrification tank (No 2 in Figure 6), while excess material are collected and removed via drainage (Figure 7).

Figure 8. Presentation of the drainage (left) and overflow &recirculation (IR) (right) system.

In the denitrification tank enter both the pretreated stream and the recirculation from the aeration tank, in which nitrification takes place.

The denitrification stage consists of an anoxic tank equipped with a mixing device that guarantees mixing of the liquor. The mixed liquor from the denitrification tank enters the aeration tank (No 3 in Figure 6) where the biological processes of oxidation of the organic load, nitrification and stabilization of sludge is taking place. The necessary oxygen for the aforementioned processes that are realized inside the aeration tank is provided by the use of 2 air diffusers, which also ensures mixing of the liquor.

Division of the suspended solids and the treated effluent is materialized through an ultrafiltration membrane. The installed membrane consists of hollow fiber, ultrafiltration modules. The pore's diameter is 0.03μm, while the total filtration area of the membrane is 34 m^2. The modules operate under negative pressure with the filtration way going from the outside of the hollow fiber towards the inside. As a consequence, solids are withheld in the retentate on the outside of the hollow fibers while the permeate flows inside and is collected by the collection manifold in the module to be subsequently transferred to a permeate accumulation tank and then discharged or used for non-potable purposes such as irrigation. Excess sludge is distributed back to sewage network. Discharge to wastewater collection system is a viable consideration where the retentate comes from a satellite treatment facility and the volume of the retentate is relatively small in comparison with the entire flow of the central wastewater treatment plant.

Figure 9. Presentation of the biological unit containing (from the left to the right) the MBR, aeration, anoxic and equalization tanks (left) and detailed view of the MBR tank (right).

1.1.2.4 MBR maintenance

Cleaning of the membranes with air (air scouring) is performed through an aeration system that consists of blowers and coarse bubble diffusers. This operation prevents membranes fouling and clogging, while at the same time it also ensures the smooth operation of the system, by discarding deposited particles that block the membrane pores, therefore permitting the filtration of the incoming wastewater. Moreover, air scouring provides the necessary mixing force so as to preserve homogeneity of the biomass characteristics within the membrane tank. The main membrane blower has a power of 2.2 kW and its total capacity is 30 m^3/h.

For the purpose of maintaining the membrane permeability, two more methods of membrane cleaning have been implemented. The first one is the backflushing mode, where the extraction pump inverts its rotation sense and conveys a part of permeate produced from the inside to the outside of the hollow fibers to remove any material that may have been deposited on the outer surface of the fibers or inside the pores during the suction period. Backflushing mode takes place for 1 minute every 10 minutes of continuous operation. The second one is maintenance cleaning; chemical cleaning cycles consisting of sodium hypochloride (NaOCl) and citric acid that reach the membranes by backflushing clean water that is enriched with those chemicals through dosage pumps. This maintenance method is used in order to prevent the formation of biofilm on the surface of the membrane. Chemical cleaning with NaOCl takes place daily, while cleaning by using citric acid takes place twice a week. Finally, two recovery cleanings are materialized twice a year.

Table 1. Maintenance cleaning protocol.

	Quantity	Duration
	(g/cycle)	(min)
NaOCl (14%)	43	30
Citric Acid (30%)	340	40

1.1.2.5 RO unit

After leaving the membrane section, the permeate is driven into a tank by a reversible lobe pump. From that tank it ends up to the RO system (Figure 10). The RO together with the electromechanical equipment and the control monitors of the pilot unit are placed inside a second container, with dimensions 2,16 m x 3,00 m x 2,87 m, located right next to the biological treatment container.

RO systems are practically required to be incorporated in the treatment train (following MBR system) especially in the case of wastewater with high salinity. The need for RO as a post treatment level is necessary in order to comply with the environmental standards as in the case of saline wastewater. Moreover, the unit has the ability to work without RO treatment, in which case the permeate ends up straight into the effluent tank.

Figure 10. Presentation of the container that includes the RO unit and the electromechanical equipment (control room).

It has to be mentioned that dual-membrane processes, such as ultrafiltration (UF) followed by reverse osmosis (RO), are becoming increasingly attractive owing to the technology used for the reclamation of municipal wastewater due to their efficiency and simplicity in operation. In this kind of process, UF membranes applied to the secondary treatment of wastewater and RO acts as the refining treatment step. The suspended solids are removed by UF membranes while RO membranes remove dissolved solids, organic and ionic matter. A membrane bioreactor can achieve both the secondary treatment of sewage as well as the pretreatment for RO, and hence MBR-RO has a great potential for the treatment of raw sewage to produce reclaimable water (Comerton, et al., 2005) (Xiao, et al., 2014). The characteristics of both the MBR and RO membranes as well as those of the pilot unit are summarized in Table 2.

Table 2. Membrane and pilot system characteristics.

Membrane characteristics	MBR	RO	Pilot parameters	MBR	RO
Manufacturer	KOCH Membrane systems	Filmtech membranes	Manufacturer	Chemitec	Chemitec
Module type	PSH 34	XLE 4040	Configuration	Hollow fiber	Spiral wound
Nominal pore size	0.03μm	-	Operation mode	Continuous	
Surface area	34m^2	8.1m^2	Permeate volume(m^3 d^{-1})	10	-
Material	PVDF	Polyamide Thin-Film Composite	Coarse bubble aeration rate(m3 h-1)	18	-
Salt rejection	-	99,7%	Operating pressure(bar)	-0,6 to 0.6	3 to 10

1.1.3 Monitoring systems

Data collecting devices and control elements have been integrated in an online platform, aiming at controlling the unit and monitoring the operation of the pilot system through a continuous flow of relevant information. The first category includes field sensors that collect data for both wastewater and treated effluent, while the second category mainly refers to a Programmable Logic Controller (PLC) unit that allows both automation and remote control of the unit.

The sensors have been installed at crucial locations of the unit, in order to ensure the quality and integrity of the treating process. Particularly, conductivity meters have been installed in the inlet, permeate and RO effluent tank, pH sensors in the RO effluent and membrane tank, a turbidity sensor in the permeate tank, an MLSS sensor in the membrane tank, a DO sensor in the aeration tank, a nitrate and ammonium sensor in both the anoxic and aeration tanks, temperature sensor in the inlet stream, flow meters in the inlet stream and permeate, level meters both in the aeration and MBR tank and finally, an energy sensor for the whole plant. Figure 11 sums up the type and location of the system's sensors.

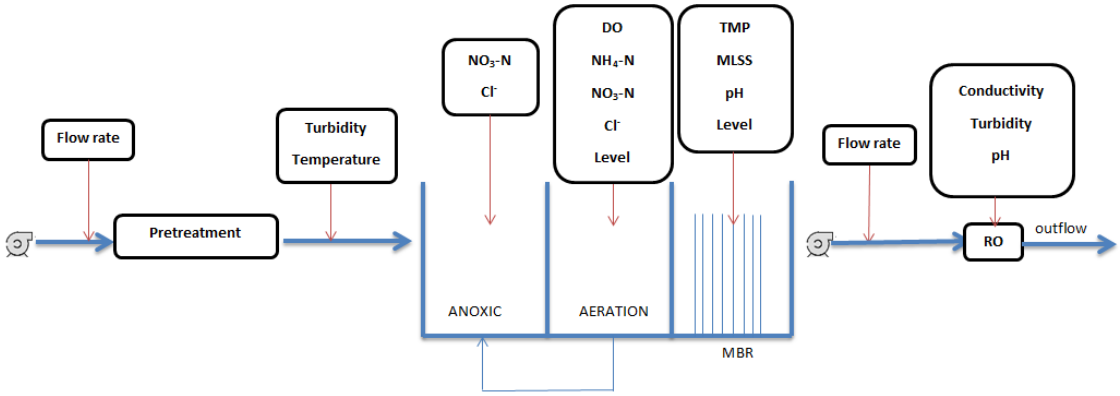

Figure 11. Depiction of the locations and types of the various sensors of the pilot unit.

After their collection, the retrieved data are uploaded in an online platform (Figure 12) which provides the following features:

- Local, remote access and control of the sensors
- Data recovery in real time and presentation through graphs
- Detection of problems and events and provision of notifications via a developed alarming system
- Data visualization for each one of the sensors
- Construction of a historical database that allows for the retrieval of specific historical data by inserting a specific data
- Ability to export data to various formats such as graphs or excel files

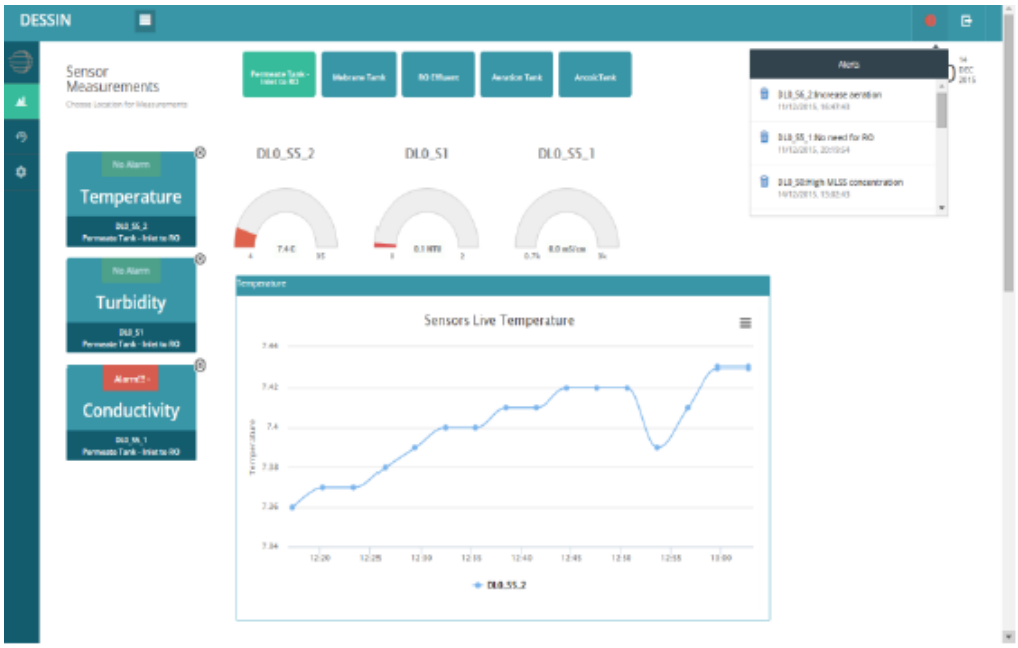

Figure 12. A view of the online platform.

Concerning the PLC system, it manages the operational parameters of every controllable element of the unit, such as pumps, valves and blowers. Consequently, it monitors and gives the ability to control flows in every pipeline, levels of the tanks and the transmembrane pressure (TMP). Moreover, the operator can insert alarm and alert values. The alarm is used to inform the operator about the possibility of a functional problem occurrence, while the alert shuts down relevant equipment in order to avoid more severe effects, thus providing constant protection for both the electromechanical equipment and the stability of the biological processes. The PLC is It is also connected with sensors and instruments, so it can adjust flow sets according to the analytical data of biology. Figure 13 presents the main screen of the PLC unit.

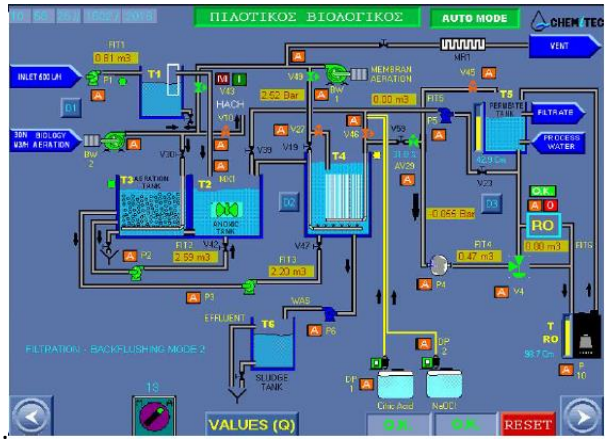

Figure 13. A view of the PLC monitor.

1.1.4 Analytical methods

To strengthen inference on the quality of the produced effluent, a series of laboratory analysis were performed in the EYDAP's laboratories. These analyses provided feedback not only for the unit but also for the sensors, in the form of cross validation. Therefore, the task of sensor calibration was done after receiving relevant indications from the laboratory results. The laboratory analysis took place twice a week, and included measurements of total chemical oxygen demand (CODt), soluble chemical oxygen demand (CODs), mixed liquor suspended solids (MLSS), mixed liquor volatile suspended solids (MLVSS), diluted sludge volume index (DSVI), biochemical oxygen demand (BOD_5), total phosphorus (TP), total nitrogen (TN), ammoniacal nitrogen (NH_4-N), nitrate nitrogen (NO_3-N), chlorides (Cl^-), total coliforms (TC), fecal coliforms (FC) and *Escherichia Coli* (EC).

Besides the above measurements, samples from the inlet, permeate tank and RO effluent were frequently analyzed for emerging contaminants and trace metals (also referred to as heavy metals). Target compounds analyzed in this study belong to two broad categories of emerging contaminants, that of the endocrine disrupting chemicals (EDCs) and the non-steroidal anti-inflammatory drugs (NSAIDs). Chemical substances belonging to the aforementioned categories present a persistent detection in the aquatic environment and have such toxicological and chemical characteristics that are of growing interest to the scientific community. Table 3 presents the target compounds that have been selected as representatives of EDCs and NSAIDs, along with their main physicochemical properties, their abbreviations and the limits of detection (LODs) for each compound.

Table 3. Target compounds, their physicochemical properties and their LODs (in ng/L).

Compound	Short form	Molecular type	MW	logKow	LOD
Nonylphenol	NP	C15H24O	220.36	4.5	3
Nonylphenol monoethoxylate	NP1EO	C17H28O2	264	4.17	2
Nonylphenol diethoxylate	NP2EO	C19H32O3	308	4.21	6
Bisphenol A	BPA	C15H16O2	228.1	2.2-3.84	10
Triclosan	TCS	C12H7Cl3O2	290	4.2-4.76	4
Naproxen	NPX	C14H14O3	230.27	3.18	3
Ibuprofen	IBU	C13H18O2	206.29	3.91	1
Ketoprofen	KFN	C16H14O3	254.3	3.12	0.5

Wastewater characteristics (chemical oxygen demand, biochemical oxygen demand, total suspended solids, total volatile solids, sludge volume index, total phosphorus, total nitrogen, ammoniacal and nitrate nitrogen, chlorides, total and fecal coliforms and *E. coli*) were determined according to Standard Methods of the American Public Health Association (American Puplic Health Association, 2012). Emerging contaminants determination in wastewater samples followed the chromatographic method developed by Samaras et al. (Samaras, et al., 2011). The procedure included solid phase extraction, while for the qualitative and quantitative analysis, an Agilent Gas Chromatograph 7890A connected to an Agilent 5975C Mass Selective Detector (MSD) was used. The Inductively Coupled Plasma Mass Spectrometry (ICP-MS) approach was adopted for the determination of the selected trace metals in the inlet flow and the MBR effluent, while for the RO effluent the selected method was Inductively Coupled Plasma Optical Emission Spectrometry (ICP-OES). For the PPs four different approaches were followed, depending on the chemical; Purge and Trap Gas Chromatography–Mass Spectrometry (P&T/GC-MS), Gas Chromatography coupled to tandem Mass Spectrometry (GC-MS/MS), Liquid Chromatography coupled to tandem Mass Spectrometry (LC-MS/MS).

1.1.5 Operating parameters

For the first operational stage, that of determining the qualitative characteristics of the unit, the operation lasted for 9 months (21/01/2016 to 20/10/2016). During this period, temperature varied between 15-25°C. The capacity of the unit was set to 10 m^3 of treated wastewater per day, while the total capacity can reach 100 m^3/d. The concentration of mixed liquor suspended solids (MLSS) in the MBR tank was set to be between 8-9 g/L. This value was achieved by daily removing excess sludge in order to maintain a solids retention time (SRT) of 20 d. Accordingly MLSS concentration in the anoxic and aeration tank remained stable at values around 6 g/L. The operational parameters of the MBR unit are listed in detail in Table 4

Table 4. MBR operational parameters.

Parameter	Units	Value
Flow (Q)	$m^3\ d^{-1}$	12
Hydraulic Retention Time (HRT)	h	3
Solid Retention Time (SRT)	d	20
Organic Loading (F M^{-1})	gCOD (gMLVSS d) $^{-1}$	0.38
Suspended Solids (MLSS)	g L^{-1}	9.2
Volatile Solids (MLVSS)	g L^{-1}	7.4
Sludge Removal (W)	L d^{-1}	84
Filtration Flux (J)	L m^{-2} h^{-1}	15-20
Filtration Flow (Q_{filtr})	L h^{-1}	500
Backflushing Flow (Q_{back})	L h^{-1}	1000

1.1.6 Results of the quality monitoring stage

The first operational stage can be divided into three discrete phases. The first phase, with duration from 21/01/2016 until 23/02/2016, corresponds to the startup period. The second stage, 23/02/2016

to 26/05/2016, refers to the winter period, while the summer period constitutes the third and last phase and lasted from 26/05/2016 to 20/10/2016.

1.1.6.1 Phase 1

The pilot unit was commenced operation in January 2016. The duration of the startup process was approximately 5 weeks, when the necessary conditions for biomass growth and nitrification-denitrification were established and approximately steady state conditions were achieved. It has to be mentioned that the system developed biomass without inoculation and during the startup period the practice of sludge removal did not take place. Figure 14 presents the concentration of the mixed liquid suspended solids (MLSS) and ammoniacal nitrogen inside the MBR tank. Also the partial use of RO and its short operation (less than 15-20 minutes) leads to low performance, so an improvement in operation of RO would be advantageous.

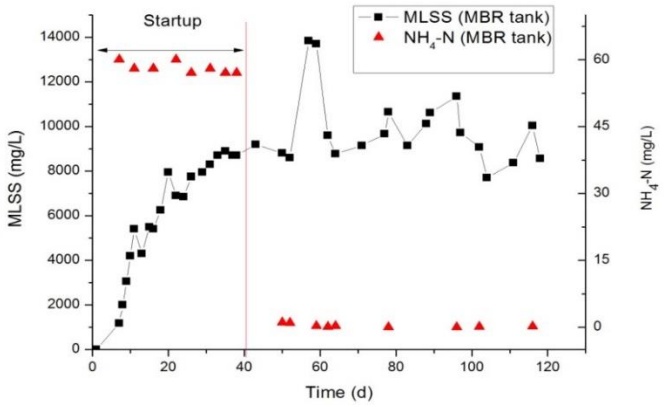

Figure 14. Evolution of MLSS and NH4-N concentrations in MBR tank.

As shown in Figure 14, the stabilization of the system and the beginning of the nitrification process were achieved around week 7, since the first operating day. Moreover, MLSS concentration rapidly increased and stabilized around high values, a fact that is anticipated by the design of the pilot unit. It is noted that the pH value inside the MBR tank during the corresponding time interval took values within the 7.5-8 range. The following graph (Figure 15) shows the temperature variation of the inlet stream and the liquor within the MBR tank for the startup period.

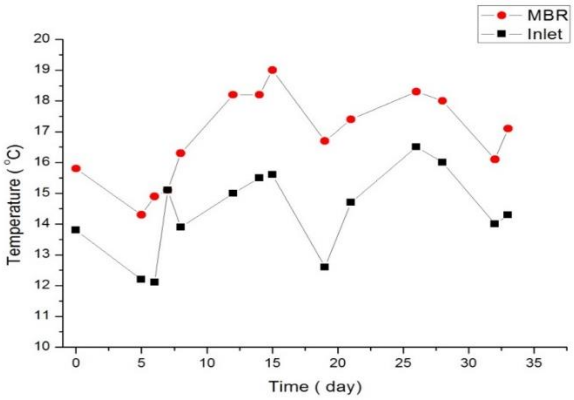

Figure 15. Temperature variation for the first phase of the system.

A thorough examination of the pretreatment unit revealed that the installed biotube filter was able to remove a substantial amount of oils and other substances that could prove harmful to the

membranes. This can be deduced from Figure 16, where a reduction of COD between wastewater before and after the filter is observed.

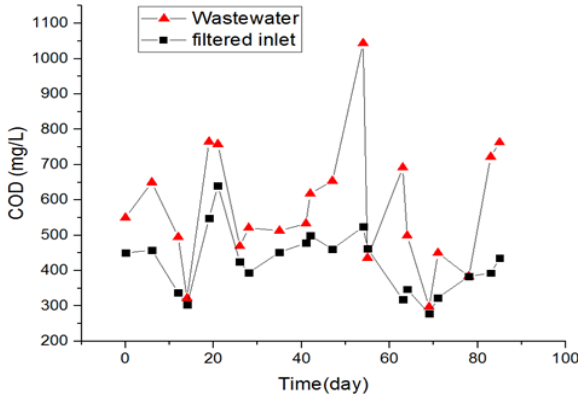

Figure 16. COD of untreated and pretreated wastewater.

The characteristics of the degritted wastewater (wastewater stream after the fine screen-grit system) and the filtered wastewater entering the equalization tank are listed in the Table 5. As can be seen from these data, pre-treated wastewater characteristics display significant fluctuations.

Table 5. Characteristics of degritted and filtered wastewater (concentrations in mg/L, average ± standard deviation).

Parameters	Degritted Wastewater	Filtered wastewater
TSS	376±373	164±72
VSS	235±112	138±46
CODt	578±176	424±86
CODs	173±30	171±25
TP	10±1	8,8±0,7
NH_4-N	57±18	55 ±15
Cl^-	184±98	157±23

1.1.6.2 Phase 2

Following the stabilization of the operation of the biological treatment, the second phase lasted approximately 100 days. During this winter period, the operation of the MBR-RO unit was closely monitored in order to make inferences regarding the system. According to the results, the system achieved to produce such a great effluent quality in terms of physicochemical parameters, as for the retrieved effluent to be under the legislation limits and be proper for reuse for non-potable uses. At the same time, the application of RO managed to further improve several qualitative aspects of the treated wastewater.

1.1.6.2.1 MBR performance and permeate quality

The operation of the MBR throughout the experimental period was stable and its performance was satisfactory. Removal of total suspended solids (TSS) of the wastewater was total (100%) throughout the operation of the pilot system (Figure 17), due to the fact that TSS have a size greater than the one of the membrane pores and, as a consequence, particles are unable to penetrate through the membrane section. Full retention of TSS by the biomembranes is the main advantage of the MBR in comparison with other conventional treatment systems, in which a settling tank is used to clarify the effluent. In addition to that, the accomplishment of a permeate stream with practically constant

characteristics is of high importance for the smooth operation of the RO unit, making the MBR system an ideal pretreatment to RO. Finally, the fact that TSS were undetectable in the MBR permeate stream along with the fact that transmeembrane pressure (TMP) had a steady value of 10 kPa nearly throughout the second period indicates that the membrane remained intact, without appreciable fouling.

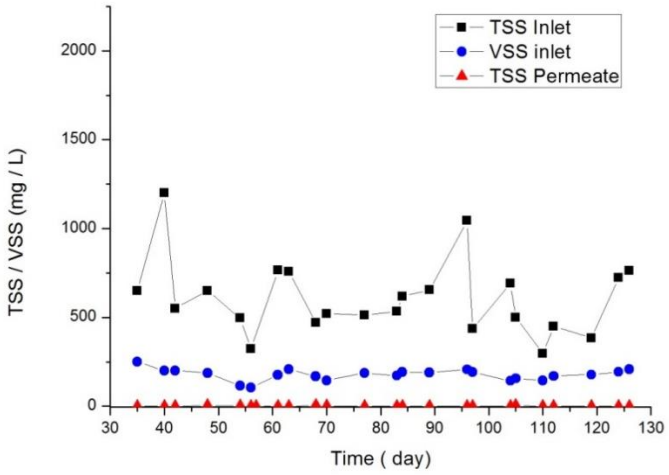

Figure 17. MBR performance in relation to TSS.

Turbidity measurements in the treated wastewater were particularly low and in accordance with the concentrations of suspended solids in the permeate. As shown in Figure 18, turbidity values in the permeate of the MBR tank were systematically lower than 0.5 NTU. An important fact that is mentioning is that the retrieved values allude to the same time as the lab samples, specifically at around 9:30 am. The spike occurring around day 100 might imply the existence of a breach in the membrane which usually goes along with an increase of microorganisms (Hai, et al., 2014). This is one of the reasons that emphasize the importance of continuous monitoring of turbidity as an indicator of microorganism concentration. Figure 19 shows the intraday variation of turbidity for six random days within the second period. The spike in turbidity values in this graph is not correlated to any type of membrane breaching, but rather with the daily scheduled maintenance cleaning. This argument is in agreement with the study of Branch et al. (Branch, et al., 2015) that showed that after Cleaning-In-Place (CIP), turbidity immediately increases and returns to its average values after about 4 hours.

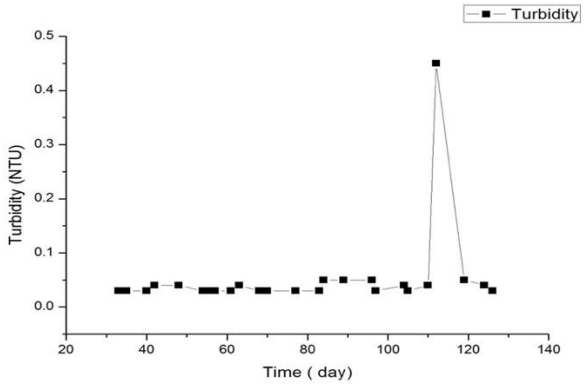

Figure 18. Turbidity measurements in the MBR permeate.

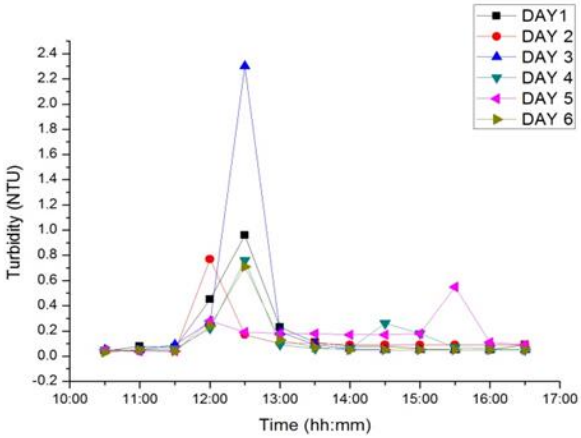

Figure 19. Intraday turbidity in the MBR permeate.

During the operation of the MBR, COD removal was very high and the percentage removal of COD was systematically higher than 95%, while the average effluent total COD was as low as 23 mg/L. Figure 20 depicts the concentration of COD in the influent and MBR permeate. The performance of the MBR can be considered particularly satisfactory and is in good agreement with corresponding studies found in literature, where the average COD removal ranges from 85 % to 98 %. In their study, Barreto, 2016 showed that membrane bioreactors can achieve removal rates up to 99% for COD inlet values varying between 600-1500 mg/, due to high MLSS values in the MBR tank (Barreto, et al., 2016).

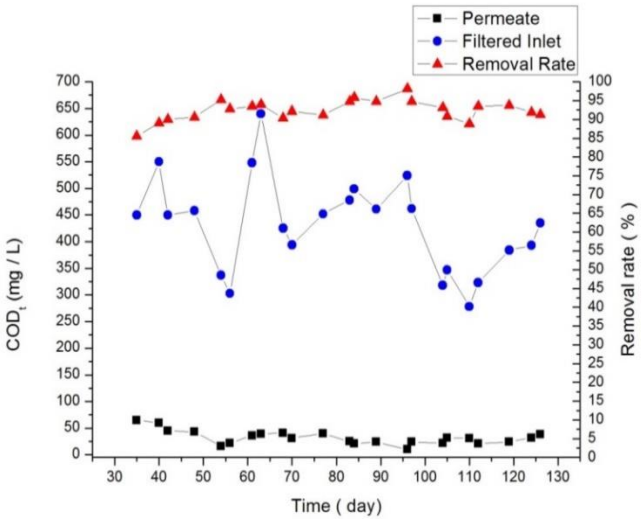

Figure 20. MBR performance in relation to COD removal.

Figure 21 introduces the variation of MLSS and MLVSS in relation to the system's running time. The data of the graph have derived from laboratory analyses and from sensors installed inside the MBR tank as well.

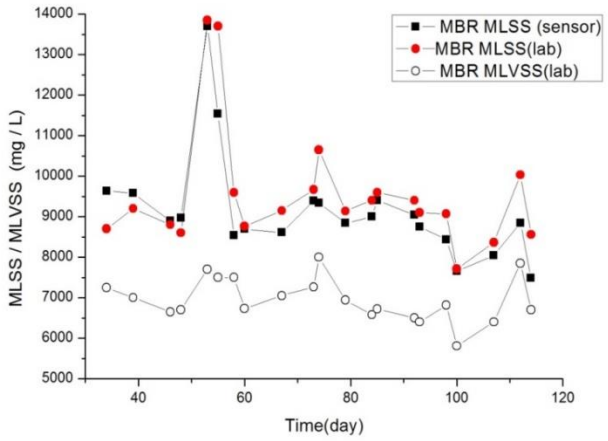

Figure 21. MLSS & MLVSS concentrations inside the MBR tank.

MLSS values inside the MBR tank ranged at high values, more specifically above 8000 mg/L and although the tank is small (1.5 m^3), MLSS concentration presented great stability. The graph comparison of the lab results with the sensor measurements proves that the installed MLSS sensor provided reliable data. This fact is noteworthy, since the existence of the sensors in the context of the integrated monitoring system allows for the remote control of the unit, providing its safety by leading to alarm conditions and ultimately to unit shutdown -if needed- when key values overcome the programmed upper threshold.

The settling characteristics of biomass were satisfactory throughout the second period. Figure 22 presents the diluted sludge volume index (DSVI) which is a measure of sludge settleability. DSVI ranged at satisfactory levels, fluctuating between 60-140mL/gSS with an average value of 100 ml/gSS, thus indicating a biomass with acceptable settling properties (Noutsopoulos, et al., 2007).

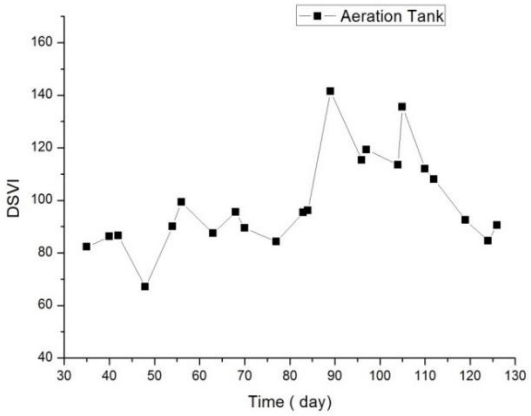

Figure 22. Sludge settleability index.

As shown in Figure 23, during the winter operational period of the MBR unit, complete nitrification was observed. The concentration of ammoniacal nitrogen was always below 0.5 mg/l NH_4-N. The increased nitrification ability of the MBR is related to the higher sludge retention Time (SRT) achieved. In their research, Cote et al. demonstrated that an increase of the SRT from 5 to 10 days

resulted in an increase of the ammonium removal rate from 80% to 99%, while Fan et. al. (1996) found that for the same increase in SRT, the nitrification efficiency increased from 94% to 99%

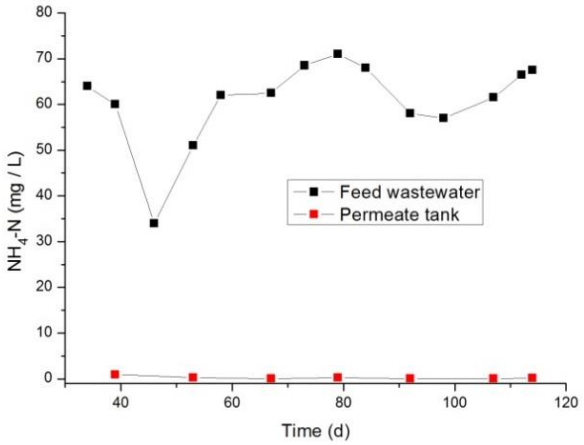

Figure 23. MBR performance in respect to ammoniacal nitrogen removal.

MBR membranes have been reported to achieve a significant decrease of microorganism concentration, varying from 4 to 8 log units, mainly through size exclusion (Cartagena, et al., 2013). The parameters that were selected as representative indicators and therefore were repeatedly analyzed in the MBR permeate and RO effluent, were the Total and Fecal coliforms (TC and FC), as well as *E.coli* (EC). These parameters were chosen because they are representative indicators for the existence of other microorganisms. More specifically, a decreased concentration of coliforms in general reveals absence of other microorganisms and fecal coliforms have additionally been correlated with the existence of fresh fecal matter, while the decrease of *E.coli* are related to virus absence (Hai, et al., 2014). Figure 24 shows that *E.coli* and Fecal coliforms were below the limit of detection of the analytical method, which indicates that the membrane was not breached during the operational period. Additionally, the TC content of MBR effluent was rather low with values ranging from 250 to500 cfu/100 mL. Traceable TC content in the MBR effluent might be a result of formation of microbial colonies in the permeate's pipe line (Zhang & Farahbakhsh, 2006). These results are in good agreement with those reported by Zhang et al (Zhang, et al., 2016), who attributes high TC values to the formation of biofilm in the internal space of the permeate pipe line.

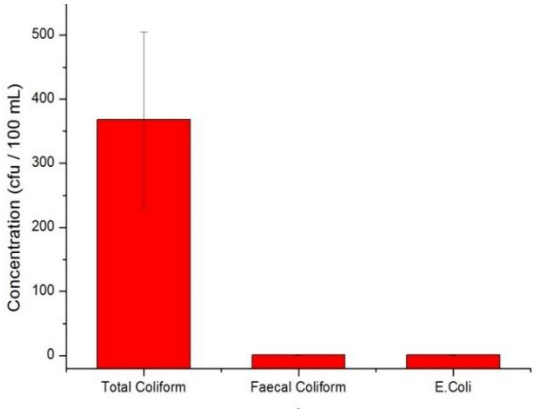

Figure 24. Concentration of biological parameters in the MBR permeate.

1.1.6.2.2 RO performance and effluent quality

Further treatment of the MBR permeate by the RO contributed in a significant reduction of the conductivity of treated wastewater. Monitoring of conductivity and pH was accomplished via the on-line sensors, which provided information about of both the inlet and effluent of the RO. Conductivity is the single most important and most commonly monitored system parameter in an RO plant. The RO flux and recovery rate are greatly affected by the conductivity of the feed water. As conductivity rises, the same happens with osmotic pressure, thus making the RO system less efficient at a given pressure and temperature. Therefore, the installation of on-line sensors is of great importance since they provide for the identification of changes in permeate flow rate due to feed conductivity fluctuations (Tam, et al., 2005). As shown in Figure 25, conductivity values in the final effluent were consistently below 0.3 mS / cm.

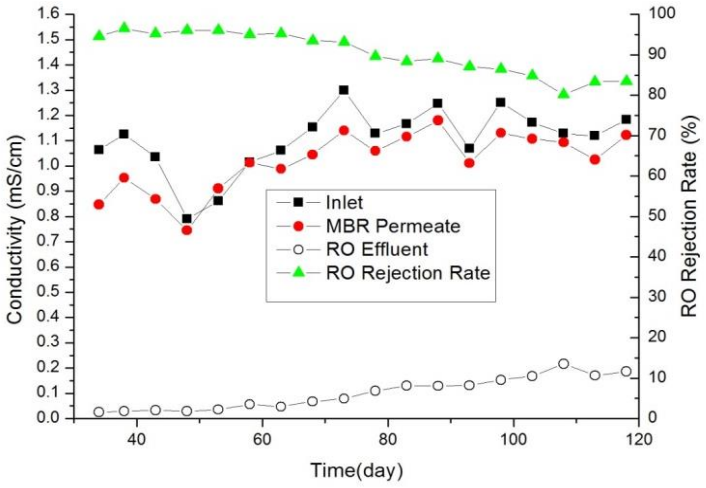

Figure 25. Ion rejection rate for the RO.

Figure 25 presents the conductivity rejection rate, through comparison of the RO feed stream (which in this case is the MBR permeate) with the RO effluent. The rejection rate is defined as the percentage difference between the conductivity of the feed water and that of the effluent. These results display the fact that conductivity was reduced by the RO, but remained unaffected by the MBR. RO rejection averages at values over 85% (Figure 25). These rejection rates are rather low for such a system, since based on the relevant literature, MBR-RO systems have removal rates of the order of 97-99%. This

low rejection rate percentage observed can be attributed to the low conductivity values of the MBR permeate. A similar pattern was recorded for pH (Figure 26). It is of significant importance that both conductivity and pH in the RO effluent kept increasing in time while rejection rate decreased. This indicates that the RO membranes have sustained fouling or scaling, although anti-scalants were added regularly into the system in order to minimize chemical precipitation on the RO membrane surface (Witgens, et al., 2005).

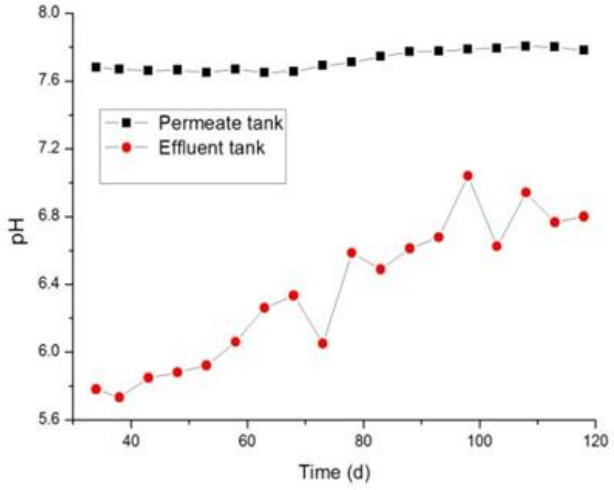

Figure 26. Evolution of pH in the RO effluent.

The performance of the RO membranes is also linked to the removal of total dissolved solids (TDS), which in this study varied around 71%. This value is considered very low for RO membranes. Table 6 presents the results of the laboratory analyses on the MBR permeate, RO effluent and RO concentrate.

Table 6. TDS removal.

TDS (mg/L)	MBR permeate	RO effluent	RO condensate
Mean	672	179	570
Standard deviation	62	55	25

In addition to the aforementioned features, RO was also tested for its ability to remove nutrients. Removal of total phosphorus (TP) by the RO was complete. In the effluent stream, the concentration of TP remained constantly under the LOD of the analytical method. On the other hand, removal of nitrogen was not complete, with its concentration reaching 12 mg/L in the RO effluent. In relation to the microbiological parameters, RO presented excellent performance, as it was expected due to the small size of the membrane pores. All the microbiological indicators remained under LOD of the analytical methods. The absence of E.Coli or Total Coliforms in the RO effluent indicates their complete rejection. Finally, chlorides in the RO effluent were less than a quarter in comparison with the RO inlet.

1.1.6.3 Phase 3

The third phase includes the summer period and spans from 26/05/2016 to 20/10/2016. All operational parameters remained constant and equal to the ones of the second period. During this period the unit remained out of order for a short time interval, due to mechanical problems

concerning mainly the blowers. In the next paragraphs the performance of the pilot MBR-RO unit for this third phase is analyzed.

1.1.6.3.1 MBR performance and permeate quality

The following two graphs present the removal of TSS (Figure 27) and COD (Figure 28) that the MBR unit achieves.

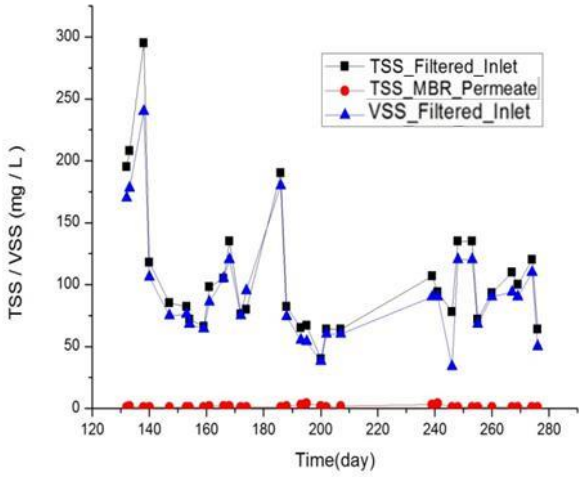

Figure 27. TSS removal by the MBR during the third phase.

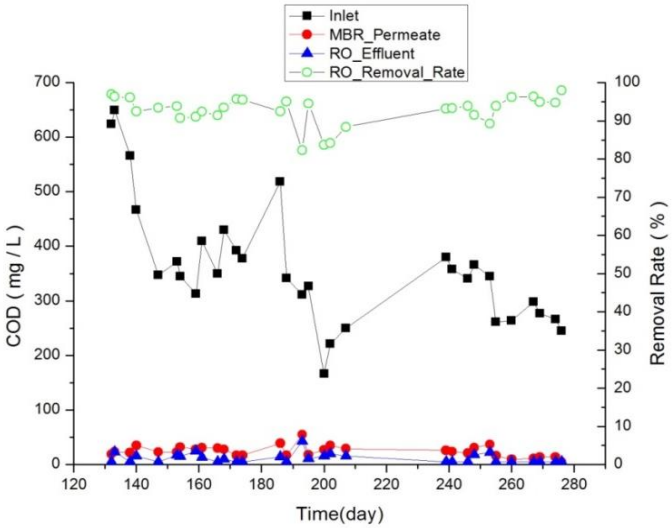

Figure 28. COD removal by the MBR during the third phase.

It is evident that TSS removal was complete in this third phase as well, with the TSS concentration in the MBR permeate being always below the LOD of the analytical method. Concerning COD, its concentration in the MBR permeate varied at very low values in this phase as well. It has to be mentioned that COD of the untreated wastewater presented a declining trend and was generally lower in comparison with that of the second phase.

Figure 29 presents the turbidity of the MBR permeate flow. Results of turbidity for this phase are in good agreement with phase 2, with turbidity values being below 0.3 NTU.

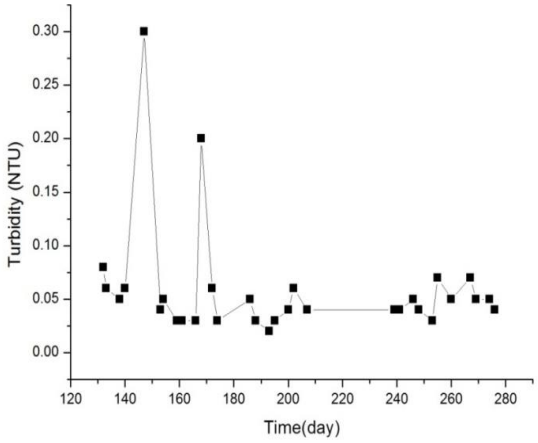

Figure 29. Turbidity of the MBR permeate during the summer period.

As it can be seen from the above diagram, there is a time period of around 30 days where there are no data available. This happened because the unit was shut down for about two weeks in order to fix certain mechanical malfunctions and two more weeks were needed in order for the system to become stable again.

Figure 30 depicts the variation of MLSS and MLVSS inside the MBR tank. As in the previous period, the data used to create this graph were obtained both by sensor and laboratory analyses.

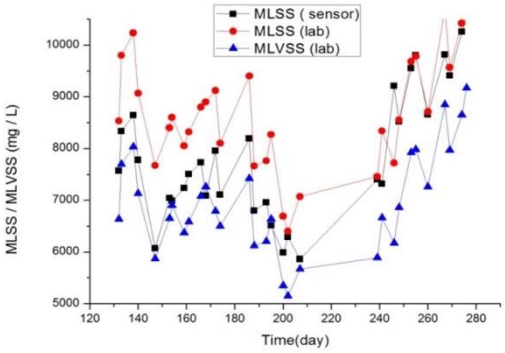

Figure 30. MLSS/MLVSS concentration in the MBR tank during the third phase.

Examination of Figure 30 reveals that MLSS had extreme variations and there were time intervals in which MLSS concentrations had values below 7000 mg/ L. The cause of this behavior is related to the several operational problems the unit faced during this phase. Moreover, Figure 30 shows that there are points at which differences between the sensor and laboratory values can be observed. This bias that the sensor had developed was eradicated though maintenance. Figure 31 presents the sludge settlability which varied at satisfactory levels, with DSVI always being below 120 ml/gSS.

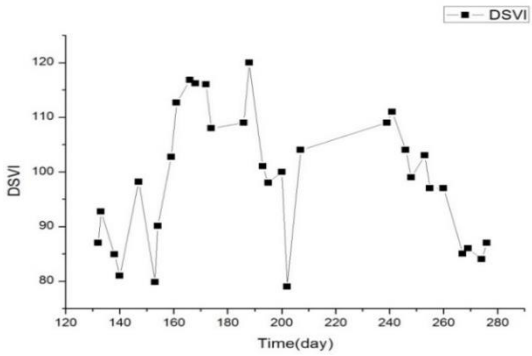

Figure 31. DSVI for the third phase

Figure 32 describes the nitrifying capacity of the pilot unit. It is obvious that although several operational problems occurred during the third period, the system managed to achieve complete removal of ammoniacal nitrogen through nitrification.

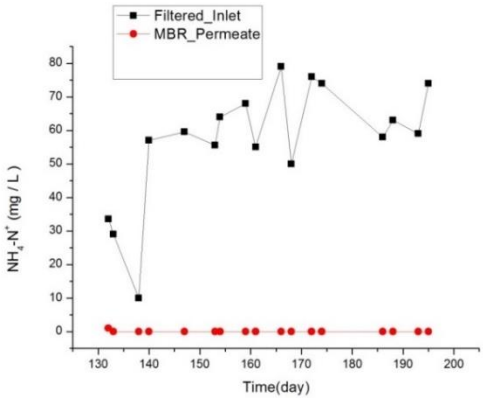

Figure 32. MBR performance in relation to NH4-N removal for the third period.

1.1.6.3.2 RO performance and effluent quality

As in the case of the second period, in this third period, further treating the MBR permeate with RO contributed in removing a significant amount of dissolved ions in the treated stream. As it can be seen in Figure 33, conductivity of the final effluent was always below 0.3 mS/cm.

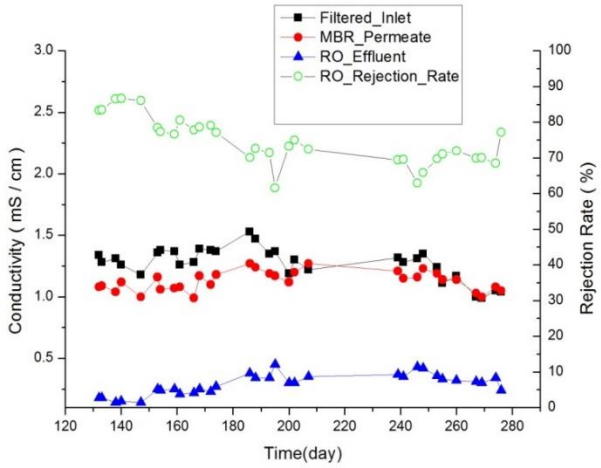

Figure 33. Conductivity of the RO feed and effluent in the third phase.

Figure 34 depicts the chloride concentration of the influent, MBR permeate and RO effluent. As it was expected, chlorides are reduced by approximately 70% by the RO. The data used in the graph were produced by laboratory analyses.

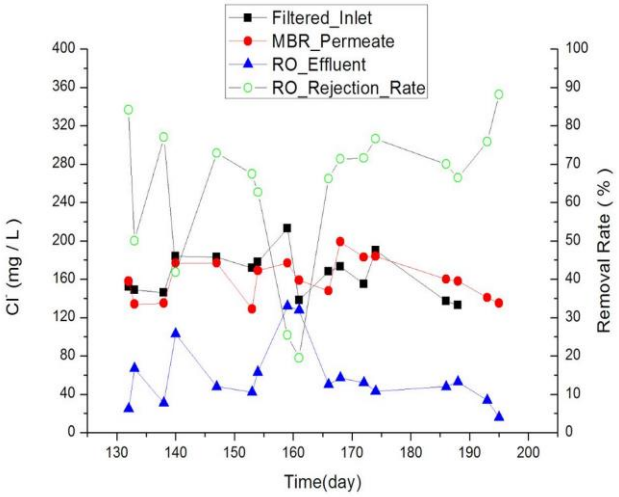

Figure 34. Removal of chlorides by the RO.

It has to be noted that during the third period RO had excellent performance in relation to the selected microbiological parameters. The removal of E.Coli, total and fecal coliforms was complete, with the respective concentration always being below the LOD of the analytical method.

1.1.7 Aggregated results and comparison with the Greek legislation

Table 7 presents the aggregated results for the second phase and Table 7 for phase 3 and both tables make a comparison of the study's results with the corresponding limits set by the Greek legislation for wastewater reuse in the case of peri-urban green (JMC 145116,2011).

Table 7. Performance of the MBR-RO pilot system (concentrations in mg/L,TC, FC, EC in cfu/100mL, turbidity in NTU) and comparison with the Greek legislation (JMC 145116,2011) for the second phase. Values represent mean± standard deviation.

Parameters	Influent[1]	MBR effluent	RO effluent	Legislation limits[2]
TSS	166 ±72 [3]	<DL[7] for 80% of samples	<DL[7]	≤2 for 80% of samples[5] ≤10 for 80% of samples[4]
BOD_5	141 ±64 [3]	0.9 (average) 1.6 for 80% of samples	≤1 for 80% of samples	≤10 for 80% of samples[4,5]
CODt	430±86 [3]	30±9.5 [3]	< 10 (average)	
CODs	171±25 [3]	25±9.5 [3]	< 10 (average)	
TN	81(average)	-	12 (average)	≤15[4,5]
NH_4-N	61±15 [3]	0.33±0.3 [3]	-	≤2[4,5]
TP	9±0.7 [3]	5 ±1 [3]	≤5	
Turbidity	-	0.05 (median)	-	≤2 (median)[4,5]
TC	>10^7	307±390 [3] 578 for 80% of samples 1115 for 95% of samples	ND[8]	≤2 for 80% of samples[5] ≤ 20 for 95% of samples[5]

FC	>10[7]	1±1.8 [3]	ND[8]	-
EC	>10[7]	0.8±1 [3] ≤ 2 for 80% of samples ≤ 2 for 95% of samples	ND[8]	≤5 for 80% of samples[4] ≤50 for 95% of samples[4]

[1] refer to filtered wastewater; [2] refer to the Greek legislation regarding wastewater reuse (Joint Ministerial Decision 354/8-3-2011); [3] average ± standard deviation; [4] refer to the limit values set in Greek legislation for wastewater reuse for unrestricted irrigation and/or industrial reuse; [5] refer to the limit values set in Greek legislation for urban reuse and/or groundwater recharge; [6] refer to the limit value set in Greek legislation for every type of reuse for WWTPs with a population equivalent greater than 100,000; [7] Limit of detection; [8] Not detected.

Table 8. Performance of the MBR-RO pilot system (concentrations in mg/L,TC, FC, EC in cfu/100mL, turbidity in NTU) and comparison with the Greek legislation (JMC 145116,2011) for the third phase. Values represent mean± standard deviation.

Parameters	Influent[1]	MBR effluent	RO effluent	Legislation limits[2]
TSS	106 ±72 [3]	<DL[7] for 80% of samples	<DL[7]	≤2 for 80% of samples[5] ≤10 for 80% of samples[4]
BOD_5	141 ±64 [3]	0.9 (average) 1.6 for 80% of samples	≤1 for 80% of samples	≤10 for 80% of samples[4,5]
CODt	342±86 [3]	23±9.5 [3]	< 10 (average)	
CODs	172±25 [3]	23±9.5 [3]	< 10 (average)	
TN	51(average)	-	15 (average)	≤15[4,5]
NH_4-N	60±15 [3]	0.3±0.3 [3]	-	≤2[4,5]
TP	9±0.7 [3]	7 ±1 [3]	≤5	
Turbidity	-	0.04 (median)	-	≤2 (median)[4,5]
TC	>10[7]	307±390 [3] 578 for 80% of samples 1115 for 95% of samples	ND[8]	≤2 for 80% of samples[5] ≤ 20 for 95% of samples[5]
FC	>10[7]	1±1.8 [3]	ND[8]	-
EC	>10[7]	0.8±1 [3] ≤ 2 for 80% of samples ≤ 2 for 95% of samples	ND[8]	≤5 for 80% of samples[4] ≤50 for 95% of samples[4]

[1] refer to filtered wastewater; [2] refer to the Greek legislation regarding wastewater reuse (Joint Ministerial Decision 354/8-3-2011); [3] average ± standard deviation; [4] refer to the limit values set in Greek legislation for wastewater reuse for unrestricted irrigation and/or industrial reuse; [5] refer to the limit values set in Greek legislation for urban reuse and/or groundwater recharge; [6] refer to the limit value set in Greek legislation for every type of reuse for WWTPs with a population equivalent greater than 100,000; [7] Limit of detection; [8] Not detected.

Comparing the aggregated results with the limits set by the Greek legislation for wastewater reuse, it becomes evident that the MBR achieved to produce retrieved water that lies within the legislation limits for all physicochemical parameters that were monitored during the second phase of operation. During the third phase of operation the concentration of total nitrogen exceeded the legislation limit of 15mg/l, due to limited denitrification.

The installed sensors revealed that turbidity was always below 2 NTU, which is the corresponding limit set in the legislation. BOD_5 of the effluent was below 2 mg/L, while the average COD of the effluent was 30 mg/L for the second and merely 25 mg/L for the third period. TSS were constantly undetectable, proving that the MBR technology is ideal as a pretreatment method for the RO feed stream and also secures the quality of the effluent.

In the RO effluent, all microbial and organic pollutants were constantly under the LOD of the analytical method. For all monitored parameters, the final effluent fully met the limits set in the

Greek legislation. However, it has to be noted that nitrogen had a rather high concentration in the final effluent and the system could not fully remove chlorides.

1.1.8 Heavy metals and priority pollutants

The most important factor that defines the success of a water treatment process is no other than the effluent wastewater's quality. There are numerous quantifiable parameters that collectively assess quality, some of which are indirect and act as indices of the presence of biochemical substances, while others are of direct nature, measuring a specific compound or microorganism. Among the latter, priority pollutants (PPs) and heavy metals are of paramount importance in wastewater urban reuse, where the legal framework regarding urban reuse is gradually becoming stricter worldwide.

PPs are substances that pose a danger to both human health and the environment and may be present in water (Kislenko, et al., 2011). Within these substances several groups of compounds can be identified such as Volatile Organic Chemicals (VOCs), Organotins, Polycyclic Aromatic Hydrocarbons (PAHs), Alkylophenols, Chlorobenzenes, Pesticides, Phthalates and others (Gasperi, et al., 2009). On the other hand, the most commonly detected toxic heavy metals (trace metals) in wastewater include Arsenic (As), Lead (Pb), Mercury (Hg), Cadmium (Cd), Copper (Cu), Chromium (Cr), Nickel (Ni), Silver (Ag) and Zinc (Zn) (Akpor, et al., 2014). Trace metals pose a serious threat to humans and to the aquatic environment since they can be absorbed, accumulated and biomagnified and can cause several known diseases, due to their toxic nature above certain concentrations (Herojeet, et al., 2015). Moreover, it has been found that they can affect several organs such as the kidney and induce malfunctions to the neurological system (Lohami, et al., 2008). It has to be noted that Cd, Hg and Pb are highly toxic to humans and animals but are less toxic to plants, while Zn, Ni and Cu are, when present in excess concentrations, more damaging to plants than to humans and animals (Tiruneh, et al., 2014). Heavy metals and PPs can be introduced into a municipal sewage network through various paths such as water runoff, groundwater and sanitary, light industrial, domestic or commercial sewage. Several past researches have investigated the source of both PPs (Soonthornnonda & Christensen, 2008); (Rule, et al., 2006), and heavy metals (Sorne & Lagerkvist, 2002).

Therefore, European Union (EU established the Water Framework Directive (2000/60/EC) (WFD) a legislative tool for protecting the aquatic environment as well as for armoring water quality. Article 16 of the WFD develops the European Union (EU) strategy against pollution of water by chemical substances. A list of 33 priority substances has been conclusively proved and most of the list's entries are organic contaminants (hydrocarbons, organochlorine compounds, organic solvents, pesticides, and chlorophenols), four of them are toxic metals and one is an organometallic compound (tributyltin). Additionally, WFD distinguishes priority substances, for which their emissions should be decreased to the greatest possible extent from priority hazardous substances, the use of which should be ceased or emissions, discharges and losses should be eliminated by 2020. Priority hazardous substances are toxic, persistent and have the tendency to bio-accumulate. The first list in the WFD was substituted with Annex II of the Directive on Environmental Quality Standards (Directive 2008/105/EC), which set environmental quality standards (EQS), while Directive 2009/90/EC layed down technical specifications for chemical analysis and monitoring of water status and brought in a list of 11 substances under review for being future entrances in the PP list. Last of the directives was Directive 2013/39/EU, which brought further inclusions to the previous and updated the initial list of 33 PPs, adding another 12 elements, compiling a list of a total of 45 compounds. This regular update of the EU directives underlines the importance of the water quality standards applied and gives insight to future directions.

In Greece, legislation concerning wastewater reuse introduces certain thresholds which are determined by the end use of the water. In particular, the limit values defined for the Greek National legislation regarding wastewater reuse for unrestricted irrigation and urban use were introduced by the JMD 145116/2011. A modification of the Joint Ministerial Decision 145116/2011 (JMD) occurred via the Government Gazette B 69/2016 (GG), which introduced 3 new PPs and more precise quality standards. In respect to heavy metals and PPs, there are two tables for each category which contain 19 and 40 compounds respectively.

In this context, monitoring of heavy metals and PPs is essential in applications of water reclamation. However, apart from those two categories of pollutants, it is considered appropriate to investigate an even wider spectrum range of substances, by including emerging contaminants (Sauve & Desrosiers, 2014) such as various compounds that belong to the endocrine disrupting chemicals (EDCs) and the non-steroidal anti-inflammatory drugs (NSAIDs), which, despite not being included in the list of PPs yet, have gained a lot of attention in research due to their persistent detection in the aquatic environment and their possible conceivable effects.

The influent of the pilot unit was tested for the occurrence of certain emerging contaminants belonging to the EDCs and NSAIDs (Figure 35), as well as for all heavy metals, trace elements and PPs that are specified in the Greek legislation for water reuse. In the first group of chemicals, all components were found to be present in the influent stream, with concentrations ranging from 0.2 μg L^{-1} up to 8.8 μg L^{-1}. From those, the only pollutant that is subject to legislation is Nonylphenol 4 (NP), which happens to be the most abundant in the examined wastewater. According to a previous study, NP concentration is higher in wastewater coming from runoff samples near light industries (Rule, et al., 2006). NP has been found to cause inhibition of wheat growth, affect chlorophyll and several enzymes and thus is highly toxic for wheat and probably for many other plants (Zhang, et al., 2016). Therefore, NP should be monitored regularly, especially in winter months where it has been found that influent concentrations are higher (Gao, et al., 2017).

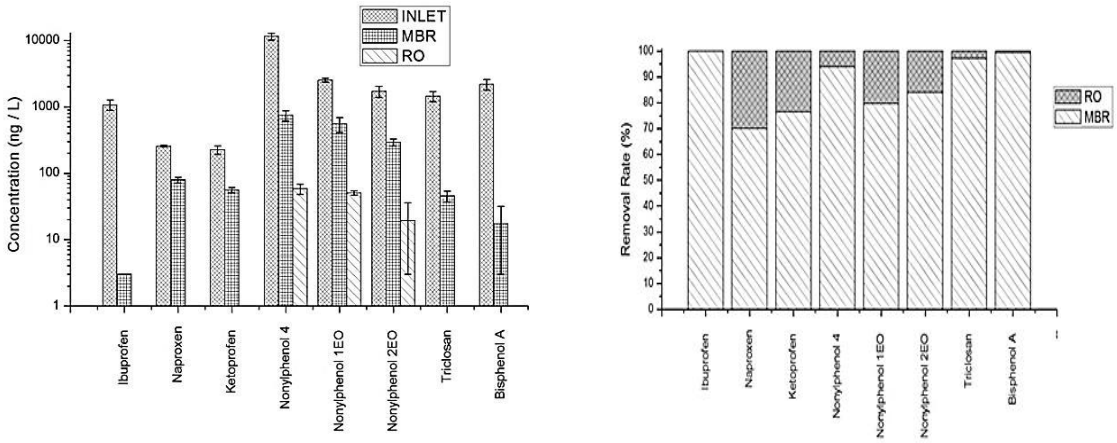

Figure 35. (left) EDC's and NSAIDs average concentrations in the inlet, MBR permeate and RO effluent, (right) contribution of MBR and RO to the total removal of EDC's and NSAIDs.

Figure 35a presents the average concentrations and the standard deviation of the selected emerging contaminants in the influent wastewater, in the effluent of MBR tank and the final effluent (RO effluent), while Figure 35b exhibits the relative contribution of the removal of each target compound at MBR and RO unit. Based on the results, the MBR tank achieved a removal of greater than 99% for IBU, greater than 90% for TCS and NP, greater than 80% for NP2EO, whereas the removal of all the

other target compounds was greater than 70%. Besides their high removal, the MBR effluent concentrations of NP and its ethoxylates (NP1EO and NP2EO) were rather high (to the order of 200-800 ng/L). These results were anticipated, since in UF filtration the removal of EDC's and other organic compounds is achieved through the absorption of the substances from particulate matter and thus only hydrophilic substances can be removed, while more polar molecules present a lower removal rate (due to small SRTs). Contrariwise, NF filtration removes such particles through size exclusion (Wintgens, et al., 2002). In any case NP permeate concentration was lower than the threshold value of 2 μg/L which has been set in Greek legislation for NP for wastewater reuse for WWTPs with a population equivalent greater than 100,000.

These results are in a good agreement with Clara et al. (2005), suggestion that SRTs greater than 10 d add strength to the elimination of some biodegradable compounds like Ibuprofen and Bisphenol A. Moreover, Stasinakis et al. (2010), showed that a greater biodegradation of 4-n-Nonylphenol and Triclosan was achieved when the SRT was set to 20 days, comparing to 3 and 10 days. Last but not least, in relation to the RO implementation, a recent study appears to follow the same removal pattern of NP as the present one, since the compound never exceeded 120 ng L^{-1}, starting from an initial concentration of around 10^3 ng L^{-1} (Al-Rifai, et al., 2011).

Concerning heavy metals and trace elements, the chemicals under investigation were the ones specified in JMD 145116/2011 with one addition; silver (Ag). From those 20 compounds, only nine were identified in the examined wastewater, while all the other analyzed compounds were found to range in values below their respective limit of detection of the analytical method (LOD), which was 0.005 μg L^{-1} or 0.001 μg L^{-1}, depending on the element. The detected metals were Aluminum (Al), Copper (Cu), Iron (Fe), Lithium (Li), Manganese (Mn), Nickel (Ni), Lead (Pb), Vanadium (V) and Zinc (Zn). In a study performed by Sorne & Lagerkvist (2002), regarding urban wastewater, it was found that Cu mostly derives from households, specifically from copper pipes and taps. In the case of Zn, the load is equally divided between households and businesses (mainly car wash enterprises), while Pb originates mostly from commercial activities. Another study indicates that in the case of Cu, Pb and Zn, light industrial sources own a greater diffusion share (Rule, et al., 2006). Moreover, the influent analysis comes in good agreement with other studies regarding the ranking of concentration magnitude of metals in raw wastewater. More specifically, the occurrence of heavy metals in urban wastewater seems to follow –with slight variations- this sequence: Fe>> Al> Zn> Mn> Cr> Cu> Ni> Pb> Cd (Ustin, 2009); (Gulyas, et al., 2015); (Karvelas, et al., 2003). The influent metal concentration order produced from this study is Fe> Al> Zn> Mn> Cu> Pb> Ni> Li> V, so the only obvious difference is that Pb has a greater concentration in the studied sample, while Cr was below its LOD.

Regarding PPs, from a total of 45 compounds, only four were present in the wastewater sampled. More specifically, these were Chloroform ($CHCl_3$), Trichloroethylene (TCE), Tetrachloroethylene (PCE) and Benzene (C_6H_6), none of which is considered as a hazardous priority substance. All of the aforementioned compounds belong to the VOC PPs. Concerning $CHCl_3$, a study of Rule et al (2005), has found that it is the only solvent that was found to have concentration greater than its LOD on domestic level. While Chloroform concentration in that study was found greater in domestic sewage, for TCE and PCE the authors suggest that dry cleaning was the reason why their concentration was greater in samples retrieved from the town center, where commercial activities take place. For $CHCl_3$, another study indicates that it has a far greater concentration in the water supply in comparison to domestic sewage, proposing that chlorination must be the main source of chloroform in wastewater (Wilkie, et al., 1996). Finally, other studies suggest that the four compounds that were found in the wastewater sample are usually undetected or found around the quantification limit (Gasperi, et al., 2009).

The removal of heavy metals was complete with only Pb and Mn being detected in a concentration level of less than 1 μg L^{-1} and consequently the effluent stream fully met the legislation standards. Concerning the PPs, all of them were not detected in the MBR effluent with the exception of $CHCl_3$, the concentration of which rose from the influent to the MBR effluent and experienced only a slight decrease from the application of the RO. This deviant behavior is attributed to the volatile nature of $CHCl_3$, which might have caused a wrong influent concentration value. Still, all PPs had effluent values below of those set by the legislation. The concentrations (μg L^{-1}) of the influent and the MBR and RO effluent are presented in Table 9, while Table 10 compares the removal rates of heavy metals and PPs of this unit to other ones.

Table 9. Concentrations of detected PPs and heavy metals in the influent MBR permeate and RO effluent streams (in μg L-1).

Substance	Wastewater	MBR permeate	RO effluent	Legislation Limit
Al	480	120	-	5000
Cu	31	5	ND[1]	200
Fe	770	310	ND[1]	3000
Li	5	4	ND[1]	2500
Mn	42	6	0.39	200
Ni	5	<5	ND[1]	200
Pb	6	<5	<2.4	100
V	1	<1	ND[1]	100
Zn	110	64	ND[1]	2000
$CHCl_3$	0.18	0.27	0.23	2.5
TCE	0.23	ND[1]	ND[1]	10
PCE	0.14	ND[1]	ND[1]	10
C_6H_6	0.1	ND[1]	ND[1]	5

[1] Not Detected

Table 10. Comparison of MBR, RO and combined MBR-RO removal rates for selected metals and PPs.

MBR	RO	MBR-RO	Reference
Cu(84%), Al(75%), Fe(60%),Li(20%), Mn(86%), Zn(42%), TCE(>99.9%),PCE(>99.9%), C_6H_6(>99.9%)	Cu(>99.9%), Fe(>99.9%),Li(>99.9%), Mn(93.5%), Zn(>99.9%), C_6H_6(>99.9%) $CHCl_3$(15%)	Cu(>99.9%), Al(>75%),Fe(>99.9%),Li(>99.9%), Mn(99%), Zn(>99.9%), TCE(>99.9%),PCE(>99.9%), C_6H_6(>99.9%)	Present study
Cu(90%), Fe(85%), Mn(82%), Zn(75%)	-	Cu(>97.1%), Fe(>99.3%), Mn(>99.1%), Zn(>99.8%)	(Marleni, et al., 1-6 December 2013)
Cu(95%), Zn(94%), Fe(97%)	-	-	(Fatone, et al., 2006)
Cu(85%) [1], Zn(93%) [1] , Fe(90%) [1], Al(94%) [1]	-	-	(Carletti, et al., 2008)
Cu(31%) [1], Zn(60%) [1],	-	-	(Gurung et al., 2016)
Cu(>81%), Fe(>88%), Mn(>54%), Zn(26%), PCE(>99.9%), $CHCl_3$(>99.9)	-	-	(Mansell, et al., 2004) [2]

[1] Refer to average value, [2] Metal data retrieved indirectly through Conklin et al (2007), who used the raw data to extract the removal rates. Values refer to a Zenon pilot unit, [3] Values refer to case B, which treats only municipal wastewater with similar consistency with this study's influent

MBR data of Table 10 indicate that Cu and Mn removal rates are consistent with the ones in the cited studies. However, the removal rate of Zn agrees only with the one reported in the study of (Mansell, et al., 2004) Mansell et al. (2004) and (Gurung, et al., 2017), but is less than half in comparison to other studies, while the removal of Fe is less than the ones observed in the rest of the studies. Another point worth mentioning is the low decrease rate of the $CHCl_3$ by the RO. A previous study found that RO can remove at least 80% of the inflowing $CHCl_3$ and also concluded that by increasing its concentration from 100 to 500 μg L^{-1} that rate decreased (Mazloomi, et al., 2009)

1.1.9 Optimization phase

Optimization of the system lasted 370 days. During this period, transmembrane pressure (TMP) was monitored and chemical additives were inserted into the MBR tank in order to examine whether additives moderate membrane fouling or if the cleaning protocol followed is sufficient. Moreover, different SRTs were examined in order to observe their impact on both effluent's quality and greenhouse gas emissions (GHG). More specifically, from 10/10/2016 until 22/12/2016 the system operated with SRT=20 days, from 25/12/2016 until 11/02/2017 the system operated with SRT=15 days and from 14/02/2017 until 7/03/2017 the system operated with SRT=10 days. In addition, from 10/06/2017, TMP started being monitored with the system operating with SRT=20 days again and with higher daily capacity, 17 m^3/day instead of 12 m^3/day, in order to create more harsh conditions in terms of membrane fouling. Up until 14/09/2017 membranes were maintained with the standard protocol and on that day, chemicals started being added daily to the system, specifically 68 g/day of polyaluminium chloride 14 % in Al_2O_3, in order to achieve a concentration of 9mg Al/L.

Figure 36 presents the evolution of COD in the MBR permeate over the optimization stage, where SRT was sequentially changed from 20, to 15 and finally 10 days. The graph displays an obvious pattern between the ability of the MBR to remove COD and the set SRT. More specifically, there is an increasing trend of COD in the MBR permeate as SRT decreases. Moreover, the data of Figure 36 reveal another important issue, that is, the higher variation of COD in the third period. This behavior was expected due to the low retention time of solids in the system.

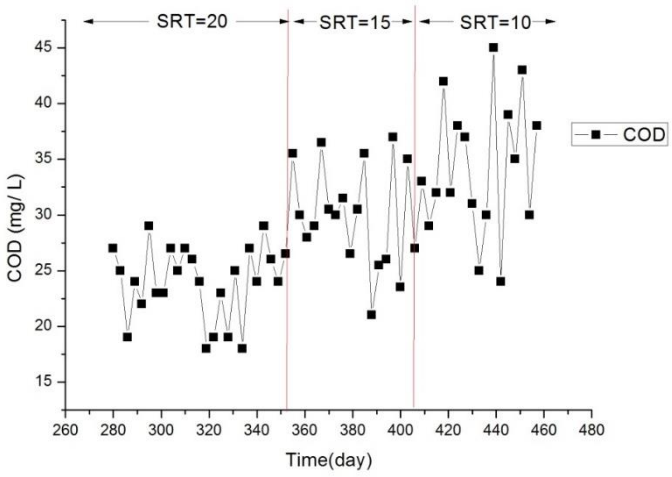

Figure 36. COD variation for different SRT values.

Figure 37 presents values of BOD_5 for different SRTs. It is evident that regardless of the different SRT levels, the MBR system managed to effectively eliminate BOD_5, thus producing a permeate stream of high quality. The perturbations observed ended up to very low values and, in total, BOD_5 for all three SRT values had an average close to zero.

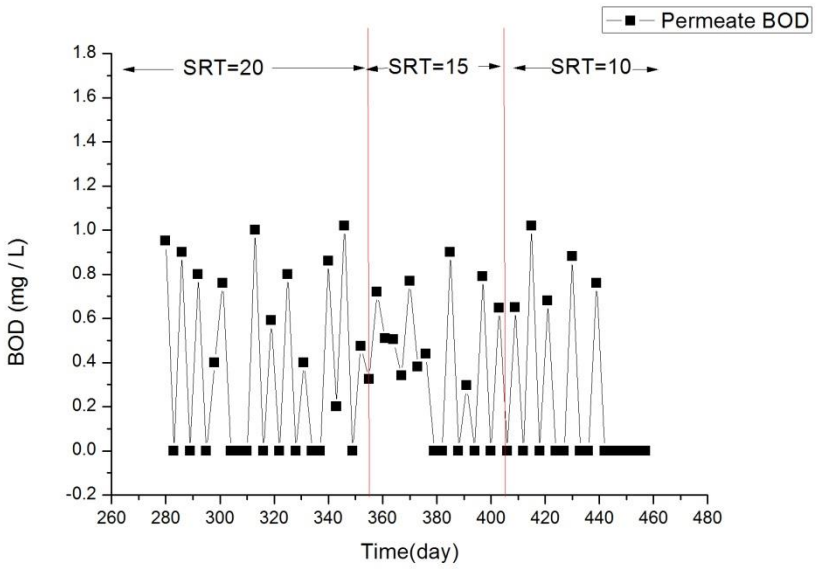

Figure 37. BOD variation for different SRT values.

Figure 38 depicts the evolution of DSVI during the optimization phase. Just as with the relevant COD graph, in this case a pattern emerges. Particularly, DSVI increases with a decrease of SRT from 20 days to 15 and finally 10 days. This escalating trend indicates that with a lower retention time of solids, sludge settleability decreases.

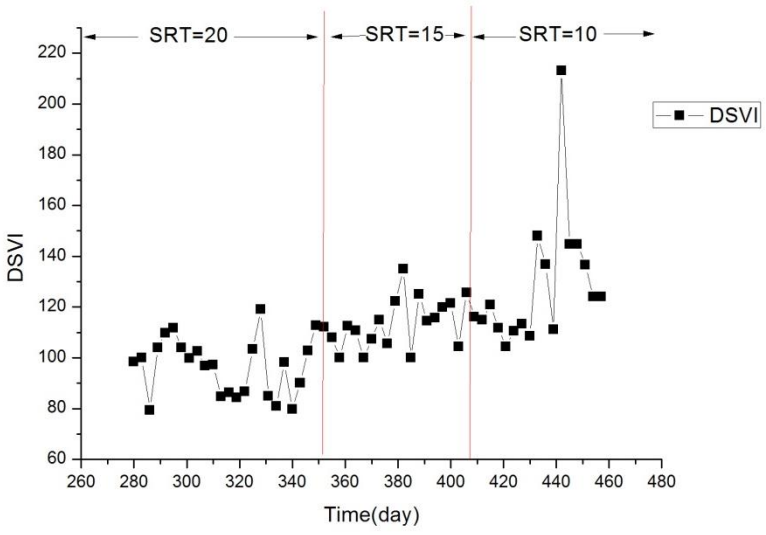

Figure 38. DSVI variation for different SRT values.

Figure 39 presents the produced GHG, based on the onsite emissions as well as the offsite emissions. No significant change between the three SRT levels seems to be taking place, in relation to the daily production of emissions. However, it has to be noted that the biggest amount of GHG emissions is caused by offsite emissions due to the high energy used by the system. The energy used was around 54 kWh/day, which produced around 33 kg of $C0_2$-eq. The energy amount used by the unit is higher than expected due to the operation of the RO.

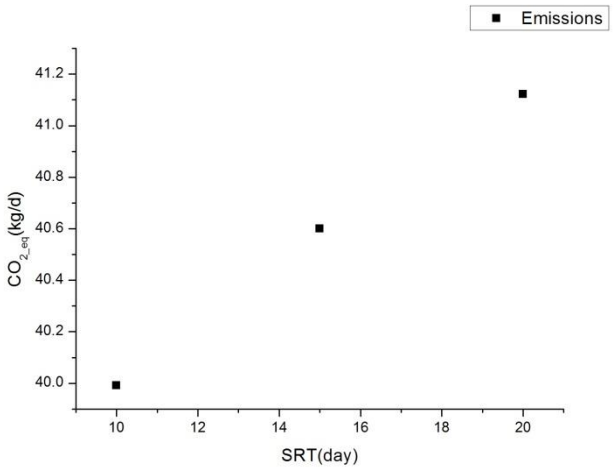

Figure 39. Greenhouse gas emissions in relation to different SRTs.

Concerning TMP, it gradually increases, building up irreversible fouling despite the cleaning protocols followed. Moreover, as shown in Figure 40, the maintenance protocol managed to reduce fouling more drastically during the beginning of the monitoring phase, but gradually lost its effectiveness. However, since additives were included in the maintenance protocol, fouling rate reduced and therefore, the rate within which TMP increased slowed down. It has to be noted that before the entrance of additives in the system, a recovery cleaning was performed, the effect of which is not visible in the graph, due to the fact that membranes were regularly maintained.

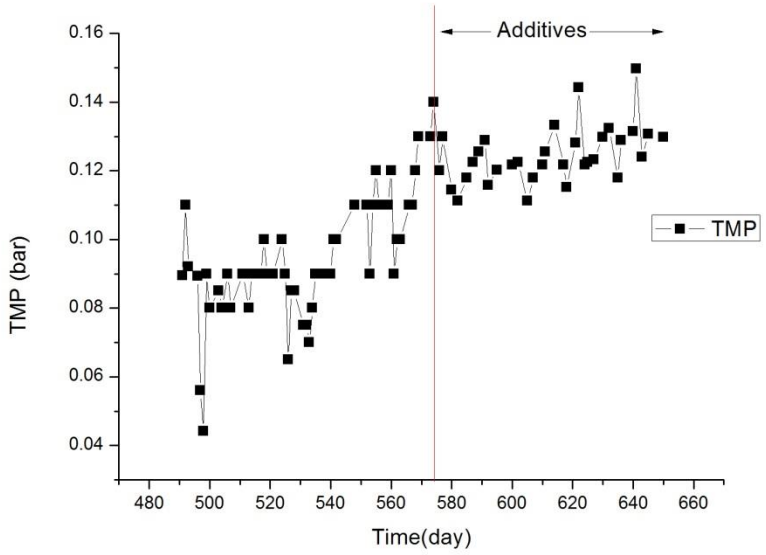

Figure 40. Transmembrane pressure of the system before and after additives.

As regards membrane permeability, it presented –as expected- the same behavior as TMP. More specifically, permeability decreases overtime and when the system was augmented additives the fouling rate decreased. In order to witness and better understand the effect of additives, a linear model was fitted for both the period with (Figure 41) and without additives (Figure 42). Comparison of the two lines reveals that the rate of fouling and therefore permeability deterioration decreases with the additives. More specifically, the slope of the line without additives is a1 = -0.7, while when additives existed in the system the slope is a2 = -0.59. This change in the slope highlights the action of additives. However, this change in the fouling rate is not surprising enough to adopt addition of chemicals in the MBR tank. The maintenance protocol is sufficient.

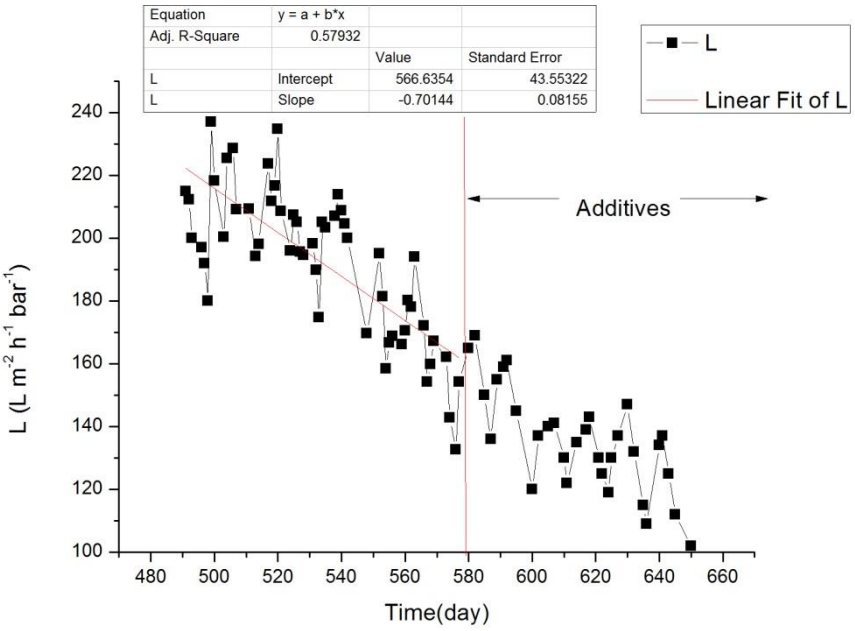

Figure 41. Membrane permeability before and after additives, with a linear fit for the phase without additives.

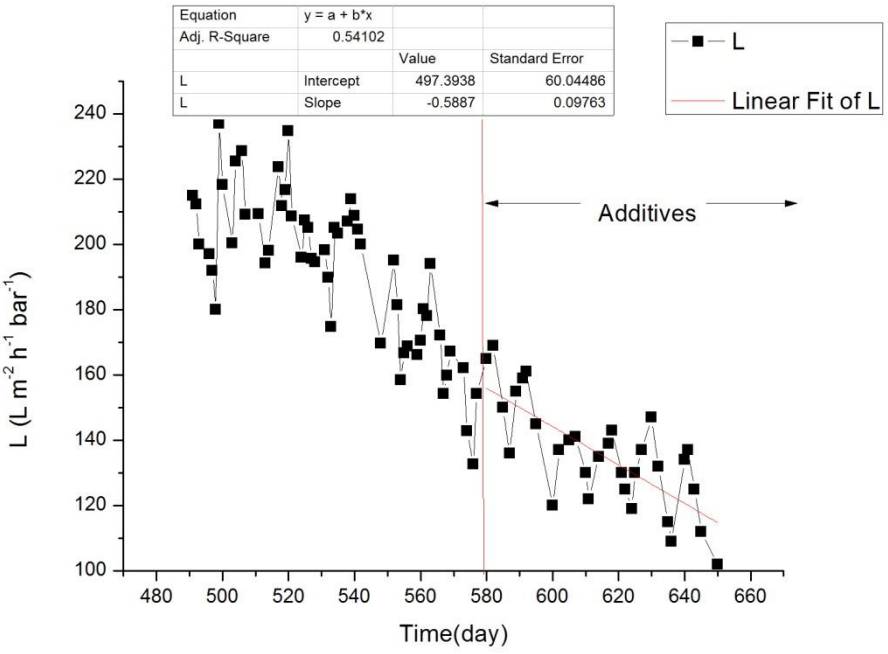

Figure 42. Membrane permeability before and after additives, with a linear fit for the phase with additives.

1.1.10 Conclusions

The results of this project lead to the conclusion that the installed MBR-RO pilot unit can produce water of excellent quality and be in line with the standards that are specified in the Greek National legislation regarding wastewater reuse for unrestricted irrigation and urban reuse. The system presented very satisfactory operational stability and high performance. The elimination of organic carbon and pathogenic content was complete. The filtration process managed reduction of pathogens without the addition of chemicals, thus avoiding the production of secondary pollutants. TMP remained steady at low values, proving that the combination of backflushing with maintenance cleaning is very effective. The use of additives reduced membrane fouling –as expected- but the reduction was not radical enough to justify the entrance of additives into the maintenance protocol. Concerning the optimal SRT, presented graphs supported the SRT under which the unit was designed, namely 20 days. Additional, the experimental results support the conclusion that the application of sewer mining practice through the implementation of an on-site compact treatment system consisting of a *pre-treatment unit* followed by a *membrane bioreactor* and a *UV disinfection unit* can reliably meet all the national and international criteria set for all types of non-potable wastewater reuse at a rather moderate cost. Such a dual membrane scheme in the context of a sewer mining application has proven to be a viable solution for water reuse in combination with fresh water saving in highly urbanized, space-limited environments. Considering also the fact that in the future European regulations are certainly going to adapt by adding more priority pollutants in the list of monitored compounds in combination with the gradual tightening of the Environmental Quality Standards highlights the importance of technologies, such as the MBR-RO one, that can meet those criteria. Nevertheless, the application of the integrated MBR-RO process is financially justified only in the case of saline wastewater.

1.2 Temperature sensors network for studying urban heat island effect

1.2.1 Introduction

Human societies are based on natural ecosystems not only for securing essential supplies such as food, water, materials, and energy, but also for amusement and recreation. This wide range of benefits is collectively described with the term “ecosystem services” (Daily et al., 1997). A major component of particular importance to arid climates provided by the ecosystem services approach is the mitigation of heat island effects due to irrigation of urban green areas.

An urban heat island (UHI) is an urban area or metropolitan area that is significantly warmer than its surrounding rural areas due to human activities. In the majority of the cities, this difference is more pronounced at night. Seasonally, UHI shows up both in summer and winter. The phenomenon was first investigated and described by Luke Howard (1818).

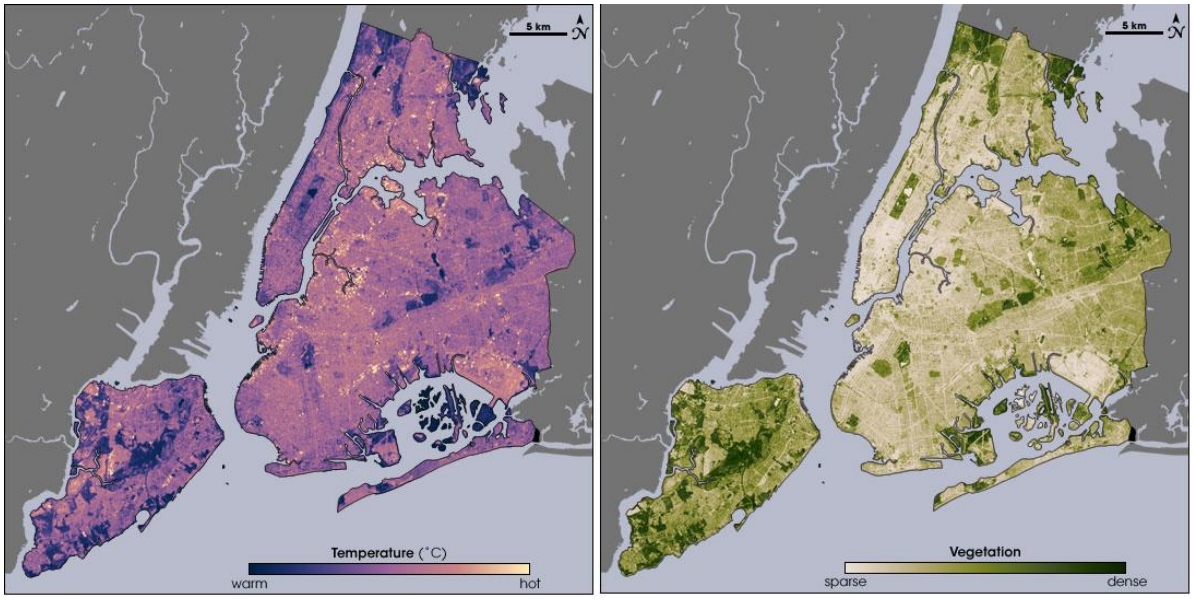

Figure 43. Spatial temperature variation (left) and vegetation density (right) maps of New York (Wikipedia, 2017).

There are several causes of an urban heat island (UHI):

- Decrease of the reflection coefficient. Roads and buildings have basically dark surfaces, which absorb significantly more solar radiation. This causes urban areas to heat more than suburban and rural areas during the day (Solecki et al, 2004).
- Thermal properties of surface material. Materials commonly used in urban areas for pavement and roofs, such as concrete and asphalt, have significantly different thermal bulk properties (including heat capacity and thermal conductivity) and surface radiative properties (emissivity) than the surrounding rural areas. This causes a change in the energy budget of the urban area, often leading to higher temperatures than surrounding rural areas (Oke, 1982).
- Reduced evapotranspiration. Another major reason is the lack of evapotranspiration through lack of vegetation. This translates into reduction of the latent heat (Rozos et al., 2017) and an increase in sensible heat (Figure 43).
- Urban canyon effect. Other causes of a UHI are due to geometric effects. The tall buildings within many urban areas provide multiple surfaces for the reflection and absorption of sunlight, increasing the efficiency with which urban areas are heated. This is called the "urban canyon effect". Another effect of buildings is the blocking of wind, which also inhibits cooling by convection and prevents pollution from dissipating (Nunez and Oke, 1977).
- Increased heat production. Waste heat from automobiles, air conditioning, industry, and other sources also contributes to the UHI.

Besides the radical solution of urban redevelopment, a more feasible solution is to increase the amount of well-watered vegetation. This includes:

- Green roofs: Green roofs (Figure 44) are another method of decreasing the urban heat island effect. Green roofery is the practice of having vegetation on a roof; such as having trees or a garden. The plants that are on the roof increase the albedo and decrease the urban heat island effect (Zinzi and Agnoli, 2012).
- Planting trees in cities: Planting trees around the city can be another way of increasing albedo and decreasing the urban heat island effect. Trees absorb carbon dioxide and provide shade. It is recommended to plant deciduous trees because they can provide many benefits such as more shade in the summer and not blocking warmth of winter (Rosenfield et al., 2014).
- Green parking lots: Green parking lots use surfaces other than asphalt and vegetation to limit the impact urban heat island effect.

Green roofs have been proven to contribute in the reduction of the energy required for the cooling of a building. According to Zinzi and Agnoli (2012) "*green roofs performances strongly depend on the water content of the systems with the adopted model. A well wet green roof has good cooling performance, but relaying on the rainfall does not ensure effective energy performances during the dry Mediterranean hot season, especially in the centre and the south east of the basin. Green roofs improve the heating performances as well, when compared with the conventional roofs*". Furthermore they have concluded that "*wet green roof is the best performing solution, thanks to a cooling demand similar to the cool roof and a heating demand slightly higher than the conventional roof. This configuration leads to 45% total energy savings. Actual rainfall and dry green performances practically give the same performance with 13% energy savings respect to standard, with a 10% reduction of the cooling demand.*" In other words, and according to Sinzi and Agnoli (2012), only the irrigated green areas contribute significantly to the reduction of the UHI effect.

Figure 44. Example of green roof.

Alexandri and Jones (2006) have concluded that there is an important potential of lowering urban temperatures when the building envelope is covered with vegetation. Air temperature decreases at roof level can reach up to 26.0°C maximum and 12.8°C day-time average (Riyadh), while inside the canyon decreases reach up to 11.3°C maximum and 9.1°C daytime average, again for hot and arid Riyadh (Figure 45).

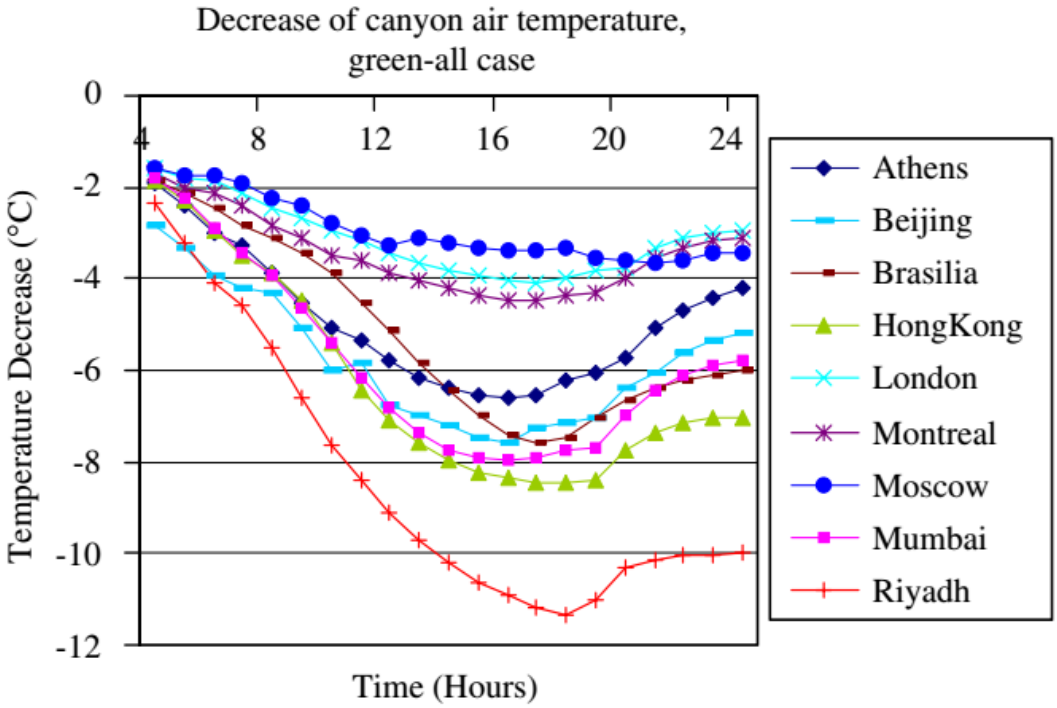

Figure 45. Air canyon temperature decrease when both roofs and walls are covered with vegetation.

The previous findings were the motivation to deploy a network of temperature sensors to study the potential benefits of irrigating with treated water a green area in KEREFYT, the research centre of Athens Water Supply Company. The case study area employs a sewer mining unit (Makropoulos et al., 2017), from which the treated water is used for irrigating a green area of 50 m^2 (Figure 46).

Figure 46. Location of meteorological sensors and irrigated area at EYDAP's Center for Research and Applications of Sanitary Technology (KEREFYT).

1.2.2 Materials and methods

The installation of the automatic meteorological metering system at EYDAP's Center for Research and Applications of Sanitary Technology (KEREFYT) includes a master measuring station and 2 satellite ambient temperature sensors. The parts of the system are:

- The master station at the location: (lat, long) = (38.07820, 23.77987). It consists of a mast on the roof of the 2-storey building of KEREFYT, a watertight box mounted on the mast containing the logger and other electronic equipment, and the A.3, A.4 and A.5 sensors. This station is powered by electricity from mains 220V / 50Hz.
- Remote ambient temperature sensors (A.1 and A.2) at locations: (38.07811, 23.77905) and (38.077954, 23.779458) respectively.
- The data logger, which processes and stores the values of the various measurements.
- Communication and data acquisition software, installed on the system computer inside the building.

Note: Coordinates are given in a geographic coordinate system with id EPSG:4326.

On the roof of the two-story building is installed the 1.5 m mast made of corrosion-resistant material on which the meteorological sensors are attached. The protective case containing the data logger and other electronic systems that need protection (e.g. battery, charger, etc.) are also mounted on the mast.

The satellite temperature sensors (A.1 & A.2) are placed on poles of length 0.80 - 1 m. The wiring of the two sensors to the data logger is on the ground and the cables are shielded by a spiral protective hose. The length of the wiring is less than 120 m and 90 m for sensors A.1 and A.2 respectively.

A.1 AMBIENT TEMPERATURE SENSOR

The ambient temperature should be measured with a sensor protected from direct sun exposure (ventilated protective cage). For this reason, the cage consists of multiple layers of thermoplastic material that allow the free circulation of air while protecting against rain and exposure to solar radiation.

This sensor measures the temperature over the irrigated area:

- It provides measurements over the -40 ° C to +60 ° C temperature range.
- It has accuracy of not worse than ± 0.4 ° C.
- It is suitable of transferring the signal to at least 120 meters.
- It is installed on a pole 0.8 m - 1 m above ground.

A.2 AMBIENT TEMPERATURE SENSOR

This sensor measures the temperature over an area with natural vegetation. The specifications are similar to A.1.

A.3 COMBINED TEMPERATURE-RELATIVE HUMIDITY SENSOR

This multi-sensor is place on the roof of the building. This sensor is placed in a naturally ventilated protective cage consisting of multiple layers of thermoplastic material allowing free air circulation while protecting against rain and exposure to solar radiation. The sensor is accompanied by a suitable bracket for supporting it.

The temperature sensor has:

- measuring range: -40 ° C to +60 ° C
- accuracy @ 23 ° C: ± 0.1 ° K

The relative humidity sensor has:

- measuring range: 0-100% RH.
- minimum cable length: 3 meters.
- accuracy: ± 1%.

A.4 WIND SPEED SENSOR

This sensor is placed on the roof. The specifications of the wind speed sensor are:

- measuring range: 0 to 75 m/s, ± 0.1 m/s
- sensitivity threshold: 0.80 m/s.
- distance constant: 3.0 m.
- operating temperature: -55 ° C to +60 ° C.
- operating relative humidity: 0-100% RH.
- external power supply not required
- made of non-oxidized materials.

A.5 RAINFALL GAUGE

This sensor is placed on the roof. The rainfall gauge is using the technology of tipping bucket. The gauge has:

- sensitivity: 0.2 mm
- water harvesting area: 200 cm^2
- capacity: 120 mm/h
- materials resistant to UV radiation and ice

Figure 47. Temperature sensor A1 on the irrigated area.

Figure 48. Temperature sensor A2 on the area with natural vegetation.

Figure 49. Multi-sensor on KEREFYT building roof.

1.2.3 Case study & Results

The sensors described above were installed in KEREFYT on 23rd September 2016. During the 14 months operation of this network of sensors (at the time of this document writing) it has been obtained time series with a time step of 10 minutes for: temperature at the irrigated area, temperature at the area of natural vegetation, temperature at the roof of the building, precipitation at the roof of the building, relative humidity at the roof of the building and wind speed at the roof of the building. These time series are shown in the following figures.

The following figure displays the fluctuation of the temperature at the roof of the KEREYF building (Figure 49). The daily fluctuation appears to be close to 12 °C. The maximum temperature on the roof during the period of the experiment was 42.3 °C recorded on the 1st July of 2017 and the minimum was -3.1 recorded on 9th of January of 2017.

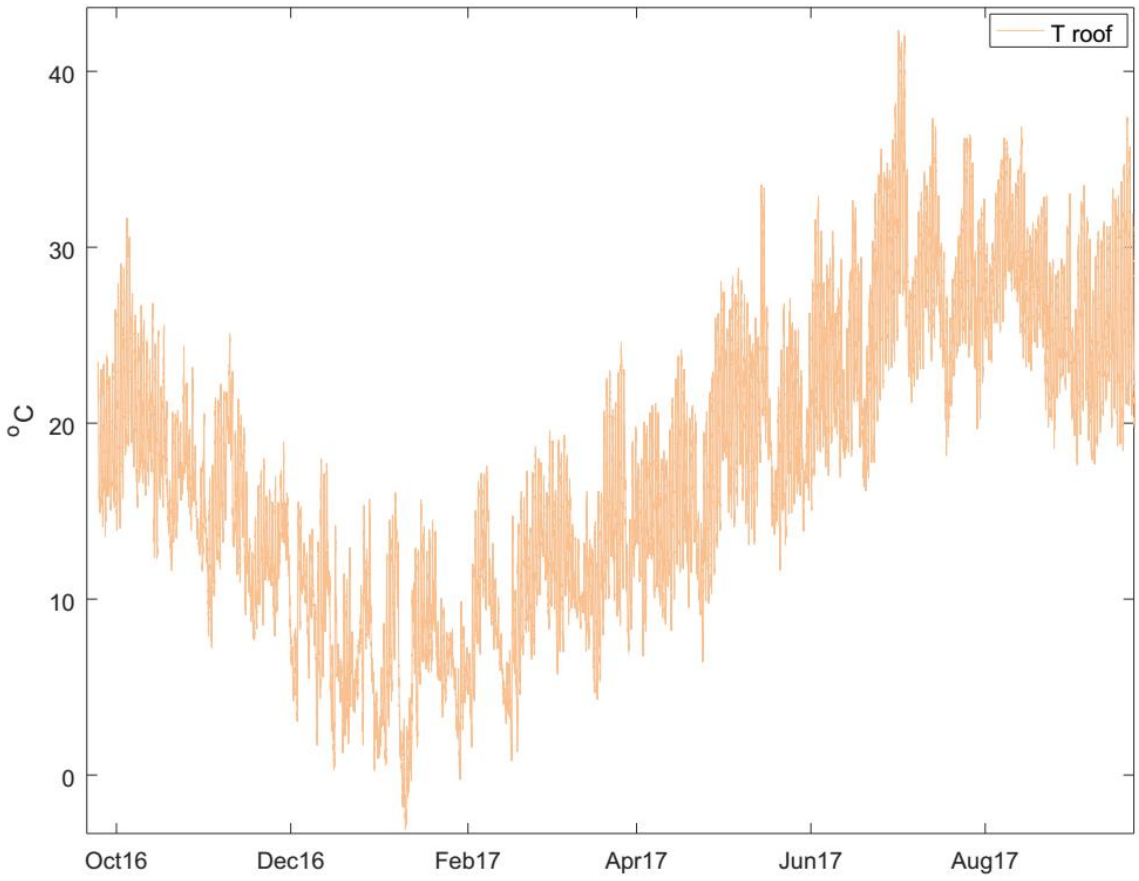

Figure 50. Temperature fluctuation at the roof of the KEREFYT building.

The following figures display the relative humidity and the wind speed (m/s) measured at the roof of the KEREFYT building. According to Figure 51 the relative humidity tends to be very high during the cold season whereas it fluctuates around 40% during summer. According to Figure 52 the area is not characterized by strong winds. The wind speed usually does not exceed the 5 m/s, whereas the strong winds at this location are around 10 m/s. The maximum value recorded was 22 m/s on 20th of January 2017 at 13:30. It is not clear if this is a measurement error or an extreme event.

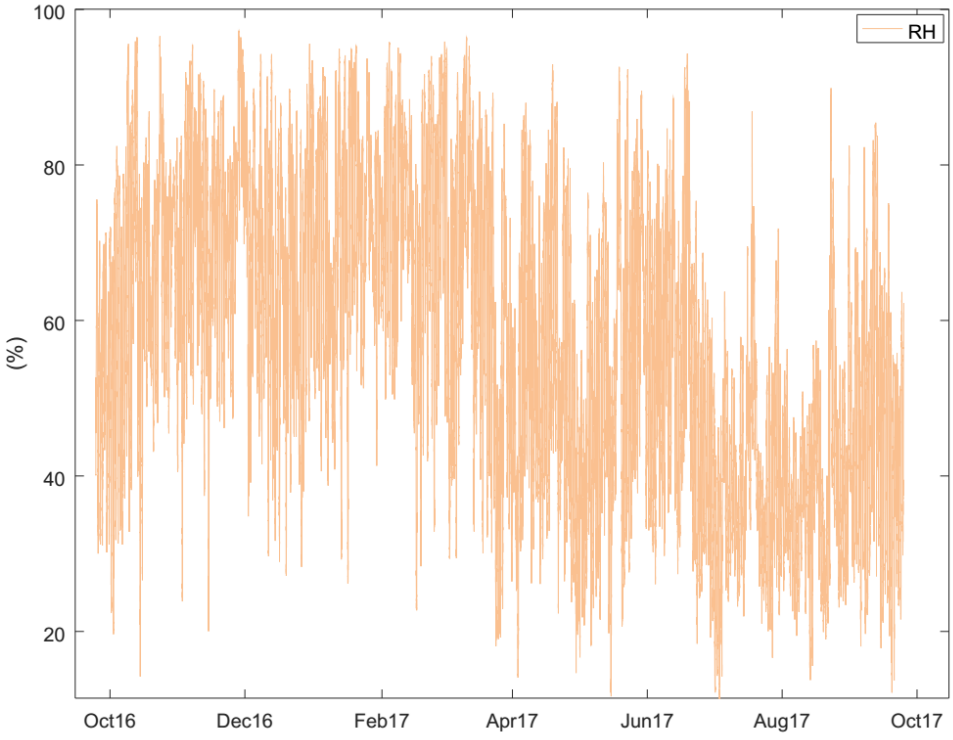

Figure 51. Relative humidity at the roof of the KEREFYT building.

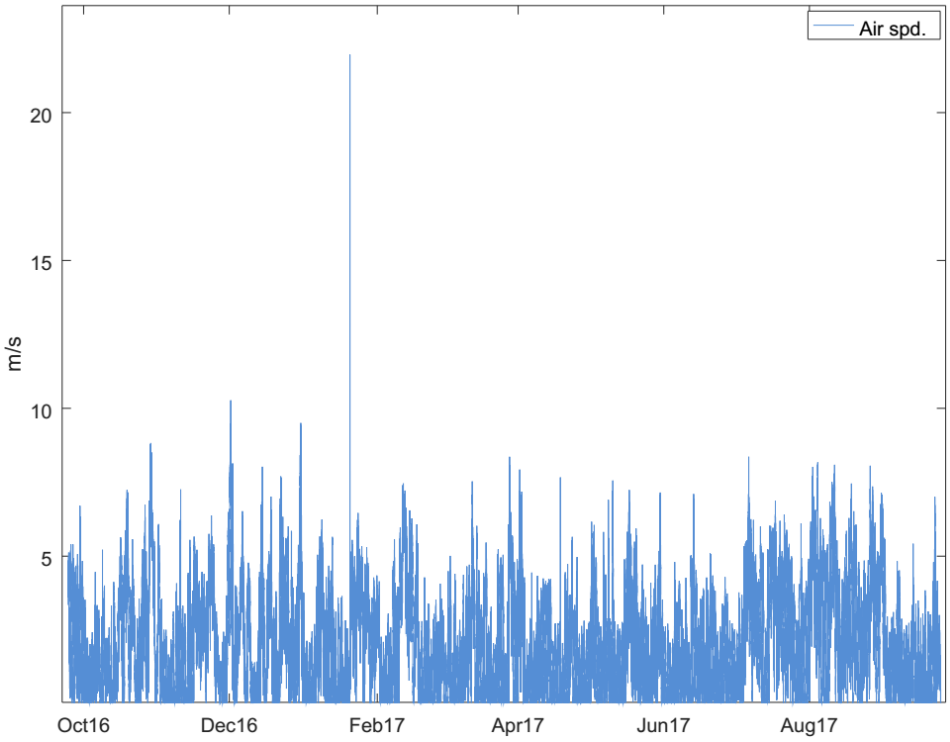

Figure 52. Wind speed (m/s) at the roof of the KEREFYT building.

The following figure displays the fluctuation of the temperatures at the KEREFYT building roof and at the irrigated area. The two time-series exhibit similar maximums, whereas the irrigated area exhibits lower daily minimums and sudden temporary temperature drops, which coincide with the irrigation schedule. The irrigated green area has also lower temperatures during the night.

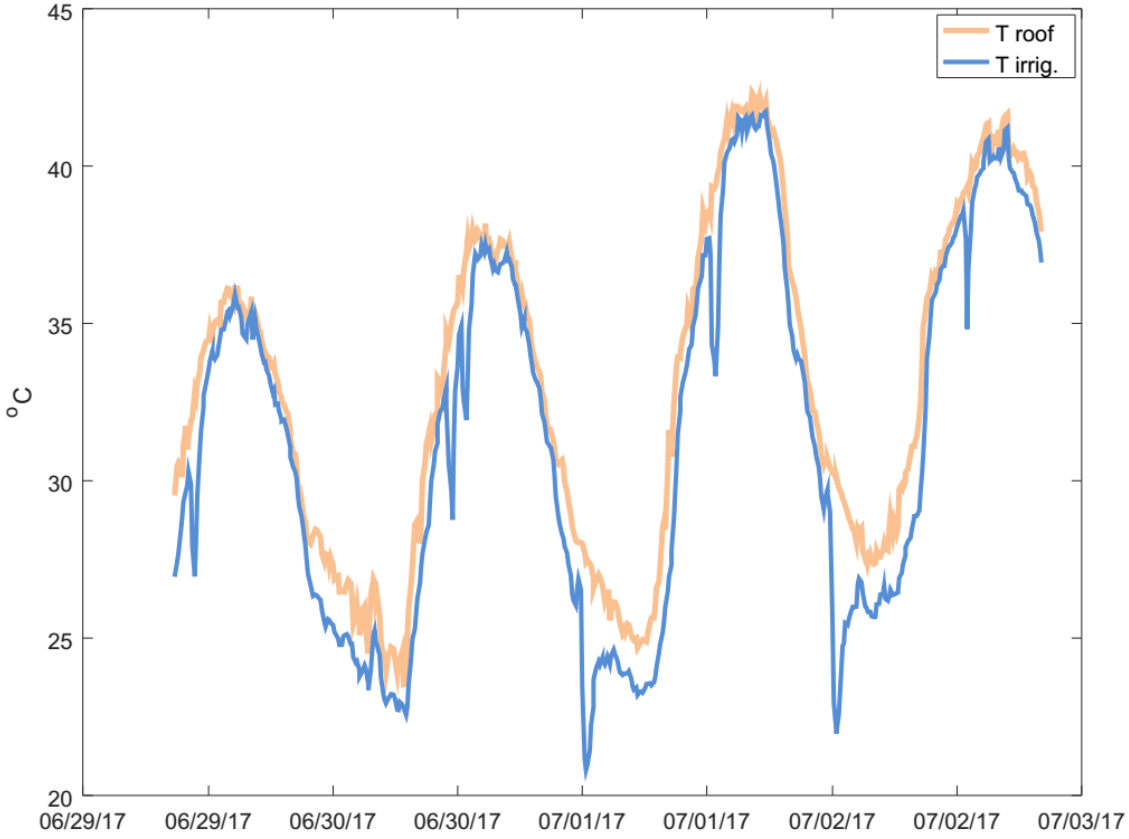

Figure 53. Comparison of roof temperature against temperature at the irrigated area.

The following figure displays the fluctuation of the temperatures at the KEREFYT roof and at the naturally-vegetated area. The naturally-vegetated area exhibits higher temperatures during day and lower temperatures during night.

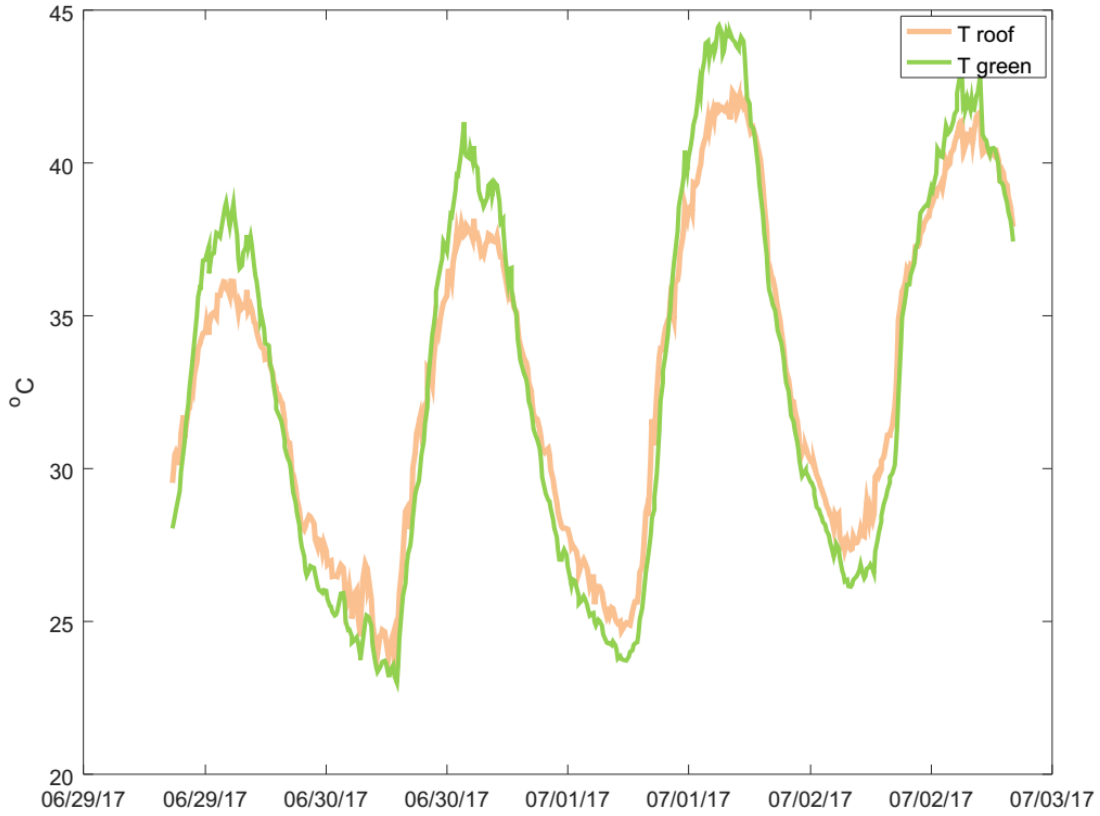

Figure 54. Comparison of roof temperature against temperature of naturally-vegetated area.

1.2.4 Conclusions

In this experiment, the ambient temperature was measured at three locations of KEREFYT, the research centre of Athens Water Supply Company. These locations are spread over an area of 1 hectare. The objective was to investigate the UHI effect and the influence of natural and irrigated green areas on it. For this reason, the first sensor was placed over a green irrigated area, the second at a naturally-vegetated area and the third on the roof of a building. The sensors are measuring the temperature every 10 minutes. After more than 1 year of measurements, the initial conclusions are the following.

The temperature of the irrigated green area was systematically lower than the temperature of the other two locations regardless the time of the day and the month of the year. More specifically, out of the 52618 records, only 1482 have temperatures of the irrigated area greater than the temperatures of the roof. Similarly, only 4285 records have temperatures of the irrigated area greater than the temperatures of the naturally-vegetated area. The annual average temperature difference between irrigated area and roof is -0.8 °C, and between irrigated area and naturally-vegetated area is -0.5 °C. It should be noted that during the hot period, the maximum temperature drop that was observed on the irrigated area during irrigation was close to 7 °C (see Figure 53). This is very close to the value estimated by Rozos et al. (2017), who coupled an urban water cycle model with a heat transfer model to simulate the energy fluxes of this area.

At any time of the year, the temperature of the naturally-vegetated area is higher than the temperature of any other area (including roof) during daytime. However, during night, the temperature of the vegetated area is lower than that of roof. On average and over the whole year, the temperature of the naturally-vegetated area is 0.2 °C lower than the temperature of the roof. This behaviour has been reported by many scientists. For example, Runnalls and Oke (2000) have described a similar pattern of diurnal evolution of temperatures related to the urban heat island during calm and clear conditions (see Figure 55).

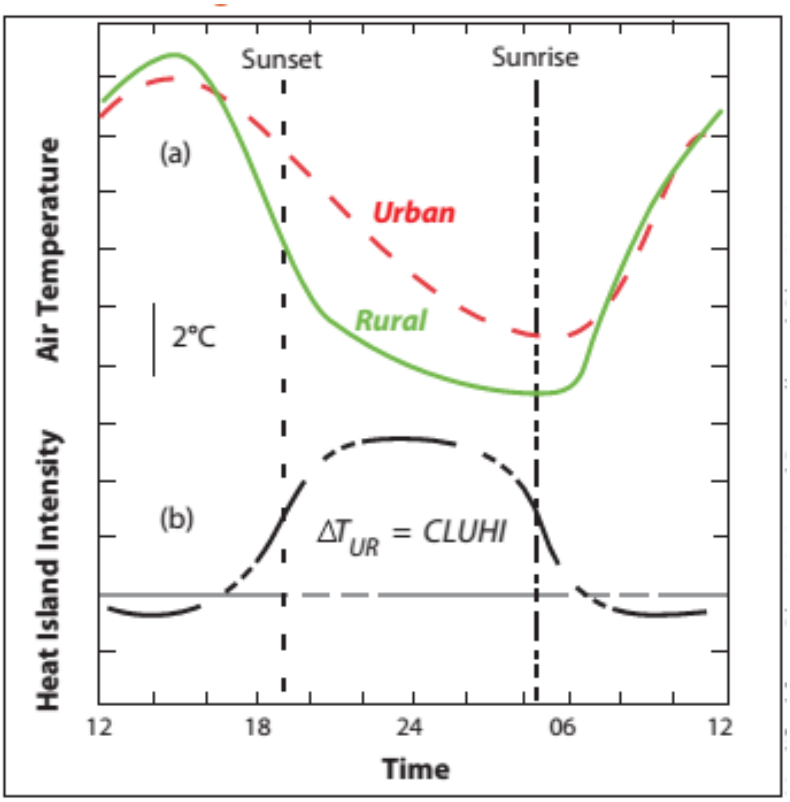

Figure 55. Comparison of roof temperature against temperature at the irrigated area.

Future work that could be done based on the findings of this experiment could be to reschedule the irrigations of the green area to take place during the most hot period of the day, and for longer periods (reducing the flows on the same time) to maximize the temperature drop. This is expected to both intensify and prolong the beneficial effects of the irrigated green areas on the UHI. Finally, regarding the naturally-vegetated area, another location could be selected for the installation of the sensor to investigate to what extend the diurnal pattern observed in Figure 55 is location depended so other parameters should be also taken into account and further studied.

2 Guidelines and recommendations for transfer to other water scarcity sites

2.1 Upscaling sewer mining at a city level

2.1.1 Introduction

Sewer mining is a water recycling technique which is based on extracting wastewater from local sewers for reuse applications (after treatment). Typical uses of the recycled water are toilet flushing, laundry uses, cooling process and irrigation (Hadzihalilovic, 2009; Marleni et al., 2012). According to Makropoulos and Butler (2010) it can be classified as a Decentralized option because of being applicable at a development level (for example, up to 5,000 households). This is also highlighted in Marleni et al., (2012) where it is argued that the this practice is not intended for individual use (indoor appliance) rather than implemented in collective/cluster scale developments. Furthermore, the latter authors remark that these systems are not managed by central water utilities (or governmental organization) rather than by private establishments under some license agreements.

A typical sewer mining scheme is consisted of a connection to the wastewater system, a network of pipes for transporting wastewater to treatment site, a compact wastewater treatment plant (the actual sewer mining unit), and a network of pipes for distributing recycled water. It can also include a discharge connection to return approved residuals and sludge back to centralized wastewater system. The residuals are allowed to be returned to the network as long as they fulfill certain regulations regarding their composition. According to Sydney Water (Sydney Water, 2008), the residual discharge of sewer mining is more likely to contain grit, more concentrated wastewater (in terms of organic matter) and some additives from the treatment such as iron, aluminum, sulphate, etc.

Current projects of sewer mining are installed until now mainly to irrigate parks and sports fields. Most of them are operating in Australia where the climate is dry and water should be treated carefully. Some characteristic examples of wastewater reuse are: Olympic Park, Pennant Hills Golf Course, Beverley Park Golf Course, Mascot Airport in Sydney, Kogarah Council, Southwell Park in Canberra, Rocks Riverside Park in Brisbane or Council House 2 Office Building in Melbourne (Sydney Olympic Park Authority, 2006; Sydney Water, 2009). It is worth highlighting that in all the aforementioned cases the wastewater is reused for non-drinking uses. For instance, the Sydney Olympic park was the first large scale urban recycling scheme. It is able to supply almost 50% of water demand of the park. While Pennant Hills Golf Club's which sewer mining treatment process is able to produce 100 million liters of recycled water each year and it has cut its potable water use by 92%. Kogarah Council became the first council in Sydney to pilot sewer mining. Up to 125 million liters of water are produced each year to irrigate parks, playing fields and the Beverley Park Golf Course.

Typical steps of a sewer mining treatment plant

The extent of the treatment process is determined by the requirements of the water quality of the end-use. It is important to select the treatment level appropriate to provide the quality required for the purpose. The typical treatment steps of a sewer mining unit are, preliminary, primary, secondary, tertiary and (in some rare cases) advanced treatment. Although, these steps may be modified in order to meet the quality required by the end-use. A brief description of each step is given below.

Preliminary treatment: Remove large components.

Primary treatment: Aims to remove some suspended solids and organic matter. This step can be followed be an advanced primary treatment with chemicals in order enhance the results.

Secondary treatment: This step targets in removing a large portion of the remaining suspended solids as well as organic matter. Furthermore, at this step a disinfection process is employed (with UV exposure or filtration technologies). Finally, in some cases prior tertiary treatment, a nutrient removal procedure is applied.

Tertiary treatment: This step results in removal of suspended solids, further disinfection of the treated product, as well as nutrient removal.

Advanced treatment: In some cases, where the quality requirements of the end-use are high, an additional step is employed in order to remove dissolved and suspended materials.

Sewer mining drivers

The use of decentralized recycling technologies, particularly sewer mining (SM) schemes, provides a range of advantages which can have strong impact on communities and environment (CRC Construction Innovation, 2006). A summary of the advantages is given below:

- Reduction of water demand and need for further water infrastructure in urbanized areas.
- Minimal environmental impact and flexibility due to the compact size of SM unit.
- Reduced discharge from central wastewater treatment plants.
- The in-site treatment reduces the cost of transporting the water from the central treatment plant to the reuse site.
- SM is scalable and adjustable thus it is suitable for wide range of uses and purposes.
- Inexpensive operation. The literature (Mallapa, 2006) reports that the cost of SM unit may vary with conditions and capacity but bare minimum costs range from $1.00/kl (1000 liters) for a 100-1000 kl plant with a capital expenditure of $900,000 to $2.74/kl and capital expenditure of $1,000,000.
- Sewer networks can be seen as assets rather than liabilities.
- Water can be treated differently depending on end-use.

Sewer mining barriers

Despite public perception, concerns and inadequate regulatory frameworks that may consist potential barriers towards SM implementation there are engineering issues that have to be addressed. A sewer network is a system where multiple physical, biological and chemical processes take place. Prior implementing SM the dynamics of the system should be investigated in order to identify the robustness and reliability of the system (Markopoulos et al., 2017). As mentioned earlier SM involves the extraction of wastewater from the system, and in some cases the return of the redundant sludge (treatment residuals) back to the system. Both wastewater extraction and sludge return could result in altering the biochemical process that take place downstream of SM unit, thus unintentionally lead to degradation of infrastructure. Typical issues are odour and corrosion. Both of them are related with the production of hydrogen sulphide in sewer pipes.

The production mechanism, the properties, and the effects of hydrogen sulphide (which is the main cause of odour and corrosion issues) in sewer networks are extensively described in section 2.1.2. These aspects are essential to study the effects of sewer mining practices in sewer networks and should be taken into consideration when implementing such schemes. In section 2.1.3 2.1.5 2.1.4

It is unambiguous that a critical and important part of successful sewer mining projects is initial design and planning. In general, there are many considerations that should be taken into account, such as: The capacity of the centralized system, alternative options for water reuse and recycling, alternative uses for the recycled water, sewer network dynamics, social, health and environmental impacts, as well as, financial issues such as capital, operating, and maintenance cost. All the above should be incorporated in a holistic risk-based approach in order to safely infer about the performance of the system regarding water quantity and quality requirements.

2.1.2 Properties, production and effects of hydrogen sulphide

Urban sewage networks usually contain organic and inorganic components. The organic compounds are imposed in microbial transformations (in the sewer network), where some of the organic matter is removed during transportation (Nielsen et al., 1992). For this reason, the sewer network must be regarded as an integral part of the wastewater treatment system.

Dissolved oxygen, ammonium, sulphate and organic compounds are natural components in sewage, while nitrate is usually not present in significant concentrations in domestic sewage (Bentzen et al., 1995). Traditionally, the organic matter of wastewater is characterized by total COD and BOD.

According to Koutsoyiannis (2011), the decay of organic matter can be aerobic and anaerobic. Aerobic decay takes place when there is adequate oxygen in the wastewater. The microorganisms that exist in the wastewater oxidize the organic matter and thus carbon dioxide (CO_2), water (H_2O), nitrate (NO_3^-) and sulphate ion (SO_4^{--}) are released.

On the hand, when there is no oxygen, another category of microorganisms cause the anaerobic decay of the organic matter. The process results to simpler organic compounds and inorganic matter,

such, hydrogen sulphide (H_2S) and ammonia (NH_3). Some of these byproducts can cause unpleasant odour in the atmosphere.

Hydrogen sulphide can be found in wastewater in two main forms, as dissolved gas (un-ionized) or as ion of hydrogen sulphide (HS^-). The ratio of those forms highly depends on sewage pH (Figure 56). When pH<5 then the ratio of H_2S as dissolved gas is 99%; while when pH>9 then the ratio of HS^- is 99%. The balance between two forms is achieved when pH=7. H_2S is fairly soluble in water, and in normal sewage water temperatures (~20° C) it can be dissolved with concentration ~3850 mg/l (for 20° C). For each increase in temperature (from 20° C) the solubility decreases about 2.5%. Furthermore, other forms of sulphide exist. These forms (which are generally insoluble) are observed with the presence of ionized metals (e.g., Fe, Zn, Cu) that combine with sulfur. This part is usually small and does not exceeds 1mg/l (Koutsoyiannis, 2011). In all such combinations, as well as in H2S and HS^- sulfur is in an electronegative state. In this state it is simply called sulphide (Pomeroy, 1990).

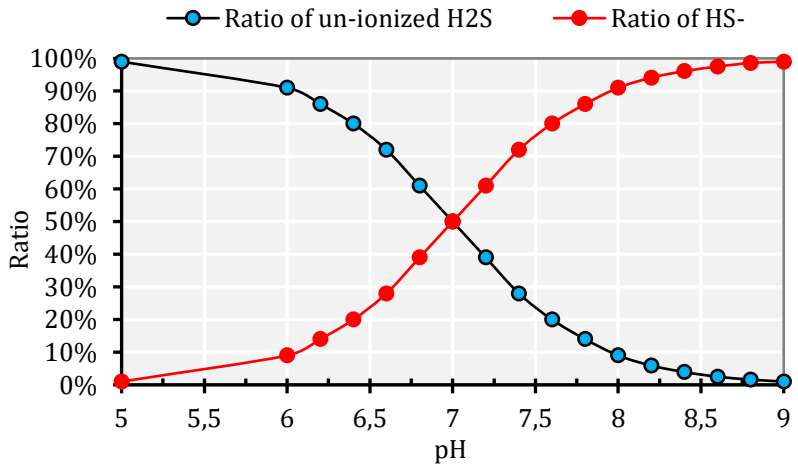

Figure 56. Ratio of H_2S, as dissolved gas (un-ionized) and as ion of hydrogen sulphide (HS^-).

In waste waters of normal pH values (6.5 to 8), sulphide may be present partly in solution as a mixture of H2S and HS -, and partly as insoluble metallic sulphides carried along as part of the suspended solids. In analyses of waste waters, a distinction is made between dissolved sulphide and insoluble sulphide. The concentrations are normally expressed in terms of the sulfur content. The amount of insoluble metallic sulphide does not ordinarily exceed 0.2 to 0.3 mg/l if the sewage is of residential origin, but the amount may be larger in sewers containing trade wastes (Pomeroy, 1990).

In general, it can be said that sulphide build-up is mostly observed in gravity sewers with large pipes, low flow conditions and insufficient re-aeration at relatively high temperatures (see section 2.1.2.4). Although, it is also observable in pressure mains, where there is absence of oxygen. Another factor that affects the sulphide build-up is industrial wastewater which usually contains high organic matter and sulphur. Despite the apparent odour (see Table 11) issue, hydrogen sulphide can cause many problems in humans and sewer networks (see section 2.1.2.1) and thus it should be taken into consideration when designing such networks.

Table 11. Odour and human health-related effects of hydrogen sulphide in the atmosphere (Hvitved-Jacobsen et al., 2013).

Odour or human effect	Concentration in
Threshold odour limit	0.0001–0.002
Unpleasant and intense smell	0.5–30
Headache; eye, nose and throat irritation	10–50
Eye and respiratory injury	50–300
Life threatening	300–500
Immediate death	>700

2.1.2.1 Problems regarding hydrogen sulphide

Most of problems that caused by hydrogen sulphide generation are related with its gas form and not the dissolved form. The main problems are briefly summarized below (Koutsoyiannis, 2011) and classified based on their origin. Problems [1], [2], [3] and [4] are related with the toxicity of H_2S (section 2.1.2.2), while [5] its corrosive effects (section 2.1.2.3):

[1] Intense unpleasant smell.
[2] Creation of toxic atmosphere which in turn contributes in formulating a dangerous environment.
[3] Problems related with the implementation of anaerobic treatment process in the main waste water treatment plant (WWTP).
[4] Furthermore, high concentrations of H_2S increase the required quantity of chlorine when such process are applied.
[5] Corrosion of pipe walls (especially those constructed from concrete, asbestos-cement and steel).

Recently, Marleni et al., (2013) presented a review on the Impact of water source management practices in residential areas on sewer networks.

2.1.2.2 Toxicity of H_2S

Hwang et al., (1995) argued that main cause of odour in sewer networks is the presence of H_2S VOCs (Volatile Organic Compounds). In addition, the odour of H_2S is familiar to people due to its presence in nature. This in turn leads to depreciation of its toxic character and thus has lead in many deaths. Furthermore, the smell of H_2S is concealed (i.e., quickly lost) as the concentration increases. Although, the hazard remains. Common examples that resulted death are, oil refineries, tanneries, viscose plants, sewer networks, and many other chemical industries, where men have occasionally been exposed to H_2S in high concentrations. Even the exposure to H_2S from swamps and from natural hot springs can be deadly. Several lives have been lost as a result of bathing in hot sulfurous spring waters in closed rooms (Pomeroy, 1990). Nowadays these issues are even closer to the center of discussion, thus resulting in reducing such accidents.

The odour formation is mostly supported by same factors (except for pipe material) that encourage the biochemical transformation processes (Hvitved-Jacobsen & Vollertsen, 2001). One of the most important factors that affects the odour attributed to H_2S is the pipe material. Pipes form plastic/PVC have slower surface recreation that leads to low H_2S absorption in the surface of the pipe - which translates in greater accumulation of H_2S - thus ultimately leads to increased odour issues (Nielsen et al., 2008). This kind of problems mostly arise in: 1) large intercepting sewers with low slope, 2) downstream of pressurized sewer mains and 3) in pipe sections with high turbulence (Vollertsen et al., 2008).

2.1.2.3 Corrosive effects of H_2S

Besides odour, another characteristic of H_2S is its corrosion-causing property. Actually, the corrosion is not caused by H_2S itself but from sulfuric acid (H_2SO_4) which is released by the (biological and chemical) oxidation of the former when it is released as gas to the atmosphere in the presence of moisture in the sewer pipe. The moisture in the pipe is attributed in the evaporation of sewage water and then in water condensation on the exposed wall of the pipe. Factors that activate the oxidation are corrosion-causing bacteria, humidity, temperature, and pipe age and material (Marleni et al., 2013). It is noted that the most common bacteria for biological oxidation are acidithiobacillus thiooxidans (Okabe et al., 2007). Apparently, older corroded concrete pipes are more vulnerable (compared to new pipes) to the corrosion-causing effects (Witherspoon et al., 2004). This is attributed to the high alkalinity of newer pipes (with pH ~11-13); where in such conditions certain bacterial cannot survive. Generally, in aged concrete sewers the pH is decreased to ~6-7. This creates favorable conditions for the bacteria; hence the pH is further decreased while simultaneously the rate of corrosion is increasing. Jensen et al., (2008) found that these bacteria are able to survive for longer than 6 months without the presence of H_2S. Marleni et al., (Marleni et al., 2013) noted the significance of this outcome for cold areas where H_2S corrosion is found to be a temporary problem rather than permanent one.

In is remarked that the concentrations of sulphide does not have to be very high in order to cause corrosion. Severe corrosion can be found in pipe sections with high turbulence, at intersections of pressurized with gravity sewers and in pumping stations (Æsøy et al., 1997). In such cases an average concentration of 0.01 mg/l of dissolved H_2S can cause extensive corrosion. In general, under normal flow conditions, sulphide concentrations between 0.1-0.5 mg/l are consider tolerable for large sewers On the other hand, for small sewer the acceptable threshold is lower and lies in the range of 0.1-0.5 mg/l (Marleni et al., 2013; Pomeroy, 1990). Hvitved-Jacobsen et al., (2002) argue that sulphide concentration above than 2 mg/l can cause severe corrosion sewage pipe.It is worth mentioning that due to the intense variability of waste water flow the peaks of sulphide concentrations can be ten times as great as these averages (Pomeroy, 1990).

The corrosion effect of H_2S has caused in numerous cases extensive damage to concrete pipes sooner than the “expiration” of the intended life. It has to be mentioned that there are cases where the pipes collapsed within 3-5 years (Pomeroy, 1990). It is clear that rehabilitation and restoration cost

of corroded sewage networks can be significantly high. Sydney et al., (1996) report that in the U.S.A, the rehabilitation of corroded pipelines are estimated to be $1.91 million/km rehabilitated pipe.

2.1.2.4 Sulphide generation and mitigation strategies

The generation of sulphide is strongly related with the sewage network design features such: materials of construction, sewer routings, pipe slopes, pipe sizes, pumping or not pumping, and other. As it was mentioned earlier, the generation of sulphide is favored in conditions without air. Such conditions arise in pressurized pipes and siphons. The quantity of H_2S increases with (Koutsoyiannis, 2011):

- Increase of retention time under conditions without aeration
- Increase of organic matter
- Increase of temperature
- In pipes with small diameters

Although H_2S can be produced in partially-filled pipes under conditions without adequate aeration. The probability and the quantity of H_2S generation increases with:

- Increase of organic matter
- Increase of temperature
- Increase of pipe wetted perimeter
- Reduce the surface width of the stream
- Reduce of flow turbulence, which results in reducing aeration rates (hence oxygen) in waste water. Turbulence is related with the slope and the flow velocity of the pipe.

The generation rate of H_2S from the flow free surface is increased when:

- Increase the concentration of H_2S in sewage
- Reduce the sewage pH
- Increase flow turbulence

2.1.2.5 Sulphide mitigation strategies

According to Koutsoyiannis (2011) the following general strategies/measures can contribute in mitigating H_2S generation:

A. For pressurized pipes and pumping stations
    - Avoid low velocities
    - Ensure adequate aeration conditions in long sewer pipes and siphons
B. For pipes with free water surface
    - During the design phase ensure proper margins for aeration and minimum flow velocities.
    - In extremely unfavorable conditions increase the pipe diameter, which results in reducing the ratio (P/B) of wetted perimeter (P) of the pipe wall to surface width (B) of the stream.

- Minimize the number of locations within the network that exhibit with high turbulence.
- Employ aeration strategies for certain pipes.

Preventing the generation of sulphide in sewerage networks can protect the pipes from sulfuric acid attacks. This is possible with a aeration and chemical based strategies (Pomeroy, 1990).

Compressed air

One way is to achieve this is to increase the dissolved oxygen of the sewage by injection of compressed air. The methods requires that the pressure main has a continuous upward slope. The air is injected at a low point, thus the generated oxygen is propagated through the pipe in the form of bubbles. Although, Pomeroy (1990) highlights that this method is not suitable for pipes with low slope because the bubbles may pass throughout the pipe without generating enough turbulence to supply dissolved oxygen as fast as the waste water requires. United States EPA provide a formula that calculates the amount of air needed (United States EPA Sulphide Control Manual 6, pages 5-8).

Refined oxygen

Another way to increase the dissolution rate is the use of refined oxygen. Again, pressure mains with low slope may still have problems (regarding sulphide generation) even if pure oxygen is injected. Pomeroy (1990) indicates that a favorable practice in order to maximize the effect of refined oxygen is to inject it on the delivery side of the pump during operational times. This way the high velocity and the maximum hydrostatic pressure of the sewage are exploited. Furthermore, the aforementioned author highlights the fact that currently there are several operational applications of this method.

On the other hand, in partly filled pipes the addition of oxygen may be unhelpful due to intense interactions between the outside atmosphere and sewer air. Hence, large amounts of oxygen will be lost.

Use of peroxide, H_2O_2 and nitrate

The use of hydrogen peroxide (H_2O_2) could be beneficial to increasing the dissolved oxygen concentration. Pomeroy (1990) argue that despite the fact that H_2O_2 does not react directly with sulphide at the concentrations found in sewage, it gradually decomposes in sewage to produce water and dissolved oxygen. Almost 50% of the weight of H_2O_2 applied is transformed to oxygen. The gains in oxygen are notable thus it is often preferred despite the high cost.

Nitrate could be an alternative solution in providing oxygen, hence satisfy the respiration rate of bacteria. This is provided via Sodium and iron salts. Pomeroy (1990) argue that this method is could be more expensive than using pure oxygen but cheaper than hydrogen peroxide which should be consider only as an emergency measure.

Chemical-based strategies

A variety of chemicals can be used in order to prevent sulphide generation or confront (and remove) sulphide concentrations already present in the network. From available chemicals the most widely used are sodium hydroxide and chlorine. The former (sodium hydroxide, i.e., caustic soda) is often used periodically in order to remove bacteria that cause sulphide generation from the slime layer. Adequate quantities of sodium hydroxide can cause a raise of pH (~12) for limited time (~30 min). An alternative to sodium hydroxide is calcium hydroxide. Pomeroy (1990) argue that the use of calcium hydroxide can cause problems with scale formation. The latter –chlorine- is the most popular substance for controlling sulphide generation. Its application is often done prior entering the treatment plant. Also it can be applied in upstream locations, in such cases there are multiple benefits, it destroys the sulphide present and simultaneously prevents further generation for ~30-60 minutes. Pomeroy (1990) argue that in in order to be effective about 50 to 150 mg per liter of sewage should be added (depending of the concentration of BOD or COD). In general, sewer networks that rely on chemicals in order to tackle the problem of sulphide face the following problems 1) a number of application stations is often required, which may be impractical 2) there is an ongoing expense of chemicals 3) continuous maintenance and monitoring.

Discussion and comments

It is clear that there are many options and tools that can be used in order to confront issues related with hydrogen sulphide. Although, it is worth highlighting that most of these strategies require engineering expertise, continuous monitoring and considering the financial cost (in some cases some measures have high capital and operating costs). Hence, proper selection of pipe material during the network design study is of paramount importance since it can prevent sulphide formation. In general, as far it concerns corrosion, it can be said that the most vulnerable pipes are those constructed by materials that have fast surface reactions; e.g., concrete and metal pipes (Marleni et al., 2013). In general, PVC/plastic pipes have slower surface reactions and thus they don't favor sulphide creation.

2.1.3 Methodology for Sewer mining placement at a city-level

Some general guidelines for the selection of the location of a sewer mining unit are provided in literature (Hadzihalilovic, 2009; Marleni et al., 2013).

[1] It has to be located near the households that will be supplied by treated water from Sewer Mining facility.
[2] It is located in a residential catchment, since the wastewater quality from residential catchment is fairly uniform quality, hence the treatment process will be relatively simple and reliable.
[3] The volume of sewage from this location is expected to increase in the future.
[4] It is located in the middle part of major sewer pipes, allowing some downstream pipes to be impacted due to the Sewer Mining facility.

Additionally, to the latter guidelines, herein we discuss the methodology developed by Tsoukalas et al., (2016; 2017) and extended by Psarrou et al. (2017) - within the context of DESSIN project - for the placement of SM units. The methodology takes into account the latter guidelines, as well as, both spatial properties and water demand characteristics of a given area of sewer mining deployment

while simultaneously accounts for the variability of sewer network dynamics in order to identify potential locations for sewer mining implementation. Specifically, it is consisted of three steps, (I) a spatial data pre-processing step during of which the spatial properties and water demand characteristics are being identified (II) a Monte-Carlo simulation (MCS) step, which involves the simulation of the sewer network in order to account for the variability of sewage discharge into the network and finally, (III) a post-processing step which comprises (III-a) the definition of appropriate metrics that quantify the output of interest and (III-b) a multi-criteria analysis of the results. A schematic description of the proposed methodology is given in Figure 57. During the first step the available spatial information (i.e., sewage network topology and assets, topography, water and land uses) is imported into the procedure in order to identify land-uses that will benefit from sewer mining (in our case green areas and parks). It involves a procedure of locating neighboring sewer network components (e.g., nodes) which are close to areas of interest. In more detail, this is done by delineating a wider area surrounding the original one (e.g., add 10 m offset to green areas) and subsequently identifying the nodes that lie into those wider areas. Finally, the paths from the identified nodes to an "*exit*" node are identified and stored. The exit node could be a WWTP or a node that links the understudy network with a broader larger network. It is worth noticing that this path is unique for each node due to the "collective nature" of sewer networks. The purpose of the second step is to propagate uncertainties related with the input parameters to the quantities of interest (e.g., BOD_5 concentration or flow of each pipe). Furthermore, the use of Monte-Carlo simulation allows the use of probabilistic functions and metrics, which in-turn provide uncertainty-aware outputs. Typical examples of uncertain parameters are the daily water consumption, daily and hourly variation coefficients of wastewater discharge and BOD_5 loading (in terms of g/cap). Alternatively, one could use a similar scenario-based approach to sample those parameters; (or in conjunction with MCS) in order to investigate the effect of certain predefined scenarios (e.g., worst, base, favorable conditions).

The third and final step involves the definition and the use of metrics i.e., utility functions or risk functions that quantify the output of interest, in our case H_2S build-up, for a chain of pipes (the paths specified in step I). We remark that BOD_5 can be directly associated with H_2S through empirically derived relationships (Lahav et al., 2006; Marleni et al., 2015). Furthermore, as a final procedure, we use multi-criteria analysis which eventually leads to derivation of a Pareto front (based on conflicting criteria – e.g., suitability of location and green area water demand), which includes all the potential locations for sewer mining.

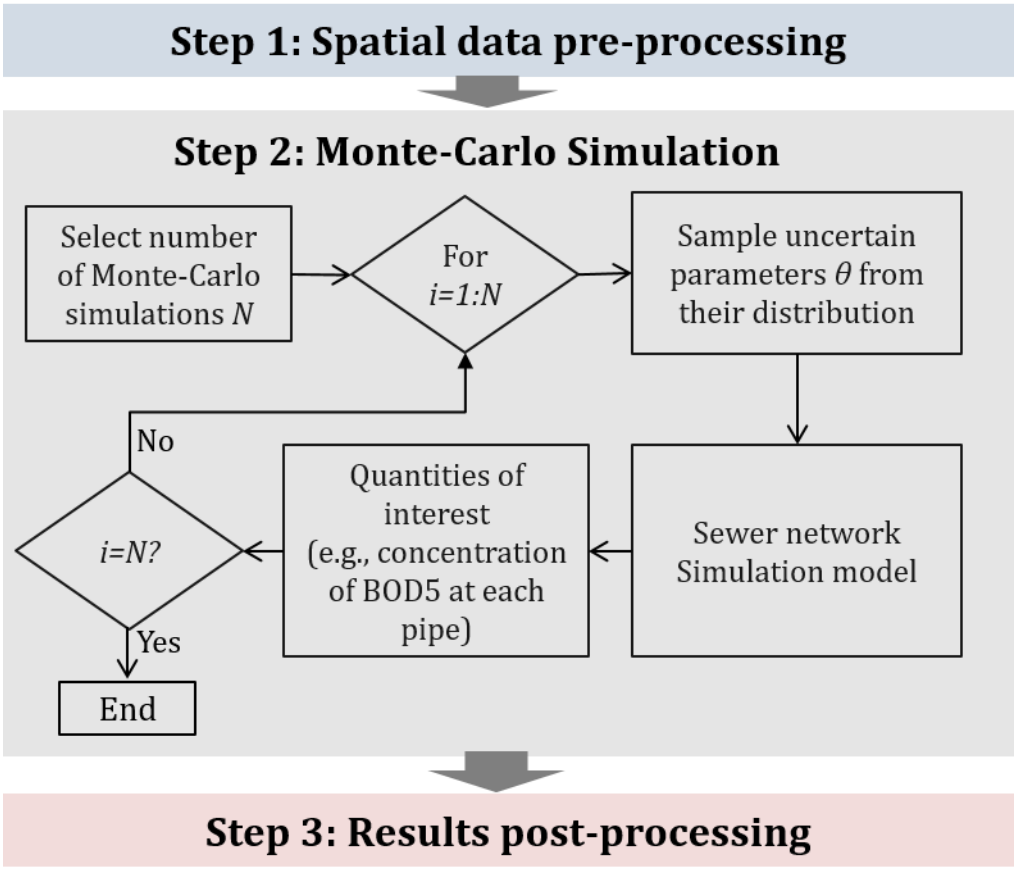

Figure 57. Overall methodological framework for the identification of potential SM locations.

The involved MCS (step II) of the proposed procedure requires the use of a simulation model in order to calculate the hydraulic outputs of interest. While any simulation model can be employed (e.g., SWMM 5.0; see also, Psarrou et al. (2017)), in this study we employed a steady state simulation model which uses the typical hydraulic equations for sewer networks as described in Koutsoyiannis, (2011). The total design discharge Q_D which is used to assess the performance of the network is calculated as the sum of sewage discharge (Q_s) and dry weather flow (Q_{DWF}). The sewage discharge can be calculated as follows:

$$Q_s = q \times E \times \lambda_L \times \lambda_S \times \lambda_1 \times \lambda_2 \,/\, 86400 \ (\mathrm{m}^3/\mathrm{s}) \quad (1)$$

Where, q is the indicative daily water consumption per capita (lpd), E is the serviced population, λ_L, is a loss coefficient of water distribution network, λ_S is a coefficient that express the percentage of water that stems to the sewage network, λ_1, is a seasonal coefficient and λ_2, is a coefficient of peak discharge. The dry weather flow can be calculated as follows:

$$Q_{DWF} = \lambda_{DWF} \times Q_s/\lambda_2 \ (\mathrm{m}^3/\mathrm{s}) \quad (2)$$

Where, λ_{DWF} is a dry weather flow coefficient (typically set to 0.2). Although, in this study we use eq. (2) in order to align with information available from previous studies, it is worth mentioning that

literature (cf., Koutsoyiannis, 2011) includes a variety of formulas for the calculation of the aforementioned quantity.

In order to assess the extent of H_2S, we decided to employ a simple qualitative indicator known as the "*Z* formula" (US EPA Sulphide Control Manual 6). The dimensionless metric *Z* was originally proposed by Bielecki & Schremmer, (1987) and Pomeroy, (1990) for a single pipe *i* in order to quantify the probability of H_2S build-up. It is expressed as follows:

$$Z_i = \frac{0.3 \times 1.07^{T-20} \times [BOD_5]_i}{J_i^{0.5} \times Q_i^{1/3}} \times \frac{P_i}{b_i} \quad (3)$$

where, *i* is the pipe index, *T* is the sewage temperature (°C), $[BOD_5]_i$ is the concentration of Biochemical Oxygen Demand of 5 days (mg/l), J_i is the pipe slope, Q_i is the discharge (m^3/s), P_i is the wetted perimeter of the pipe wall (m) and b_i the surface width (m) of the stream. It is apparent from latter equation that despite its simple form, the "*Z* formula" accounts for the hydraulic characteristics of the sewer network which, except *T* (which is usually assumed constant) all other parameters of eq. (3) are calculated using the simulation model. Furthermore, the concentration of BOD_5 loading was assumed to be invariant during the day, thus, it can be calculated by dividing the daily mass of BOD_5 with the daily sewage volume. According to Pomeroy, (1990) values of $Z_i > 7500$ indicate that there are high chances of H_2S formation which could lead to odour and corrosion problems. See also Table 12 for a wider classification.

Table 12. *Z* values and characteristic conditions *Z*, adapted from (Pomeroy, 1990).

Z Value	Possible conditions
Z < 5000	Sulphide rarely present or only in very small concentrations.
Z ~ 7500	Peak concentrations of a few tenths of a mg/l of dissolved sulphide may be reached;
Z ~ 10000	Sulphide sometimes may develop in sufficient proportion materially to increase odours,
Z ~ 15000	Odour of sewage will increase markedly at times. Rapid attack of concrete structures is
Z > 25,000	Dissolved sulphide will be present most of the time, and small concrete pipes possibly

Eq. (3) can be used for a single pipe, thus we used a modified version of index *Z* of Pomeroy for a "chain" of pipes *n*:

$$MZ_c = \sum_{i=1}^{n} a_i \times Z_i \quad (4)$$

Where, ai are weight coefficients. In this study we use weight values proportional to pipe length using the following formula, $a_i = L_i/L_{tot}$, where, L_i is the length of pipe *i*, and L_{tot} is the total length of pipes of chain (*i* = 1, ..., *n*). It is worth mentioning that literature includes a variety of metrics (Boon, 1995; Hvitved-Jacobsen et al., 2013; Lahav et al., 2006; Marleni et al., 2015), other than Pomeroys' Z, that could be used to quantify (with higher precision) the amount of H2S in terms of mg/l. Since we performed *N* model simulations (step II) we have *N* values of *MZc* for each path and for each green area, therefore we are able to calculate $Q[MZc]_x$ which represents the value of the desired

quantile *x*. For example, the 75th quantile value indicate that 75% percent of *MZc* are below $Q[MZc]_{75}$ value. Through this way we impose an additional reliability criterion for H2S build-up. Finally, for each green area, among all available paths we select the one with (optimum) minimum $Q[MZc]_x$ value. To this point we have located the nodes with minimum $Q[MZc]_x$, thus we could fuse it with information regarding the water demand in the areas of interest (green areas). We select as approximate indicator for water demand the area of the park. Similarly, the actual water demand of each area could be more accurately calculated if relevant information was available. It is worth mentioning that the use of multi-criteria analysis allows the inclusion of other metrics regarding other aspects of the network, hence, provides a powerful tool for exploring alternative options and decisions.

2.1.4 Case study & Results

The methodology is demonstrated in a sewer network designed for the city of Kalyvia Thorikou in Greece (Figure 58). The network has not been constructed yet, although it is foreseen to accommodate an area of 98 ha from which 17 ha are green areas. It is part of a larger engineering project of Saronikos municipality (service 10 - 15 thousand people) which aims at extending the existing sewage network of coastal zone. It is consisted of 1030 pipes of total length ~38 km, while their diameter varies from 0.2 m to 0.5 m. The pipe slope varies from 2‰ to 150‰, with an average slope of 35‰. The understudy area can be considered appropriate for testing the proposed methodology, since it is consisted of various network elements and has adequate number of green areas which could benefit from sewer mining practices.

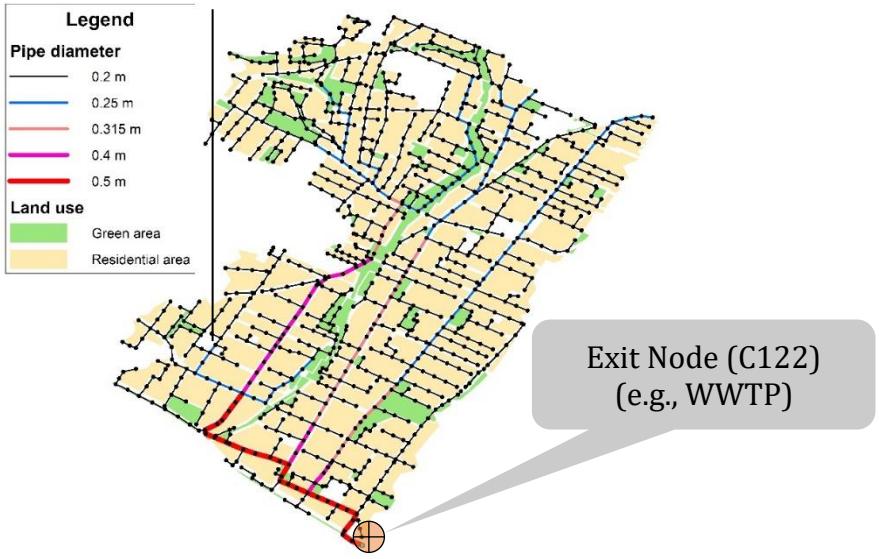

Figure 58. Case study sewer network and land uses – Kalyvia Thorikou, Greece.

The design period of the network was assumed, $T = 40$ years, as in the original study of Hydroexigiantiki, the engineering firm which conducted the study of the above network. The design population (E) is adjusted using the compound rate formula $E = E_o \times (1 + \varepsilon)^n$, where, E_o is the current population, ε is the increase rate (assumed 1.5%) and n is the extrapolation year ($n = 0, ..., T$). The value of n can be varied in order to assess the performance of the system at different time periods. In this study, q was assumed to be equal to 250 l/day, λ_L was assumed equal to 0.725 for

year 0 and 0.85 for year 40. Similarly, λ_s, was assumed equal to 0.625 for year 0 and 0.65 for year 40. The values of λ_L and λ_s for intermediate years can be calculated using linear interpolation. The value of λ_{DWF} was set equal to 0.2. Finally, we assumed λ_1 and λ_2 as uncertain parameters that follow uniform distribution; i.e., we assumed λ_1~Uniform[0.7, 1.3] *and* λ_2~ *Uniform*[0.8, 1]. As far it concerns parameter *n,* we employed three scenarios, 0, 20 and 40 years. Also, the mass of BOD_5 was varied using three scenarios 40, 50, and 65 g/(day cap). The maximum allowable number of simulation runs for the MCS step was set equal to 500. The desired quantile *x* (i.e., reliability level) for the calculation of $Q[MZ_c]_x$ was set to 75%.

Figure 59 illustrates the final result of the post-processing step III in a form of a Pareto front, using as objectives the minimization of modified *Z* index and the maximization of green area. It is notable that one could also interpret those two objectives as the simultaneously maximization of suitability and benefit from sewer mining practices respectively. The suggested procedure located three potential locations for sewer mining units' placement that optimize both criteria simultaneously, while on the other hand discarded other inferior locations. Additionally, the map depicted in Figure 60 provides a visual summary of all the green areas (green polygons) of the case study, as well as the three areas (red polygons) identified by the proposed methodology since they were suitable for SM placement. Furthermore, in order to visually illustrate the concept of optimum path it presents the selected optimum path (magenta line) for the green area with ID3. This path has the lowest *MZ* value compared to all other alternative paths of ID3.

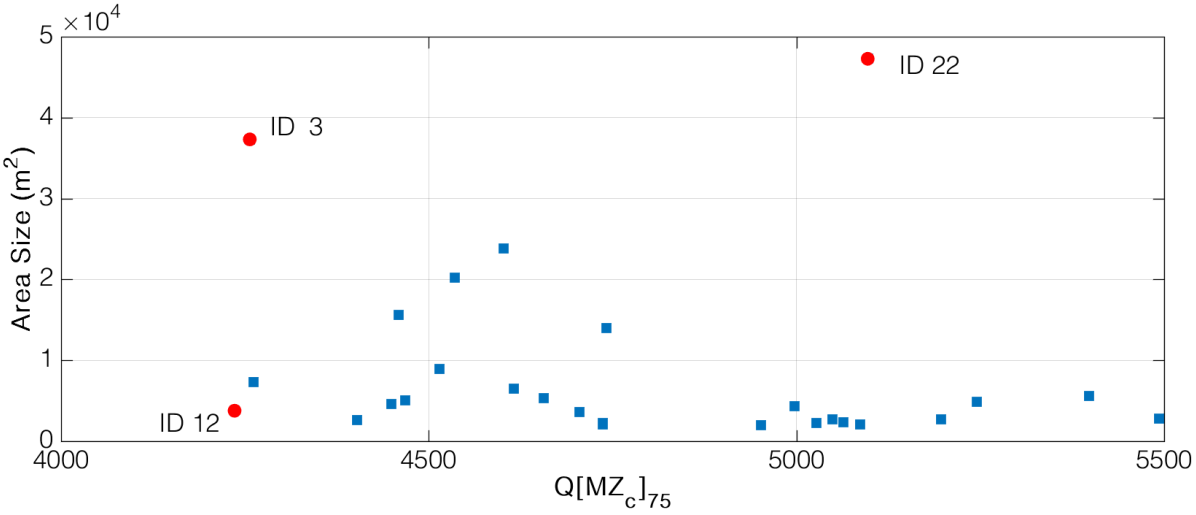

Figure 59. Derived Pareto front based on modified indicator *Z* (MZ) and green area size.

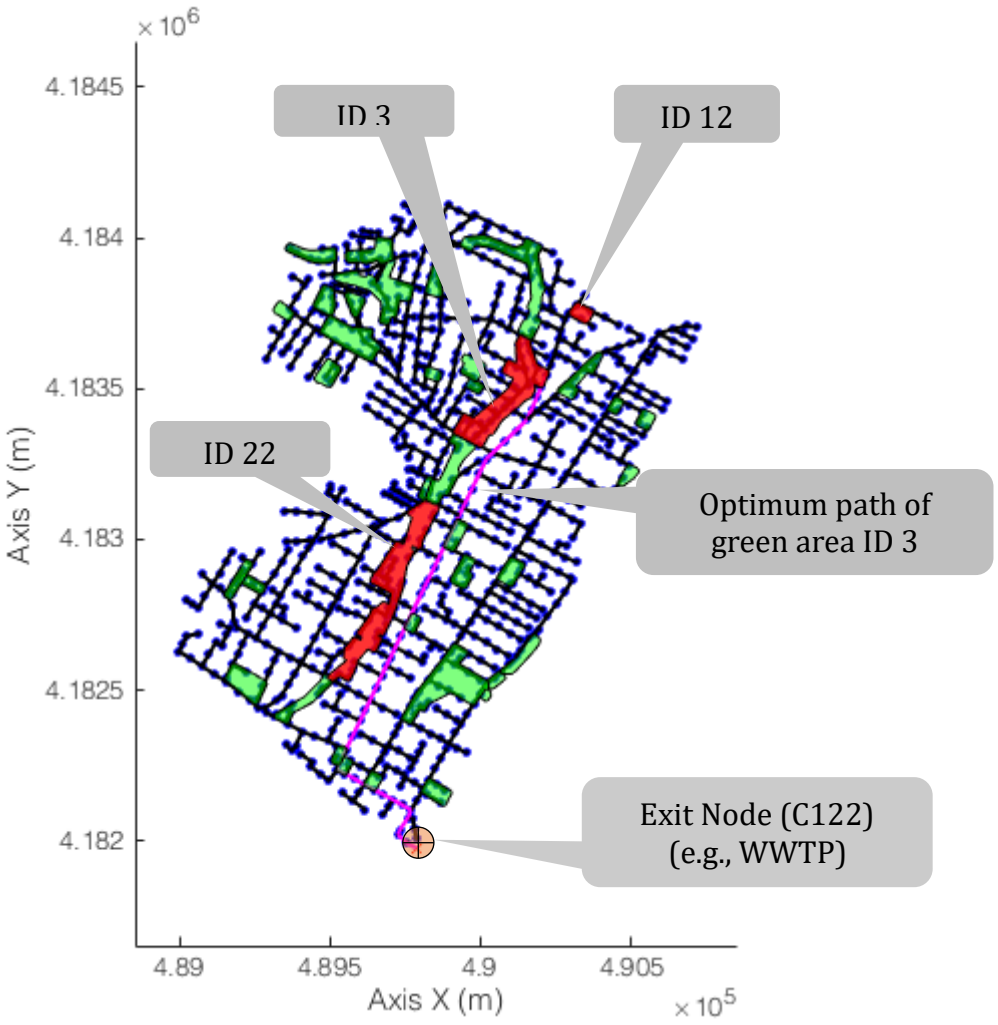

Figure 60. Proposed sewer mining locations for Kalyvia Thorikou sewer network

Figure 61 depicts the cross-section of optimum path of green area ID3 (magenta line in Figure 60). The path starts from pipe C215 which is located close to the green area ID3 and ends to C122 which is linked with the "*exit*" node of the understudy system. More specifically, the upper panel of Figure 61 shows the variability of the MZ across that path. Furthermore, the lower panel of Figure 61 shows the probability of non-exceedance the threshold values P(*Z*<7500). It can be seen that until C171 the system demonstrates high non-exceedance probabilities (~90%), i.e., high reliability. After that point the reliability decreases but it is still preserved within acceptable levels (70-80%).

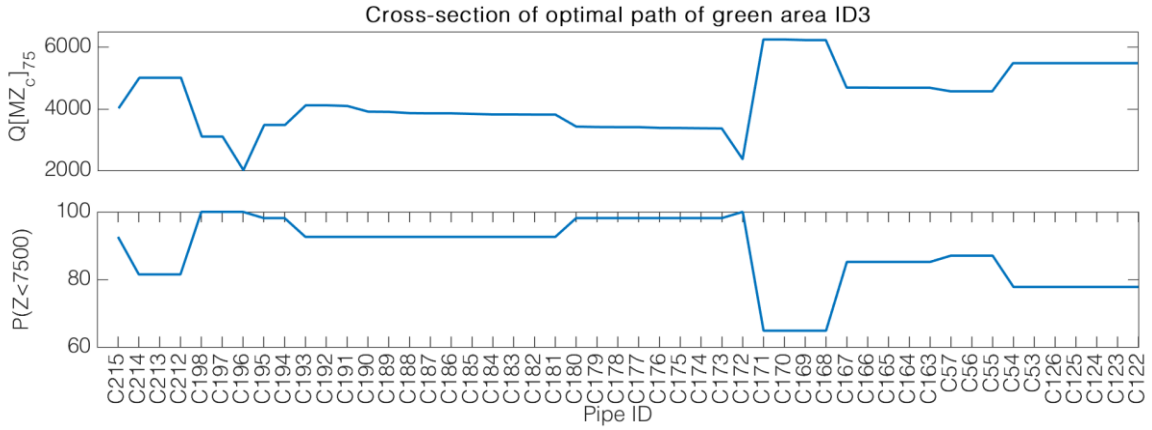

Figure 61. Cross-section of optimal path of green area ID 3. The upper panel depicts the variation of modified indicator *Z* (MZ) among longitude profile. The lower panel depicts the probability of non-exceedance of the threshold value of *Z* = 7500 among the cross-section.

2.1.5 Conclusions

In order to overcome the engineering challenges imposed by the multiple physical, biological and chemical processes that take place in a sewer network, we introduced a novel Monte-Carlo based method for the identification of potential locations for sewer mining units. The proposed risk-based approach allows to safely plan for SM deployments taking into due consideration system performance objectives regarding water quantity and quality. As such it can be used to enhance the decision-making process with useful guidelines and insights. More specifically, the proposed method has been demonstrated though a case study (Kalyvia Thorikou, Greece) where we focused on identifying optimum locations for sewer mining units subject to the generation (minimize) of hydrogen sulphide (H_2S) and water demand. The results showed that the proposed methodology was able to identify potential locations for sewer mining units' placement while simultaneously taking into consideration the spatial properties of the area as well as the variability and hydraulic characteristics of the sewer network. Ongoing work (Psarrou et al., 2017) is focused on improving the proposed framework through the integration of a dynamic simulation model, such as SWMM 5.0 into the computational procedure.

2.2 Water recycling, ecosystem services and business potential in a small-scale economy: A framework for sewer-mining implementation

2.2.1 Introduction

The economic study of the sewer-mining technology presented in the sections below, comprises part of the Demonstrate Ecosystem Services Enabling Innovation in the Water Sector (DESSIN) project, with purpose to establish a general framework for evaluating and -at a more specific level- pricing the contribution of water innovations to the value of ecosystem services. The economic analysis mainly concerns the investigation of the potential for upscaling and operating in a real business environment a wastewater reclamation pilot unit. Due to severe lack of data and experience of similar projects in real market conditions in Greece, the analysis was based on the use of the international literature as well as mathematical simulations. However, as the major target was to develop a coherent ecosystem service evaluation methodology, this obstacle was not considered preventive. Based on a combination of indicative specific-area data from Kalyvia Thorikou in the inland East Attica region (NUTS EL305 classification) and theoretical assumptions, the simulation concerns the quantification of selected assessed ecosystem services from watering a small park in the area with treated wastewater from the unit. In particular, our quantitative study estimates the value of direct and indirect expected benefits, ranging from the conservation of groundwater resources to the pricing of microclimate regulation services from the park's watering. In general, the corner stone of our methodology lies on the idea of integrated environmental-economic accounting (FAO et al. 2014). Furthermore, we examine indicative scenarios on the sewer-mining technology's diffusion potential under the assumption of learning curves and improvements that further reduce its cost. Finally, it discusses qualitatively the options on the business model for the technology's commercialization in relation to the expected new economic activities to in the area, such as tourism, urban farming and environmental education. In general, for both of our assessments -quantitative and qualitative- we followed the sequence of the main categories presented in the DESSIN Ecosystem Services Evaluation Tool (as developed in Deliverable 23.1).

2.2.2 Study description

Although no real installation of the unit took place in the selected area for simulations it was considered fit for our purposes. Kalyvia Thorikou (37°50'N 23°55'E) is located in the wider East Attica region (NUTS EL305 classification) and is a former small municipality with 14.426 permanent inhabitants (based on the 2011 recording). After administrative reforms (Kallikratis Law; 2010) it became a municipal unit of the *Saronikos Municipality* along with four (4) other independent small municipalities. The municipal unit's administration area is 70.636 km^2 at an elevation of 110 m from the (nearby) sea's surface. Economic sectors in the area concern agriculture, light industry and services (mainly banks and insurance companies). More specifically, the agricultural sector is the one we are concerned the most in our simulations as it is the one related the most to groundwater extraction, making them along with the public administration, the main beneficiaries and stakeholders in the area as they will be most affected from full-cost accounting of groundwater.

2.2.3 Issue characterization

Due to the very small size of the area, we generally do not observe an unusually intense dynamic (eg. rapid population growth or an urbanization trend) that could distort in the short-term any socio-economic or/and environmental balance. Drivers of growth in the area generally remain of low intensity and concern tourism and visitors. The number of visitors in the area has increased due to the upgrade of the transportation network in Attica as the area can also serve as an intermediate station for those travelling to the nearby sea. Although the state of environmental systems can be characterized as "good" in general, in the long-term we could fairly assume that specific environmental practices will not continue to be sustainable. In addition -as it will also be highlighted in the following sections- even if long-term environmental pressures are not considered, the area is indicative of emerging opportunities on the experimentation of new practices that deal with circular economy issues with focus on water resources. However, in short, we could define as the most significant driver the growth of family agriculture (many inhabitants cultivate crops in their own fields) via the use of groundwater resources. This trend creates a pressure towards increasing groundwater scarcity. Specifically, we could identify a need for mitigation of groundwater extraction and substitution of this practice -at least partial or full if possible- by water reclamation. Another identified driver is the increase of tourists in the area that usually seek an open public space for recreation. An ideal space for that would be a park, which would need maintenance and frequent watering. However, watering via groundwater extraction would intensify any future scarcity problem; hence water reclamation would be considered as a very reliable solution as well. In addition, the creation of a small park would also contribute to microclimate regulation in the area - both for the tourists as well as for the nearby residents.

2.2.4 Responses and beneficiaries

In our simulations we deal specifically with the above issues as pressures; on the one hand we deal with how the continuation of groundwater extraction would affect scarcity under full-cost accounting (also in order to compare this cost with the sewer-mining unit's cost) and further mitigate it through reuse and on the other hand, how could water reuse also activate other ecosystem services of profound economic value. Hence, the creation of our measures for controlling a pressure (or enhancing ecosystem services) concern the following:

1. **Groundwater scarcity assessment:** The cost of groundwater extraction (via pumping) in the Figure 62A is represented with the variable C_t and in our case, can be assumed constant for simplification. When we extract an amount of groundwater, we have to put a price covering not only the extraction cost, but the scarcity cost as well. This is a temporal cost reflecting the fact that if we extract water today, this same amount will not be available in the short future (for instance -say- tomorrow). The variable μ in Figure 62A represents the water scarcity cost; which in the economic literature is called Scarcity Rent. The scarcity rent increases the total groundwater price ($C_t + \mu_t$) until it meets the sewer mining technology -as the alternative solution- price P_s. From that point it will be cheaper to recycle wastewater than keep extracting groundwater. The crucial fact here is the time that this equilibrium occurs (the sooner it occurs, the better it is for the conservation of groundwater). To quantify the water scarcity mitigation, we can use the Recycling Multiplier concept (*RM*) (Karakatsanis 2010; Karakatsanis et al. 2014).

The *RM* provides us with how many times can –at least theoretically- an initial amount of wastewater W_o be reused by a specific coefficient m. The *RM* can be formulated as below:

$$RM = W_0/(1-m) \quad (5)$$

For our case, we can consider an *m* coefficient equal to 0,5 as the processed wastewater will be used to water a small park and will not be re-inserted to the economy (as it could be the case in industry). With significant lack of national, regional and global data on water reuse (Sato et al. 2012; UN 2012) we can resort to minimum assumptions on the impact that recycling will have on the area's total reserves. However, the cost aspect remains crucial in any case; even if the unit's small scale cannot impact directly groundwater conservation in the area, it is accepted that the faster the sewer-mining technology is improved, the sooner it will be able to operate in a market environment at lower cost. In Figure 62B we provide a theoretical depiction as well on the cost reduction rate (learning curves) of the sewer-mining technology.

2. **Microclimate regulation assessment:** The second major response concerns the evaluation of microclimate (ecosystem) services. Specifically, the control of latent heat fluxes has an impact on the local temperature and further on the household energy budget for heating and cooling. A theoretical depiction of this approach is presented in Figure 62C, where we consider a U-shaped relationship that reflects increased energy use for cooling or heating across external temperature deviations from a bioclimatic optimum (according to the literature this is ~18.3 ^{o}C). In general, for Mediterranean countries like Greece, the U-shape relationship empirically applies very well. Tyralis et al. (2017), as well as Karakatsanis et al. (2017) confirm it as they identify a general U-shaped pattern between temperature and electricity consumption for various geographical areas and at various scales. Via this model we may identify the statistical relationship between temperature and electricity use, *before* and *after* the watering of the small park with reused water. After the U-relationship and its related distribution have been revealed (see Figure 62D), we can simply calculate the impact on the household's energy *expenditure* for cooling or heating and measure the annual reduction of its energy bill payments that is exclusively due to the local regulation of temperature. The daily electricity prices are available by the *Independent Power Transmission Operator* (IPTO).

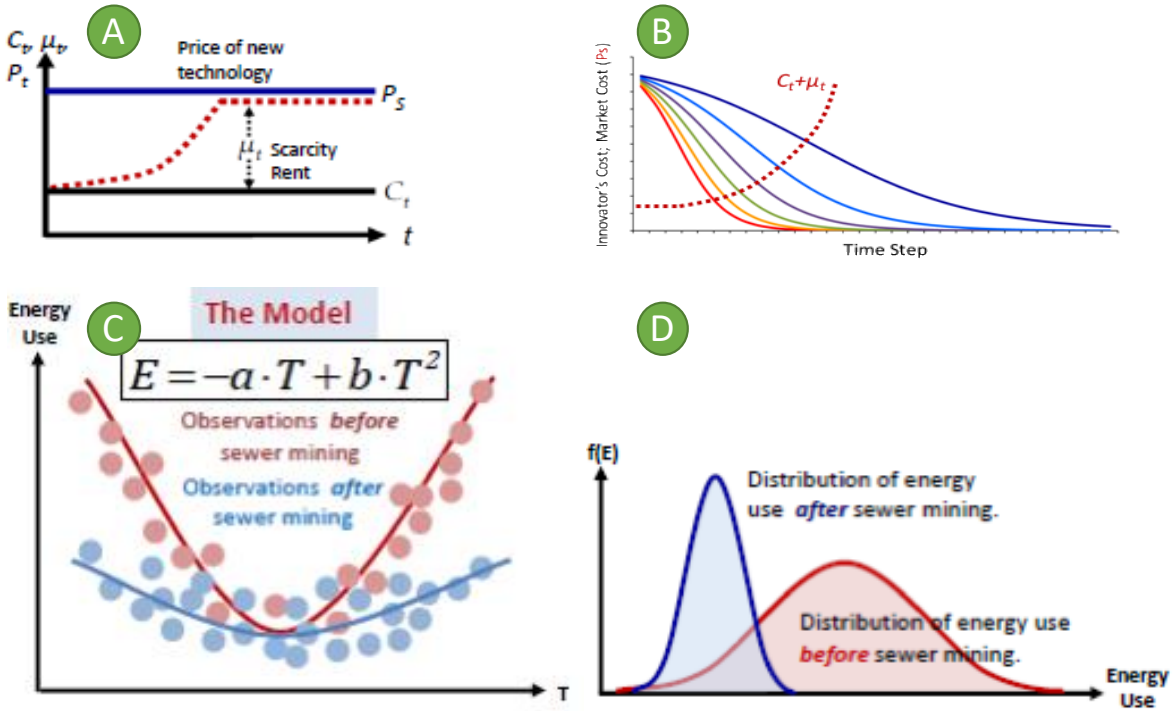

Figure 62. (A) Theoretical depiction of groundwater extraction cost, including the extraction and the scarcity cost, (B) Theoretical depiction of the sewer-mining unit's learning curves in combination to the increase of groundwater extraction total cost, (C) Theoretical depiction of the model used to assess the value of microclimate services based on temperature regulation in the park and (D) Theoretical depiction of the distribution of energy use by nearby consumers before and after the park's watering.

2.2.5 Impact evaluation of measures

The first part of our assessment concerns the application of responses on the quantitative evaluation and -in turn- mitigation of groundwater scarcity in the area. As described in the previous section, in order to apply full-cost accounting we should take into consideration not only the capital and operational costs for pumping groundwater (which consist of the cost of pump purchase, installation to a groundwater site and the related energy costs for its daily operation) but of the scarcity cost as well. The scarcity cost is independent of the extraction cost as it concerns only the effect of diminishing groundwater availability and not of the difficulty to extract more of the resource. An analytical approach of the scarcity cost concept can be found in Moncur et al. (1988). In general however the basic derivation of the scarcity cost comes from the Extraction/Reserves ratio, which in the case of exhaustible resources –as well as many cases of groundwater- is diminishing. The results of the assessment are presented in Figure 63 below:

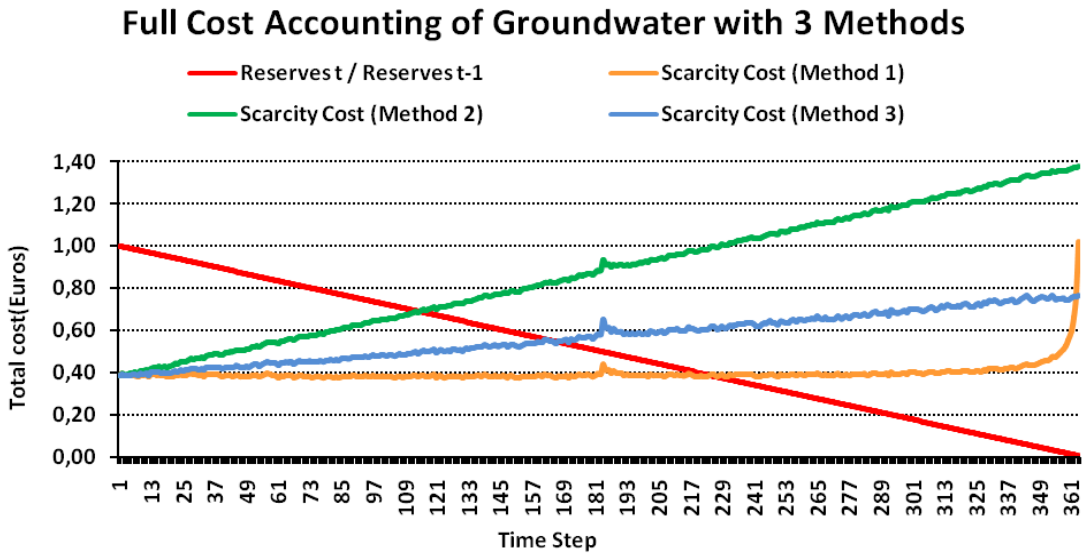

Figure 63. Results over the full cost accounting, including the extraction cost (capital and energy) as well as the scarcity cost, the latter calculated with 3 different methods.

For the composition of costs, we used data on pump capital costs, daily electricity prices from IPTO (Independent Power Transmission Operator, Greece) in order to assess the daily energy cost of pumping, theoretical evaluations of energy (electricity) use based on available pump data used in the area, as well as groundwater extraction data from Kalyvia Thorikou. It should however be denoted that for the groundwater extraction data, there is significant uncertainty as only 6 sites in the area are recorded officially. In reality, there are numerous other unrecorded sites from which many inhabitants pump water. This increases significantly all kinds of costs -and especially the capital cost as the pumped water from these sites occurs via the use of many pumps and not a single one that distributes the water to users. The basic data for the simulation on groundwater scarcity assessment are presented in the following table (Table 13):

Table 13. Data on groundwater extraction costs (scarcity costs not included)

Capital cost (Euros) / daily groundwater extraction (m^3)	Average pump coefficient	Daily average energy cost (Euros)	Total daily groundwater extraction (m^3)	Total groundwater reserves (m^3) (Assumed for the model)
0,34	0,4	0,05	2.317,81	845.000

As far as the methodologies for assessing the scarcity cost are concerned, we applied three indicators under the assumption of finite reserves (for simplicity here assumed to deplete within one year with the current daily groundwater extraction rate). Our main target is to identify which method/indicator reflects better the scarcity effect in the total price across the resource's depletion. The three indicators used were the following:

The **Extraction/Reserves** ratio. This indicator simply calculates the effect of the current extraction rate (here assumed constant on average) on remaining reserves of the resource at every time step, which is added to the extraction cost as it is. It is formulated as:

$$ER_{Ratio} = \frac{\text{Extraction}}{\text{Remaining Reserves}} \quad (6)$$

The **Reverse Current/Initial Reserves** ratio. This indicator calculates the ratio between the current and the initial reserves (before the beginning of extraction) at every time step. Then, the ratio is abstracted from the unit (1) and added to the extraction cost. It is formulated as:

$$RCIR_{Ratio} = 1 - \frac{\text{Current Reserves}}{\text{Initial Reserves}} \quad (7)$$

The **Enhanced Reverse Current/Initial Reserves** ratio. This indicator is similar to the previous indicator with the difference that it is added to the extraction cost after multiplied by it at each time step. It is formulated as:

$$ERCIR_{Ratio} = \text{Extraction Cost}\left(1 - \frac{\text{Current Reserves}}{\text{Initial Reserves}}\right) \quad (8)$$

In Figure 63 we see that the most reliable indicator for the scarcity cost is the ERCIR as it is the only one that can increase the groundwater price sufficiently to reach the alternative solution's price (here the sewer-mining technology) before the groundwater resource is completely depleted. The ER ratio is very inelastic across the resources depletion and reacts only at the final stages –which is only when the resource becomes extremely scarce. The RCIR ratio performs better than the ER, but does not manage to cover up the cost of the alternative technology even when the resource is completely depleted. The only indicator that manages to increase fast enough and reflect the scarcity cost more accurately is the ERCIR. Not only it reaches the cost of both sewer-mining technologies (MBR-UV and MBR-UV-RO) quite before the resource is depleted (it reaches the price of MBR-UV when the remaining reserves are at 50% and the MBR-UV-RO when remaining reserves are at 40%) but also becomes higher than the extraction cost by the complete depletion of the resource, reflecting more accurately the scarcity effect.

The above assessment assumed constant sewer-mining technology costs. However, the second part of the groundwater scarcity assessment concerns the potential of each sewer-mining technology to become the main solution much sooner. Considering that according to Makropoulos et al. (2017) the cost of MBR-UV is 0,86€/m^3 and the cost of MBR-UV-RO is 1,07€/m^3 that means that the first technology needs to cover a scarcity cost of 0,46€ and the second of 0,67€ to reach the extraction cost of groundwater. Assuming an average ratio of 0,08€ at each time step, we can simulate the learning curves of both technologies in Figure 64 below:

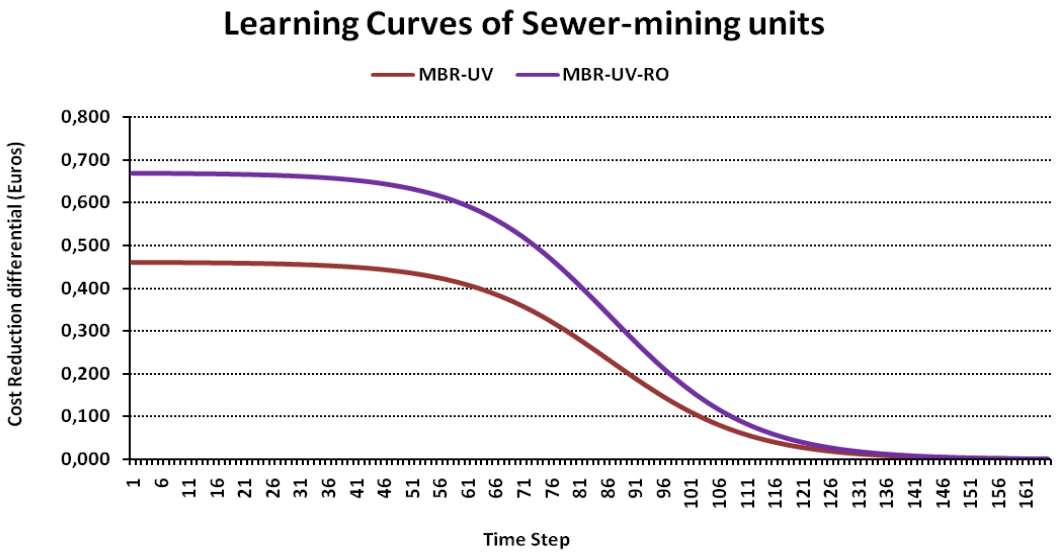

Figure 64. Simulation of cost reduction rate for both sewer-mining technologies at each time step.

Conclusively, as far as the assessment of groundwater scarcity is concerned we sum-up with the following:

The sewer-mining unit's costs concern their initial level and do not include the expected cost reduction from learning curves (which are only simulated). Hence, our assumptions have been quite strict on the unit's cost dynamics.

The groundwater extraction cost was estimated as a *weighted average cost* of each recorded site in the simulated area. However, as there is a high number of unrecorded groundwater pumping sites, the extraction cost is expected to be higher. Hence, our assumptions on the "business as usual scenario" we have been quite lenient.

The scarcity cost, is also estimated on the recorded groundwater pumping sites; hence it is also expected to be higher. If we combine this point with the previous two, we can conclude that the technology has -in overall- a high market potential.

The second part of our assessment concerns the evaluation of microclimate regulation services from a local park's watering. According to the literature examining the relationship between those two variables for Mediterranean countries we expect to find a U-type relationship, depicting that for any deviation from a bioclimatic optimum (considered ~18,3 ^{o}C) electricity use will increase either for heating (during the winter) or for cooling (during the summer). The empirical relationship based on daily data for Kalyvia Thorikou is presented in Figure 65 below:

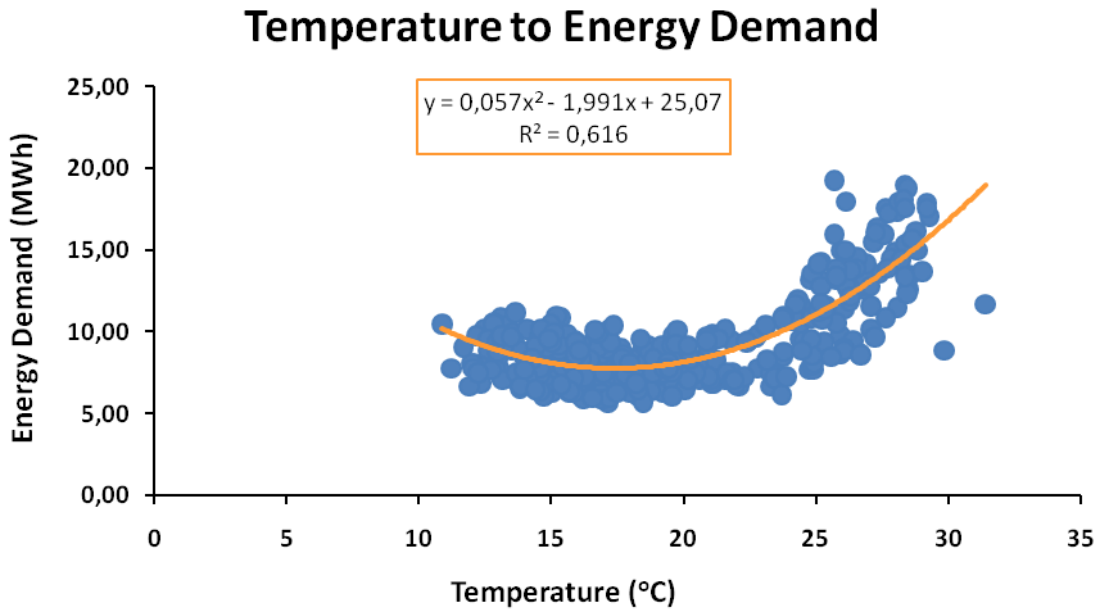

Figure 65. The relationship between temperature and electricity use in Kalyvia Thorikou based on daily temperature and electricity use data for 2014.

As expected, the U-relationship verifies for our case as well –although with significant asymmetry towards the higher temperatures. In short, this indicates that deviations towards higher temperatures are more likely to occur than deviations toward lower temperatures, which is expected in Greece. Mathematically, the relationship between these two variables is formulated as:

$$E = c - aT + bT^2 \quad (9)$$

Although the coefficient of determination, R^2, indicates that there is much uncertainty incorporated in the model, we can consider it sufficient in order to estimate the benefits from microclimate regulation in the area. The values of the parameters on which we will base our evaluation are a = 1,991, b = 0,057 and c = 25,07. The next step is to estimate the new temperatures after the park's watering. Normally, we expect that the new temperatures are concentrated in higher frequencies towards the bioclimatic optimum; hence energy use for cooling or heating will not be as high as before. We also assume that no other effect takes place for the reduction of energy use (such as enhanced building materials) but temperature. The pattern of energy use is assumed to follow (in a deterministic way) the U-curve of Figure 65, with the same daily electricity prices. Only temperature is considered variable.

Based on the simulations that took place in KEREFYT at the site of the sewer-mining technology application, we assume that a similar effect would occur in the simulated area as well. This is of course a completely theoretical assumption, however its target is to simplify the methodology. According to the above, the change in temperature distribution in the simulated area is presented in Figure 66 below:

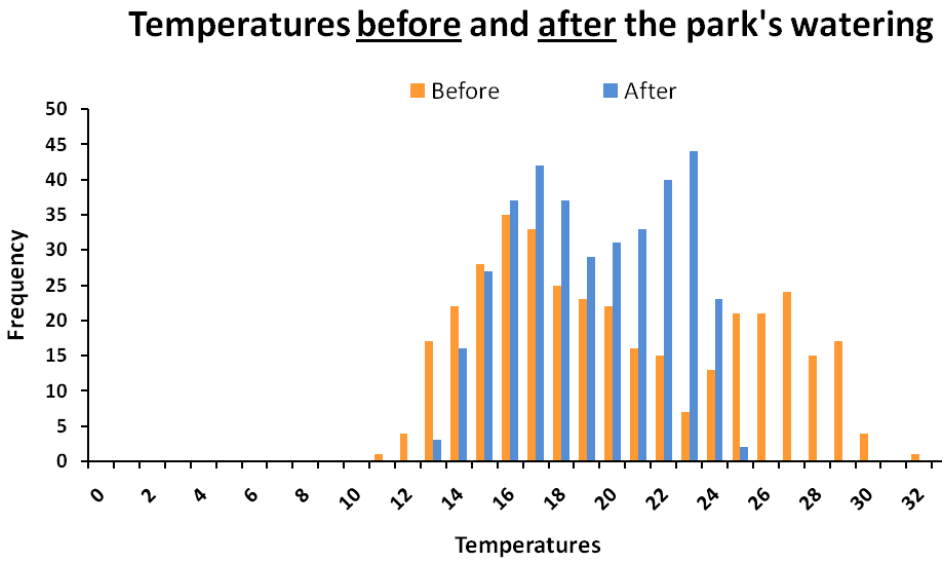

Figure 66. Distribution of temperatures in the simulated area before and after the park's watering

As expected, the temperatures after the park's watering are concentrated towards the bioclimatic optimum. In addition, we measure the temperature deviations from that optimum in Figure 67 below:

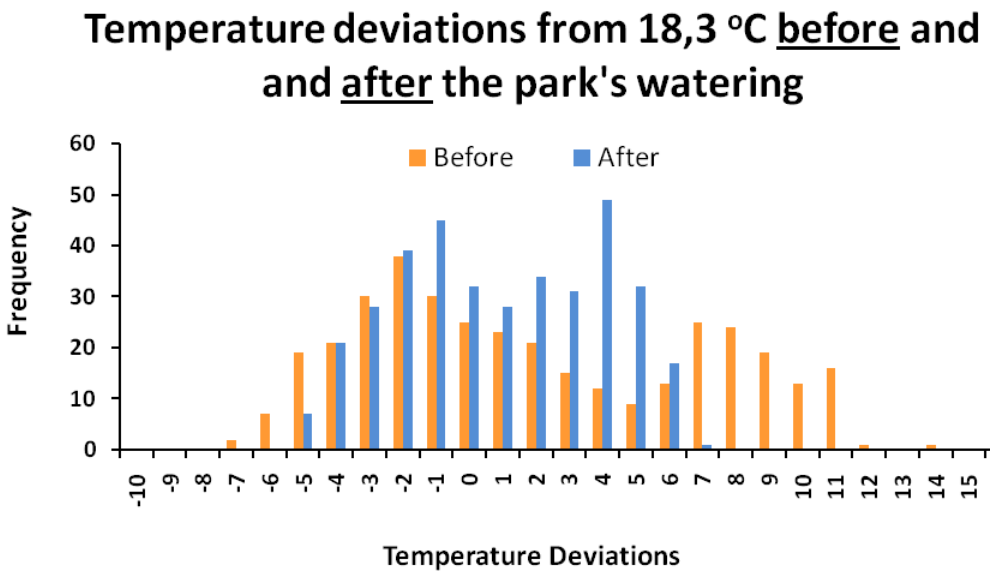

Figure 67. Distribution of temperature deviations from the bioclimatic optimum (value=0 for no deviations) before and after the park's watering.

As before, we verify that the deviations from the bioclimatic optimum have reduced significantly after the park's watering with processed water from the sewer-mining technology. Now, at a more specific level we calculate the difference between daily energy use before and after the park's watering in relation to temperature changes. The results in the change of electricity demand distribution are presented in Figure 68:

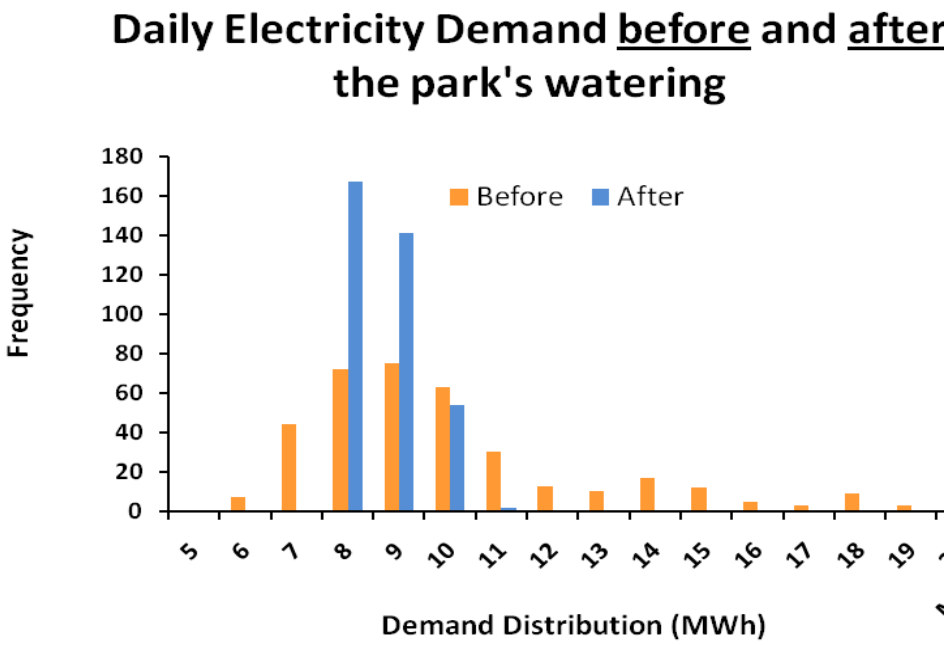

Figure 68. Distribution of energy (electricity) demand before and after the park's watering across changes in the local temperature.

Again, the results verify our initial assumptions and the theoretical depiction of the response measure presented in Figure 62D. Furthermore, we simulate the effect of reduced energy demand for cooling or heating on the total expenditure of family budgets for energy use. Total expenditure is calculated as the product of energy demand at each day (Q_i) and the average price (P_i) of electricity for this particular day *i* as:

$$Exp = P_i Q_i \tag{10}$$

However, as the daily electricity price is considered to remain unchanged in the simulation, the only way to change the total expenditure is by changing the electricity demand (as a result in change of temperature). Hence, we can calculate the change in total expenditure as:

$$\Delta Exp = P_i \Delta Q_i \tag{11}$$

Normally, it is expected that the distribution of daily expenditures will be following the general pattern of energy demand as well, although there is increased uncertainty due to the fact that the prices are not determined by the demand of such a small area but by other factors as well; hence they might not be depicting the effect of reduced energy demand in the area. The results are presented in Figure 69 below:

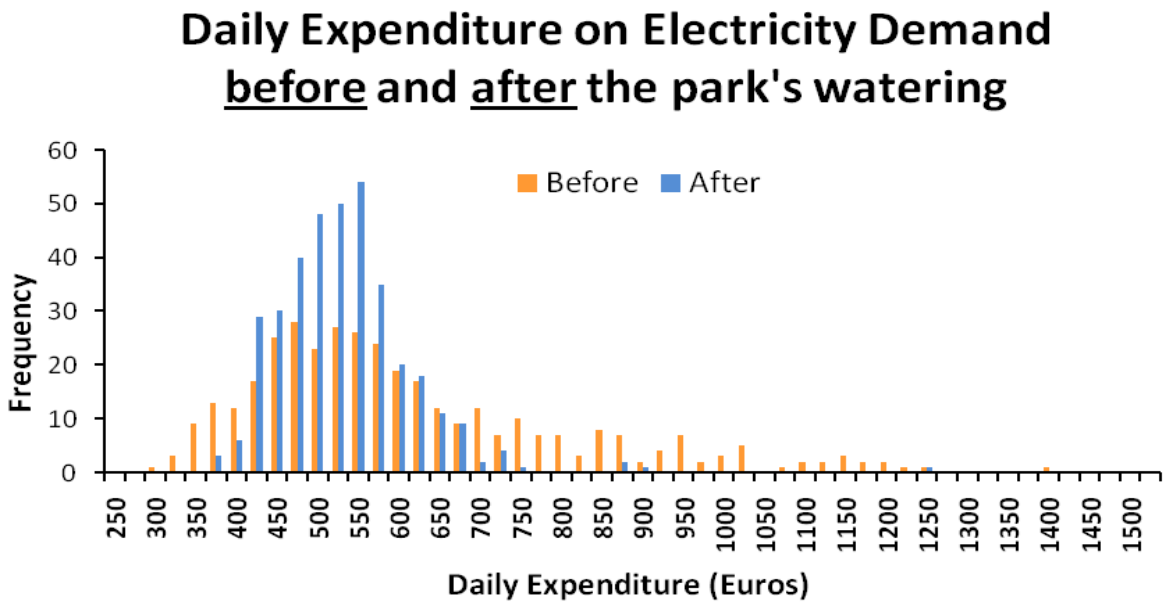

Figure 69. Distribution of expenditures on electricity demand before and after the park's watering.

As in Figure 68, the pattern for energy expenditure is similar to the pattern of energy demand. Based on the above, we finally calculated the distribution of savings from the application of the sewer mining technology for watering the park. The results are presented in Figure 70 below:

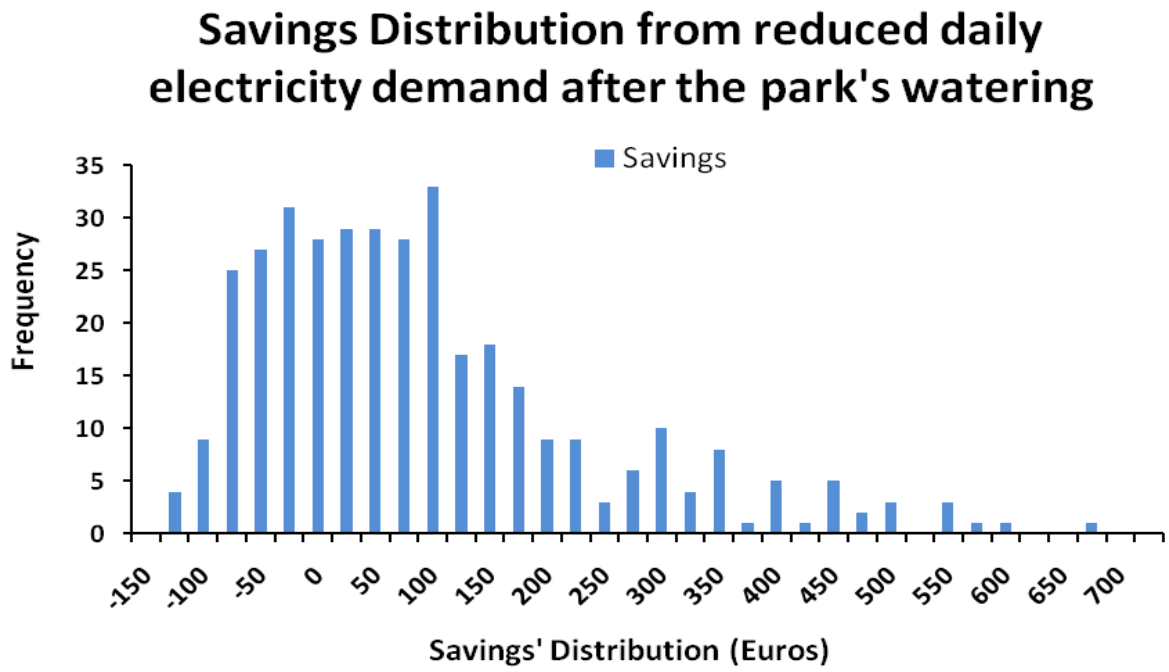

Figure 70. Distribution of energy expenditure savings after the park's watering and derived temperature regulation.

In Figure 70 we can observe that a significant part of the distribution falls in the range of -150 to -50 euros per day. This is due to the fact that the simulation on the temperatures regulation is quite simplified and in some cases –mainly those concentrated in the left part of the U-curve- resulted in

lower temperatures than before; hence leading to slightly increased energy use for heating. However, as the major part of the U-curve was concentrated in the right part (more energy use for cooling) the overall benefit was significantly positive. As the park's area is small in comparison to the whole area of municipal unit, only a small part of the population is expected benefit from microclimate regulation services. In particular, the benefits range from 130-150€ in terms of annual energy savings for the MBR-UV technology and 140-180€ for the MBR-UV-RO for a number of 20 families (consisting of 2 parents and 2 children each) assumed to reside near the park's area.

Concentrating all the elements of our analysis (see the slide) we came with the first simulated results (see table). As far as the simulation is concerned it is important to denote that the annual energy savings for a model household of four people (parents and two children) are estimated on *average* and *not discrete* electricity consumption and pricing (i.e. families with low annual income have significant reductions in energy and water bills). These savings are also a bulk estimation of the maximum annual amount that this model household would be willing to pay for microclimate regulation from the park (otherwise, if it was more expensive it would just prefer to use its electric appliances for cooling/heating).

2.2.6 Sustainability assessment

As the potential benefits of sewer mining for the circular economy and ecosystems are easily identified, a major issue –with significant social extensions- concerns the establishment of a functional business model that will ensure social acceptance and economic profitability for the operator. Empirically, models that aim at providing high value-added services with absence of subsidization or excessive bank lending at every stage of the commercial application (initial, intermediate or mature) prove to be the most resilient in time (Albach et al. 2014, p. 158). In relation to the features of small-scale applications –such as the pilot study area- two business models comprise the main candidates for the sewer mining technology commercialization: (a) full provision of the service by the municipal water company that keeps property of the distribution networks or (b) privatization of the service (e.g. by an SME), while the water supply company maintains the property of the distribution networks and receives a rent for their use (e.g. a constant monthly fee or proportional to the demand for the network use). The second business model is a type of public-private partnership (PPP); a highly common practice for new water infrastructures under formation (Marin 2009). The PPP model differs from the public supply model in the sense that all business risks and benefits are –by contract- ceded to the private counterparty. In this context, the decision between the two business models is a matter of the ratio between the marginal benefits and the marginal costs from the technology's application. Generally, the higher is the ratio, the higher is the potential for private interest and involvement.

Assuming that for small-scale applications the marginal costs between the private and the public sector do not vary significantly, the business model selection depends on the accurate valuation (and pricing) of the marginal benefits; mainly those deriving from water-enhanced ecosystem services. A general framework for quantifying the benefits of ecosystem services in macroeconomic accounts has been proposed by the UN (2014). Water-enhanced ecosystem services concern the functions of the (local) ecosystem that used to be inactive due to the limitations in available water. For example,

in the study area, the most notable derived service is microclimate regulation from watering a local park. This provides the community with direct, local and collective benefits from less energy use for heating and cooling during the year; features that are expected to promote the technology's social acceptance. Other, more entrepreneurship-oriented ecosystem services, may concern the activation of (formerly not viable) investment projects, such as touristic activities, urban farming, hydroponics and environmental education. What should be denoted is that at the small-scale it is rather the variety of ecosystem services that matters most than their scale. Hence, from a business point of view, the achievement of economies of scope (diversification of ecosystem services) is more important from economies of scale; the latter being a more appropriate target for large-scale urban webs or industrial ecology complexes (Ehrenfeld and Gertler 1997). At the small-scale, the conditions for the organization of local and transparent water-enhanced ecosystem service markets between few competitive end-users are more favorable. In such markets, a private operator (e.g. a research startup or an SME) would seem more flexible to manage the challenges of ecosystem services diversification.

The public-private partnership model is also preferred due to lower socio-economic pricing risks. Due to the potential of SMEs involvement the benefits and costs are usually better distributed; as it provides both parties with more flexibility. On the one hand it allows SMEs to implement various innovations and various forms of deals with customers, while it relieves the public company from the need of business decisions and related administrative costs. The latter can rely on a rent that mainly covers network maintenance, keeping the ability of pricing in relation to business conditions (either receive a constant rent or adjust it as a variable payment according to the network's use by SMEs).

2.2.7 Conclusions

Our priority was to develop and apply a pricing system for the diffusion of the sewer-mining technology in a market environment as an economically viable investment. An indicative small-scale area with issues of water scarcity was selected for the simulation and valuation of ecosystem services. The main scenario was to use treated wastewater from the sewer-mining unit to water a local park. Hence, our analysis was based in three (3) main pillars: (1) the quantification of water scarcity mitigation, (2) the valuation of water-enhanced ecosystem services (the major service being microclimate regulation from the park's watering) and (3) a discussion on estimated derived economic activities as well as the business model for the sewer mining technology operation.

For estimating the effect of water scarcity mitigation, we considered the case of groundwater as the most indicative due to its low recharge rates, which was also the "business as usual scenario" to the sewer-mining unit for watering the park. In general, we considered the cost of groundwater extraction to be constant and focused on the scarcity cost in time as more groundwater is extracted and is not available in the future. The extraction and the scarcity cost comprised the total price of groundwater. When this reaches the price of the sewer mining technology, the latter becomes the main solution and further groundwater extraction is abandoned (Figure 62A). We further assumed that the price of the sewer-mining technology is not static; as improvements took place, it could become a more affordable solution sooner. In relation to that we made several assumptions on the cost reduction rate (learning curves).

We further assumed that the park's watering had an impact on the local temperature and further on the household energy budget for heating and cooling. This was the main ecosystem service based on a U-shaped relationship (Figure 62B) that reflects increased energy use for cooling or heating across external temperature deviations from a bioclimatic optimum (according to the literature ~18.3 ^{o}C). Via this model we identified the statistical relationship between temperature and electricity use at an hourly base, before and after the watering of the small park. After the new U-relationship and had been revealed (blue-color schemes), we could calculate the impact on the household's energy expenditure for cooling or heating and measure the annual reduction of its energy bill payments for a model household of four people (parents and two children). Annual energy savings were also a bulk estimation of the maximum annual amount that this model household would be willing to pay for the microclimate regulation service from the park's watering via the sewer-mining unit.

The main benefit from the local environment's upgrade is the higher number of visitors for recreation. Secondary benefits concern the development of new economic activities, such as urban bio-farming and environmental education.

For the sewer-mining technology's business model, we could identify two (2) possible candidates, which are mutually exclusive: (1) A centralized operation from the municipal/public water company -that also holds property of the water network. In this model, a single company offers the full range of sewer-mining derived services and takes all related business benefits and risks. (2) A public-private partnership. In this model, private companies (e.g. SMEs) offer the full range of services taking all business benefits and risks, while the public company continues to hold property of the network, receiving a rent for its use. Selecting one of the two models would strongly depend on the scale of the application area.

Evaluated ESS:

- Microclimate regulation for reduced energy use and reduced energy bills from households. A model household of 4 people (parents and 2 children) was used for the simulation.
- Mitigation of groundwater scarcity and increase of future groundwater availability.
- A qualitative evaluation of the range of new economic activities that could be created upon the manifestation of water-enhanced ecosystem services.
- A qualitative evaluation of the optimal business model for the sewer-mining technology to be implemented in a market environment without long-term dependence on bank lending or state subsidization.

Results:

- Microclimate regulation benefits for a model household of 4 people (parents and 2 children) range between 130-180€ annually, depending on the sewer-mining unit's technology (MBR-UV or MBR-UV-RO).
- Groundwater scarcity cost mitigation ranges between 0.40-0.50€/m^3, depending on the sewer-mining unit's technology (MBR-UV or MBR-UV-RO) and the cost reduction rate (learning curve) per year. Specifically, this is achieved for an average total cost reduction rate of the sewer-mining unit ranging from 0.08-0.09€/m^3/year so that within the first five (5) years the major part of the scarcity cost will have been mitigated by both technologies.
- According to the qualitative evaluation, the increase of water availability due to the installation of a sewer-mining unit could lead to significant enrichment of economic activities in the area as well as enhancement of existing ones. The majority of these new activities relate to tourism (eg. increased number of arrivals due to the upgrade of the park's environmental state, more visits to a nearby archaeological site, environmental education activities, small-scale bio-culture and generally better value-for-money according to the Cost of Travel method).
- Two (2) candidate business models (central operation and public-private partnership) for the optimal diffusion and operation of the sewer-mining technology in a market environment. The selection of the business model is highly depended on the scale of the area.

References

Æsøy, A., Storfjell, M., Mellgren, L., Helness, H., Thorvaldsen, G., Ødegaard, H., Bentzen, G., (1997). A comparison of biofilm growth and water quality changes in sewers with anoxic and anaerobic (septic) conditions. Water Sci. Technol. 36, 303–310.

Akpor, O. B., Ohiobor, G. O. & Olaolu, T. D., (2014). Heavy Metal Pollutants in Wastewater Effluents: Sources, Effects and Remediation. Advances in Bioscience and Bioengineering, Volume 2, pp. 37-43.

Al-Rifai, J., Khabbaz, H. & Schafer, A., (2011). Removal of pharmaceuticals and endocrine disrupting compounds in a water recycling process using reverse osmosis systems. Seperation and Purification Technology, Volume 77, pp. 60-67.

Alexandri, E. and Jones, P. (2008). Temperature decreases in an urban canyon due to green walls and green roofs in diverse climates, Building and Environment, 4, 480–93.

American Puplic Health Association, (2012). Standard Methods for Examination of Waters and Wastewaters. 22nd Ed ed. Washington D.C.

Bailey, R., Janet A. K. and Bras, B. (2004a), Applying ecological input-output flow analysis to material flows in industrial systems: Part I: Tracing flows, Journal of Industrial Ecology, Vol. 8, Issue 1-2, 69-91

Bailey, R., Janet A. K. and Bras, B. (2004b), Applying ecological input-output flow analysis to material flows in industrial systems: Part II: Flow metrics, Journal of Industrial Ecology, Vol. 8, Issue 1-2, 69-91

Barreto, C. et al., (2016). Assessing the performance of an MBR operated at high biomass concentrations. International Biodeterioration & Biodegradation, pp. 1-10, In press, Corrected proof.

Bentzen, G., Smith, A., Bennet, D., Webster, N., Reinholt, F., Sletholt, E., Hobson, J., (1995). Controlled dosing of nitrate for prevention of HS in a sewer network and the effects on the subsequent treatment processes. Water Sci. Technol. 31, 293–302. doi:10.1016/0273-1223(95)00346-O

Bielecki, R., Schremmer, H., (1987). Biogene Schwefelsäure-Korrosion in teilgefüllten Abwasserkanälen.

Boon, A. G. (1995). Septicity in sewers: causes, consequences and containment. Water Science and Technology, 31(7), 237–253.

Branch, A. et al., (2015). Chemical Cleaning in membrane bioreactors: Implications for accreditation in Water Recycling. Water:Journal of the Australian Water Association, June, Volume 42, pp. 60-64.

Carletti, G., Fatone, F., Bolzonella, D. & Cechi, F., (2008). Occurrence and fate of heavy metals in large wastewater treatment plants treating municipal and industrial wastewaters. Water Science and Technology, Issue 57, pp. 1329-1336.

Cartagena, P. et al., (2013). Reduction of emerging micropollutants, organic matter, nutrients and salinity from real wastewater by combined MBR-NF/RO treatment. Seperation and Purification Technology, June, Volume 110, pp. 132-143.

Clara, M. et al., (2005). The solids retention time-a suitable design parameter to evaluate the capacity of wastewater plants to remove micropollutants. Water Research, Volume 39, pp. 97-106.

Comerton, A., Andrews, R. & Bagley, D., (2005). Evaluation of an MBR-RO system to produce high quality reuse water. Water Research, Volume 39, pp. 3982-3990.

Cote, P., Buisson, H., Poud, C. & Arakaki, G., (1997). Immersed membrane activated sludge for the reuse of municipal wastewater. Desalination, Volume 113, pp. 189-196.

CRC Construction Innovation, (2006). Barriers and drivers of new public-private infrastructure: sewer mining. CRC for Construction Innovation. Retrieved from http://eprints.qut.edu.au/26976/1/CIBE_Sewer_Mining_Case_Study_final_July.pdf

Daily G.C., Alexander S., Ehrlich P.R., Goulder L., Lubchenco J., Matson P.A., Mooney H.A., Postel S., Schneider S.H., Tilman D. and Woodwell G.M. (1997) Ecosystem Services: Benefits Supplied to Human Societies by Natural Ecosystems. Issues in Ecol. 2 1– 16.

Degremont, G., (1979). Water treatment handbook. John Wiley & Sons Inc.

Duchin, F. (2004), Input-output economics and material flows, Rensellaer Polytechnic Institute, Department of Economics (Rensellaer Working Papers in Economics, 424

Ehrenfeld, J. and Gertler N. (1997), Industrial Ecology in Practice: The evolution of interdependence at Kalundborg, Journal of industrial Ecology

Fan, X., Urbain, V., Qian, Y. & Manem, J., (1996). Nitrification and mass balance with a membrane bioreactor for municipal wastewater treatment. Water Science and Technology, Volume 34, pp. 129-136.

Fatone, F., Battistoni, P., Pavan, P. & Cecchi, F., (2006). Application of a membrane bioreactor for the treatment of low loaded domestic wastewater for water-reuse. Water Science Technology, Volume 53, pp. 111-121.

Food and Agriculture Organization of the United Nations, International Monetary Fund, Organization for Economic Cooperation and Development and World Bank (2014), System of environmental-economic accounting 2012: Central framework, available at:

Gao, D., Li, Z., Guan, J. & Liang, H., (2017). Seasonal variations in the concentration and removal of nonyphenol ethoxylates from the wastewater of a sewage treatment plant. Journal of Environmental Sciences, Volume 54, pp. 217-223.

Gasperi, J., Garnaud, S., Rocher, V. & Moilleron, R., (2009). Priority pollutants in surface waters and settleable particles within a densely urbanised area:Case studies of Paris. Science of the Total Environment, Volume 407, pp. 2900-2908.

Gulyas, G., Pitas, V., Fazekas, B. & Karpati, A., (2015). Heavy metal Balance in a communal wastewater treatment plant. Hungarian Journal of Industry and Chemistry, Issue 43, pp. 1-5.

Gurung, K., Ncibi, M. & Sillanpaa, M., (2017). Assessing membrane fouling and the performance of pilot scale membrane bioreactor (MBR) to treat real municipal wastewater during winter season in Nordic regions. Science of the Total Environment, Volume 579, pp. 1289-1297.

Hadzihalilovic, V., (2009). Sewer mining for golf course irrigation. J. Aust. Water Assoc. 36, 168–71.

Hai, F., Fagram , S. & Yamamoto, K., (2014). Removal of Pathogens by Membrane Bioreactors: A review of the Mechanisms, Influencing Factors and Reduction in Chemical Disinfectant Dosing. Water, Volume 6, pp. 3603-3630.

Herojeet, R., Rishi, M. & Kishore, N., (2015). Integrated approach of heavy metal pollution indices and complexity quantification using chemometric models in the Sirsa Basin, Nalagarh valley, Himachal Pradesh, India. Chinese Journal of Geochemistry, Volume 34, pp. 620-633.

Howard L., Climate of London Deduced from Meteorological Observations, Vol. 1, W. Phillips, London, 1818.

https://unstats.un.org/unsd/envaccounting/seeaRev/SEEA_CF_Final_en.pdf

Hvitved-Jacobsen, T., Vollertsen, J., (2001). Odour formation in sewer networks, in: Odours in Wastewater Treatment: Measurement, Modelling and Control. IWA Publishing Company.

Hvitved-Jacobsen, T., Vollertsen, J., Nielsen, A.H., (2013). Sewer processes: microbial and chemical process engineering of sewer networks. CRC press.

Hvitved-Jacobsen, T., Vollertsen, J., Yongsiri, C., Nielsen, A.H., Abdul-Talib, S., (2002). Sewer microbial processes, emissions and impacts, in: 3rd International Conference on Sewer Processes and Networks, April. pp. 15–17.

Hwang, Y., Matsuo, T., Hanaki, K., Suzuki, N., (1995). Identification and quantification of sulfur and nitrogen containing odorous compounds in wastewater. Water Res. 29, 711–718. doi:http://dx.doi.org/10.1016/0043-1354(94)00145-W

Jensen, H., Nielsen, A., Hvitved-Jacobsen, T., Vollertsen, J., (2008). Survival of hydrogen sulfide oxidizing bacteria on corroded concrete surfaces of sewer systems.

Karakatsanis, G. (2010), The Recycling Multiplier: The added value of waste, ISEE Biennial International Conference, Oldenburg and Bremen, Germany

Karakatsanis, G. et al. (2014), Entropy, recycling and macroeconomics of water resources, EGU General Assembly, Vienna, Austria

Karakatsanis, G. et al. (2017), Energy, variability and weather finance engineering, Energy Procedia 25, p. 389-397

Karvelas, M., Katsoyiannis, A. & Samara, C., (2003). Occurrence and fate of heavy metals in the wastewater treatment process. Chemosphere, Issue 53, pp. 1201-1210.

Kislenko, K., Dudutyte, Z. & Ruut, J., (2011). Baltic Actions for Reduction of Pollution of the Baltic Sea from Priority Hazardous Substances, s.l.: Life+.

Koutsoyiannis, D., (2011). Design of Urban Sewer Networks, 4th ed. National Technical University of Athens, Athens.

Lahav, O., Sagiv, A., & Friedler, E. (2006). A different approach for predicting H2S(g) emission rates in gravity sewers. Water Research, 40(2), 259–266. https://doi.org/10.1016/j.watres.2005.10.026

Lohami, M. B., Singh, A., Rupainwar, D. C. & Dhar, D. N., (2008). Seasonal varations of heavy metal contamination in river Gomti of Lucknow city region. Environmental Monitoring and Assessment, Volume 147, pp. 253-263.

Makropoulos C., Rozos E., Tsoukalas I., and et al., Sewer-mining: A water reuse option supporting circular economy, public service provision and entrepreneurship, Journal of Environmental Management, doi:10.1016/j.jenvman.2017.07.026, 2017

Makropoulos, C.K., Butler, D., (2010). Distributed water infrastructure for sustainable communities. Water Resour. Manag. 24, 2795–2816. doi:10.1007/s11269-010-9580-5

Malamis, S. et al., (2012). Assessment of metal removal, biomass activity and RO concentrate treatment in an MBR-RO system. Journal of Hazardous Materials, Volume 209-210, pp. 1-8.

Mansell, B. et al., (2004). Comparison of Two Membrane Bioreactors and an Activated Sludge Plant with Dual-Media Filtration : Nutrient and Priority Pollutant Removals. Proceedings of the Water Environment Federation, Volume 20, pp. 749-761.

Marin, P. (2009), Public-private partnerships for urban water utilities: A review of experiences in developing countries, The World Bank, Washington DC, USA

Marleni, N., Gray, S., Sharma, A., Burn, S., & Muttil, N. (2013). Modeling the Effects of Sewer Mining on Odour and Corrosion in Sewer Systems (pp. 1–6).

Marleni, N., Gray, S., Sharma, A., Burn, S., Muttil, N., (2012). Impact of water source management practices in residential areas on sewer networks - A review. Water Sci. Technol. 65, 624–642. doi:10.2166/wst.2012.902

Marleni, N., Park, K., Lee, T., Navaratna, D., Shu, L., Jegatheesan, V., … Feliciano, A. (2015). A methodology for simulating hydrogen sulphide generation in sewer network using EPA SWMM. Desalination and Water Treatment, 54(4–5), 1308–1317. https://doi.org/10.1080/19443994.2014.922899

Mazloomi, S. et al., (2009). Efficiensy of domestic reverse osmosis in removal of trihalomethanes from drinking water. Iran. J. Environ. Health. Sci. Eng., Volume 6, pp. 301-306.

Moncur, J. E. T. and R. L. Pollock (1988), Scarcity Rents for Water: A Valuation and Pricing Model, Land Economics, Vol. 64, No 1

Nielsen, A.H., Vollertsen, J., Jensen, H.S., Wium-Andersen, T., Hvitved-Jacobsen, T., (2008). Influence of pipe material and surfaces on sulfide related odor and corrosion in sewers. Water Res. 42, 4206–4214.

Nielsen, P.H., Raunkjær, K., Norsker, N.H., Jensen, N.A., Hvitved-Jakobsen, T., (1992). Transformation of Wastewater in Sewer Systems: A Review. Water Sci. Technol. 25, 17–31.

Noutsopoulos, C., Andreadakis, A., Mamais, D. & Gavalakis, E., (2007). Identification of type and causes of filamentous bulking under Mediterranean conditions. Environmental Technology , Volume 28, pp. 115-122.

Nunez, M; T. R. Oke (1977). "The Energy Balance of an Urban Canyon". Journal of Applied Meteorology. 16: 11-19.

Okabe, S., Odagiri, M., Ito, T., & Satoh, H. (2007). Succession of sulfur-oxidizing bacteria in the microbial community on corroding concrete in sewer systems. Applied and Environmental Microbiology, 73(3), 971–980.

Oke (1982). "The energetic basis of the urban heat island". Quarterly Journal of the Royal Meteorological Society. 108 (455): 1–24. Bibcode:1982QJRMS.108....1O. doi:10.1002/qj.49710845502.

Plevri, A. et al., (2017). Promoting on-site urban wastewater reuse through MBR-RO treatment. Desalinaton.

Pomeroy, R.D., (1990). The Problem of Hydrogen Sulphide in Sewers. Clay Pipe Dev. Assoc. Ltd., London, 2 nd Ed. by A. G. Boon), 1990, 24.

Psarrou E., Tsoukalas I., and Makropoulos C., (2017). A decision support tool for optimal placement of sewer mining units: Coupling SWMM 5.1 and Monte-Carlo simulation, Proceedings of the 15th International Conference on Environmental Science and Technology, Rhodes, Greece; 09/2017.

Rosenfield, Arthur, Joseph Romm, Hashem Akbari, and Alana Lloyd. (2014). Painting the Town White -- and Green. MIT Technology Review. N.p., 14 07 1997. Web. 25 Feb 2014.

Rozos E., Tsoukalas I., Ripis K., Smeti E., and Makropoulos C. (2017). Turning black into green: Ecosystem services from treated wastewater, Desalination and Water Treatment, 2017

Rule, K. L. et al., (2006). Diffuse sources of heavy metal entering an urbam wastewater catchment. Chemosphere, Issue 63, pp. 64-72.

Runnalls, K.E. and Oke, T.R. (2000) Dynamics and Control of the Near-Surface Heat Island of Vancouver, British Columbia. Physical Geography, 21, 283-304.

Samaras, V., Thomaidis, N., Stasinakis, A. & Lekkas, T., (2011). An analytical method for the simultaneous trace determination of acidic pharmaceuticals and phenolic endocrine disrupting chemicals in wastewater and sewage sludge by gas chromatography- mass spectometry. Analytical Bioanalytical Chem, Volume 399, pp. 2549-2561.

Sato, T. et al. (2013), Global, regional and country level need for data on wastewater generation, treatment and use, Agricultural Water Management 130, 1-13

Sauve , S. & Desrosiers, M., (2014). A review of what is an emerging contaminant. Chemistry Central.

Solecki, William D.; Rosenzweig, Cynthia; Parshall, Lily; Pope, Greg; Clark, Maria; Cox, Jennifer; Wiencke, Mary (2005). "Mitigation of the heat island effect in urban New Jersey". Global Environmental Change Part B: Environmental Hazards. 6 (1): 39–49. doi:10.1016/j.hazards.2004.12.002.

Soonthornnonda, P. & Christensen, E. R., (2008). Source apportionment of pollutants and flows of combined sewer wastewater. Water Research, Volume 42, p. 19891998.

Sorne, L. & Lagerkvist, R., (2002). Sources of heavy metals in urban wastewater in Stockholm. The Science of the Total Environment, Volume 298, pp. 131-145.

Stanislav E. S. (2012), Ecological economics: Sustainability in practice, Springer Science+Business Media B.V. 2012

Stasinakis, A. S. et al., (2010). Removal of selected endocrine disrupters in activated sludge systems: Effect of sludge retention time on their sorption and biodegradation. Bioresource Technology, Volume 101, p. 20902095.

Sydney Olympic Park Authority., (2006). Urban water reuse & integrated water management.

Sydney Water, (2009). Recycled water in the Sydney region - sewer mining schemes. Sydney, Australia: Sydney Water. Retrieved from https://www.sydneywater.com.au/water4life/recyclingandreuse/pdf/SewerMiningRecycled WaterMap.pdf

Sydney Water. (2008). Sewer Mining How to establish a sewer mining operation, 14. Retrieved from http://www.sydneywater.com.au/Water4Life/RecyclingandReuse/pdf/SewerMiningBrochure.pdf#Page=1

Sydney, R., Esfandi, E., & Surapaneni, S., (1996). Control concrete sewer corrosion via the crown spray process. Water Environment Research, 68(3), 338–347.

Tam, L. et al., (2005). A pilot study for wastewater reclamation and reuse with MBR-RO and MF-RO systems. Desalination, Volume 202, pp. 106-113.

Tiruneh, A. T., Fadiran, A. O. & Mitshali, J. S., (2014). Evaluation of the risk of heavy metals in sewage sludge intended for agricultural application in Swaziland. International Journal of Environmental Sciences, Volume 5, pp. 197-216.

Tsoukalas, I. K., Makropoulos, C. K., & Michas, S. N., (2017). A Monte-Carlo based method for the identification of potential sewer mining locations. Water Science and Technology, wst2017487.

Tsoukalas, I., Makropoulos, C. & Michas, S., (2016). A Monte-Carlo based method for the identification of potential sewer mining locations, 13th IWA Specialized Conference on Small Water and Wastewater Systems, Athens, Greece.

Tyralis, H. et al. (2017), Exploratory data analysis of the electrical energy demand in the time domain in Greece, Energy, Vol. 134, p. 902-918

United Nations (UN) (2012), World Water Development Report 4, UNESCO Publishing

Ustin, G. E., (2009). Occurrence and removal of metals in urban wastewater treatment plants. Journal of Hazardous Materials, Issue 172, pp. 833-838.

Vollertsen, J., Nielsen, A. H., Jensen, H. S., & Hvitved-Jacobsen, T., (2008). Modeling the formation and fate of odorous substances in collection systems. Water Environment Research, 80(2), 118–126.

Wikipedia (2017). Urban heat island, available online from https://en.wikipedia.org/wiki/Urban_heat_island .

Wilkie, P. J., Hajimihalis, G., Koutoufides, P. & Connor, M. A., (1996). The contribution of domestic sources to levels of key organic and inorganic pollutants in sewage: the case of Melbourne, Australia. Water Science and Technology, Volume 34, pp. 63-70.

Wintgens, T., Gallenkemper, M. & Melin, T., (2002). Endocrine disrupter removal from wastewater using membrane bioreactor and nanofiltration technology. Desalination, Volume 146, pp. 387-391.

Witgens, T. et al., (2005). The role of membrane processes in Municipal wastewater reclamation and reuse. Desalination, Volume 178, pp. 1-11.

Witherspoon, J., Allen, E., & Quigley, C., (2004). Modelling to assist in wastewater collection system odour and corrosion potential evaluations. Water Science & Technology, 50(4), 177–183.

Xiao, Y. et al., (2014). Advanced treatment of semiconductor wastewater by combined MBR-RO technology. Desalination, Volume 336, pp. 168-178.

Zhang, K. & Farahbakhsh, K., (2006). Removal of native coliphages and coliform bacteria from municipal wastewater by various wastewater treatment processes: Implications to water reuse. Water Research, Volume 41, pp. 2816-2814.

Zhang, Q. et al., (2016). Comparative toxicity of nonylphenol, nonylphenol-4-ethoxylate and nonyphenol-10-ethoxylate to wheat seedlings. Ecotoxicology and Environmental Safety, Issue 131, pp. 7-13.

Zinzi, M., and S. Agnoli. (2012). Cool and green roofs. An energy and comfort comparison between passive cooling and mitigation urban heat island techniques for residential buildings in the Mediterranean region. Energy and Buildings. 55. 66-76.

The research leading to these results has received funding from the European Union Seventh Framework Programme (FP7/2007-2013) under grant agreement no. 619039